



## Geochemical carbon dioxide removal potential of Spain

Liam A. Bullock<sup>a,\*</sup>, Juan Alcalde<sup>a</sup>, Fernando Tornos<sup>b</sup>, Jose-Luis Fernandez-Turiel<sup>a</sup>

<sup>a</sup> Geosciences Barcelona (GEO3BCN), CSIC, Lluís Solé i Sabarís s/n, 08028 Barcelona, Spain

<sup>b</sup> Instituto de Geociencias (IGEO, CSIC-UCM), Dr Severo Ochoa, 7, 28040 Madrid, Spain

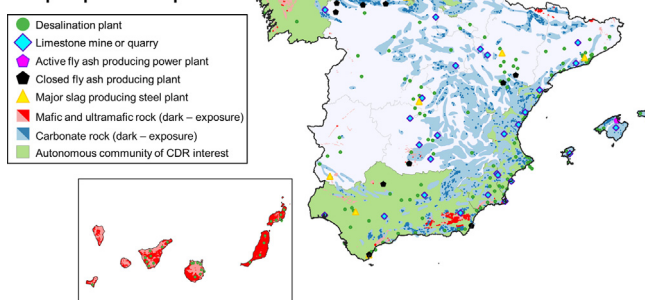


### HIGHLIGHTS

- To achieve national reduction targets, there is a need for large scale CO<sub>2</sub> removal.
- Spain may host a high geochemical CO<sub>2</sub> removal capacity thanks to its varied geology.
- We identify possible materials, localities and avenues for strategies within Spain.
- Mafic, ultramafic and carbonate rocks and industry by-products are of key interest.
- Spain's CDR potential warrants devoted studies to achieve high removal tonnages.

### GRAPHICAL ABSTRACT

#### Geochemical CO<sub>2</sub> removal prospects for Spain



### ARTICLE INFO

Editor: Daniel CW Tsang

#### Keywords:

Carbon dioxide removal  
Geological CO<sub>2</sub> storage  
Mineral carbonation  
Enhanced weathering  
Ocean alkalinity enhancement  
Spain

### ABSTRACT

Many countries have made pledges to reduce CO<sub>2</sub> emissions over the upcoming decades to meet the Paris Agreement targets of limiting warming to no >1.5 °C, aiming for net zero by mid-century. To achieve national reduction targets, there is a further need for CO<sub>2</sub> removal (CDR) approaches on a scale of millions of tonnes, necessitating a better understanding of feasible methods. One approach that is gaining attention is geochemical CDR, encompassing (1) in-situ injection of CO<sub>2</sub>-rich gases into Ca and Mg-rich rocks for geological storage by mineral carbonation, (2) ex-situ ocean alkalinity enhancement, enhanced weathering and mineral carbonation of alkaline-rich materials, and (3) electrochemical separation processes. In this context, Spain may host a notionally high geochemical CDR capacity thanks to its varied geological setting, including extensive mafic-ultramafic and carbonate rocks. However, pilot schemes and large-scale strategies for CDR implementation are presently absent in-country, partly due to gaps in current knowledge and lack of attention paid by regulatory bodies. Here, we identify possible materials, localities and avenues for future geochemical CDR research and implementation strategies within Spain. This study highlights the kilotonne to million tonne scale CDR options for Spain over the rest of the century, with attention paid to chemically and mineralogically appropriate materials, suitable implementation sites and potential strategies that could be followed. Mafic, ultramafic and carbonate rocks, mine tailings, fly ashes, slag by-products, desalination brines and ceramic wastes hosted and produced in Spain are of key interest, with industrial, agricultural and coastal areas providing opportunities to launch pilot schemes. Though there are obstacles to reaching the maximum CDR potential, this study helps to identify focused targets that will facilitate overcoming such barriers. The CDR potential of Spain warrants dedicated investigations to achieve the highest possible CDR to make valuable contributions to national reduction targets.

### 1. Introduction

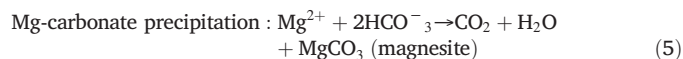
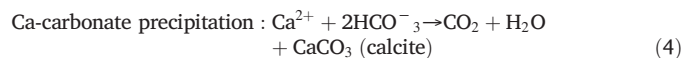
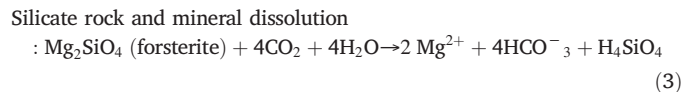
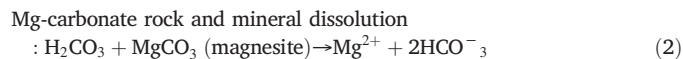
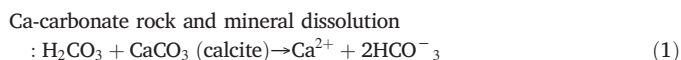
There is a growing urgency for CO<sub>2</sub> removal (CDR) strategies to reduce atmospheric CO<sub>2</sub> concentrations. Anthropogenic CO<sub>2</sub> inputs to the atmosphere are a crucial cause of global warming, and the Paris Agreement

\* Corresponding author.

E-mail address: [lbullock@geo3bcn.csic.es](mailto:lbullock@geo3bcn.csic.es) (L.A. Bullock).

goal to limit the increase in global average temperature to 1.5 °C cannot be achieved without atmospheric CDR on the order of tens of gigatonnes (Gt) CO<sub>2</sub> per year by 2100 (IPCC, 2022). This objective represents a formidable challenge, requiring an urgent assessment of different CDR strategies that can be implemented on a large multinational scale. The long-term aim of the European Union (EU) is to achieve climate-neutrality by 2050, in line with the commitment to global climate action under the Paris Agreement and the European Green Deal (no net emissions of greenhouse gases (GHGs) by 2050; European Commission, 2021). This aim will require innovative technological solutions incorporated into industrial policy and research.

On top of mindful GHG reduction efforts and increasing use of renewable energy, attention is turning to feasible CDR methods that target CO<sub>2</sub>-material reactions by both in-situ and ex-situ surface and sub-surface approaches, in dry or aqueous hosting conditions (see Fig. 1 for definitions used in this study), collectively termed geochemical CDR strategies (Energy Futures Initiative, n.d.; Canadell et al., 2021; Schenuit et al., 2021; Campbell et al., 2022). Approaches include (1) subsurface in-situ injection of CO<sub>2</sub>-rich gases into alkaline (Ca and Mg cation-rich) rocks for mineral carbonation and geological storage, (2) ex-situ ocean alkalinity enhancement and ocean liming, enhanced rock weathering and mineral carbonation of alkaline-rich materials, and (3) electrochemical separation processes. The main natural processes include:



One of the main principles is to induce or accelerate the natural chemical weathering reaction (Eqs. (1)–(3)), to form soluble bicarbonates (stabilized by Ca<sup>2+</sup> or Mg<sup>2+</sup> cations), i.e., alkalinity, or to later precipitate solid carbonate minerals (Eqs. (4)–(5)). These reactions can consume (or remove) CO<sub>2</sub> from the atmosphere (dissolution of silicates and precipitation of carbonates on land or in the ocean would result in release of some CO<sub>2</sub> due to outgassing, effectively halving the net CDR; dissolution and precipitation of carbonates results in no net CDR) and store it safely for 100's of thousands of years or longer, but are slow processes, taking similar timescales to occur in the nature (Renforth et al., 2013). Targeted CDR strategies could speed up reactions (Eqs. (1)–(3)) to occur on human timescales of several decades or faster to meet long-term international climate targets. The key questions which are being actively investigated in geochemical CDR include

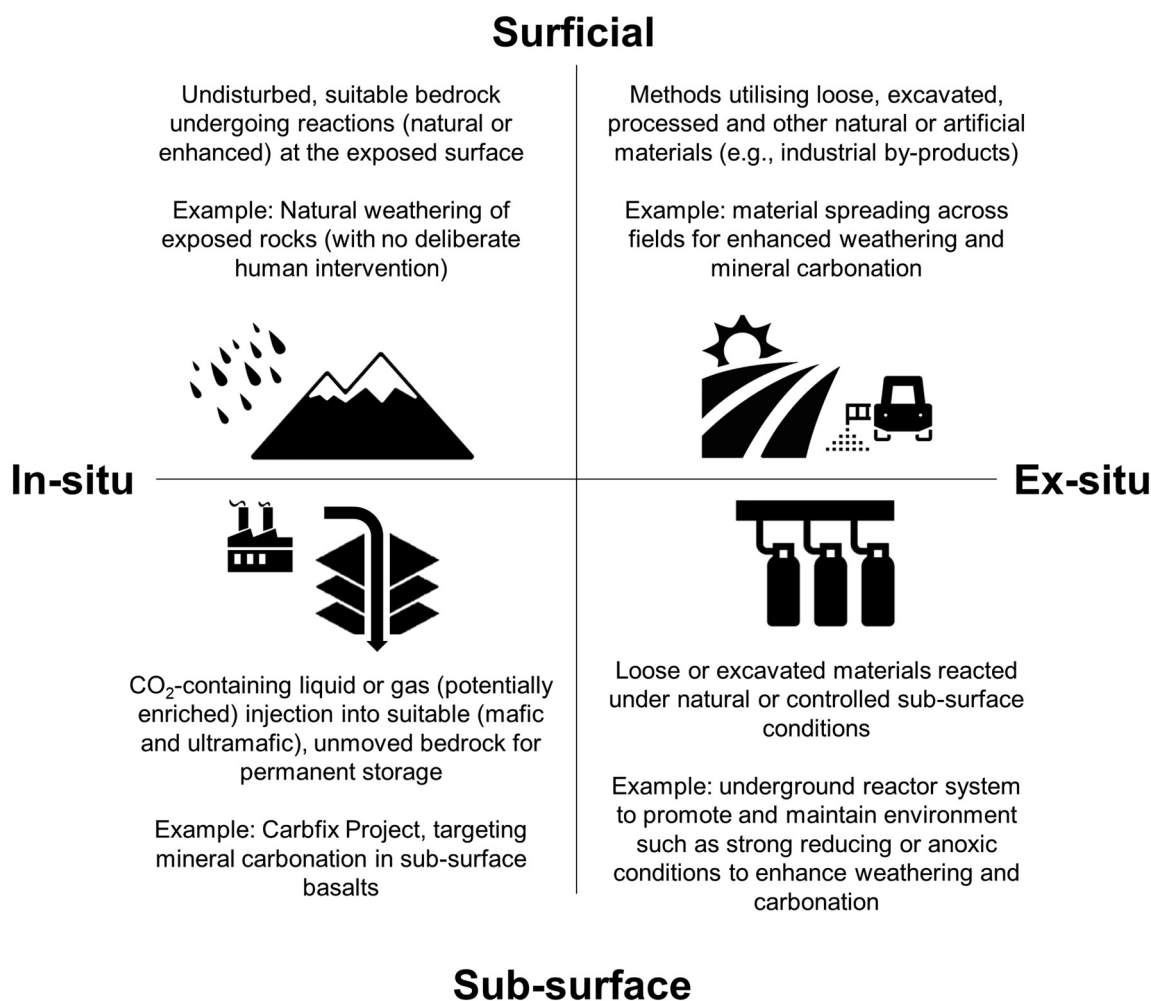


Fig. 1. Definitions used in this study of in-situ and ex-situ geochemical CDR approaches, hosted in both surficial and sub-surface settings.

determining which materials are most suitable for implementation (e.g., Hitch et al., 2010; Renforth and Henderson, 2017; Li et al., 2018; Kelemen et al., 2019; Khudhur et al., 2022), how much material is theoretically accessible to carry out geochemical CDR (e.g., Renforth, 2012; Bullock et al., 2021), where materials are located (e.g., Kremer et al., 2019; Bullock et al., 2022), what techniques can speed up reactions (e.g., Schuiling and Krijgsman, 2006; Krevor and Lackner, 2011; Hartmann et al., 2013; Kelemen et al., 2020; Xing et al., 2022) and what methods can be upscaled for large-scale CDR (e.g., Hangx and Spiers, 2009; Power et al., 2014; Matter et al., 2016; Beerling et al., 2020). Several studies have also sought to categorise the CDR potential of individual countries, including the United States (Krevor et al., 2009), United Kingdom (Renforth, 2012; Smith et al., 2014; Alcalde et al., 2018b; Kantzas et al., 2022), Japan (Myers and Nakagaki, 2020), and South Africa (Hietkamp, n.d.; Vogeli et al., 2011; Meyer et al., 2014).

Here, we examine the geochemical CDR potential of Spain. As an EU Member State, Spain is bound to adopt national energy and climate plans to make notable progress on its climate actions. Spain's governmental target is a 90 % GHG emission reduction by 2050 compared to 1990, equating to a decrease from 334.3 MtCO<sub>2</sub>eq (CO<sub>2</sub> equivalent) in 2018 to 28.9 MtCO<sub>2</sub>eq in 2050 (Sun et al., 2021), roughly a 9.5 MtCO<sub>2</sub>eq reduction per year. In a “business as usual” scenario, whereby the current policies and GHG reduction trends are projected to continue, emission levels will remain above baseline 1990 levels by 2030 (NECP, 2020; Climate Analytics, 2021), meaning more ambitious goals for reductions should be targeted. This scenario may encompass an increased recognition of geochemical CDR potential, at least on an investigative or pilot study scale.

As well as hosting several chemically and mineralogically favourable rock types that could be utilized for CDR purposes, including some already exploited by mining and quarrying activities, Spain produces several industrial waste by-products that could also be harnessed. Moreover, extensive cropland and agricultural coverage, greenhouse deployment, mined and quarried land and coastline exposure could provide geochemical CDR site opportunities across the mainland and Spanish islands. Despite the possible options, no potential geochemical CDR opportunities are highlighted in Spain's low emission development strategy (LEDS) (MITECO, 2020b), meaning this potential contribution to overall CDR and LEDS in Spain is still relatively unknown. This study provides a primary catalogue of available and accessible materials in Spain, targetable regions and some preliminary calculations of the overall geochemical CDR potential for the country. It should be stressed that any calculated maximum theoretical CDR could not be conceivably achieved, in part due to practicalities of methodological implementation, hindered access to suitable materials and the limited ability to react 100 % of available cations in human timescales (mineralogy-dependent). However, results can be used to further define Spain's overall climate targets and initiate future CDR plans and projects for academia, industry, government and other sectors of interest to achieve as much of the maximum potential as possible.

## 2. Methodology for preliminary CDR calculations

An initial assessment of the reactivity potential of materials in Spain has been made here based on their whole material (rock) geochemistry and modal mineralogies. One method that can be utilized to provide an indicator of upper limit geochemical CDR suitability is through the modified Steinhour (1959) formulae, adapted by Renforth (2019), and later implemented in Bullock et al. (2021, 2022). This calculation is based primarily on the material chemistry, giving a maximum hypothetical CDR specific capacity of a given material, through alkalinity production (“E<sub>pot</sub>” value, measured in kg of CO<sub>2</sub> per tonne of material; kgCO<sub>2</sub>/t) or via carbonation (“C<sub>pot</sub>” value), assuming 100 % mobility of aqueous complexes without consideration for reaction kinetics, timescales of mineral dissolution and secondary precipitation of non-carbonate minerals. The calculations are

made using whole rock (or material) compositions in the following equations:

$$E_{pot} = \frac{M_{CO_2}}{100} \cdot \left( \alpha \frac{CaO}{M_{CaO}} + \beta \frac{MgO}{M_{MgO}} + \varepsilon \frac{Na_2O}{M_{Na_2O}} + \theta \frac{K_2O}{M_{K_2O}} + \rho \frac{MnO}{M_{MnO}} + \gamma \frac{SO_3}{M_{SO_3}} + \delta \frac{P_2O_5}{M_{P_2O_5}} \right) \cdot 10^3 \cdot \eta \quad (6)$$

$$C_{pot} = \frac{M_{CO_2}}{100} \cdot \left( \alpha^* \frac{CaO}{M_{CaO}} + \beta \frac{MgO}{M_{MgO}} + \gamma \frac{SO_3}{M_{SO_3}} + \delta \frac{P_2O_5}{M_{P_2O_5}} \right) \cdot 10^3 \quad (7)$$

The coefficients  $\alpha, \beta, \gamma, \delta, \varepsilon, \rho,$  and  $\theta$  consider the relative contribution of each oxide to geochemical CDR (see Renforth, 2019), adjusted based on the modal carbonate content of the rock (see Bullock et al., 2021). Elemental concentrations of the materials are expressed as major element (wt%) oxides,  $M_x$  is the molecular mass of those oxides, and  $\eta$  is molar ratio of CO<sub>2</sub> to cation sequestered during weathering (here,  $\eta = 1.5$  to account for buffering in the seawater carbonate system; Renforth and Henderson, 2017; Renforth, 2019; Bullock et al., 2021). Notwithstanding the assumptions relating to reaction kinetics, the formulae are employed here for regional/large-scale estimations based on available whole rock chemistry (elemental and major element oxides for Ca, Mg, Na, K, Mn, S and P, taken from literature examples; Table SI1) of mafic-ultramafic rocks and industrial by-products, giving a value of g of CO<sub>2</sub> removed per kg of material (gCO<sub>2</sub>/kg, Table SI1; see Renforth, 2019; Bullock et al., 2021, 2022).

While the E<sub>pot</sub> and C<sub>pot</sub> values may provide a means of estimating a theoretical maximum potential, in practice, the reactivity of a material is heavily governed by mineral kinetics and the ability of the material to react in a given media setting (e.g., in water or air, under ambient or elevated temperatures, with CO<sub>2</sub> in air or concentrated) or over a given period of time (on decadal to millennia timescales). The ability for a mineral to undergo dissolution, thus releasing the necessary cations for alkalinity production or mineral carbonation, is a key variable for both quantitative and qualitative determination of material suitability for geochemical CDR applications. Dissolution of minerals may require the breaking of chemical bonds of variable strength, and may act as the rate limiting step in geochemical CDR reactions (Daval et al., 2009; Pullin et al., 2019; Khudhur et al., 2022). Therefore, mineral kinetics should also be considered for assessment of material suitability. Several studies have utilized shrinking core models to determine dissolution time and extent of a given mineral or rock (e.g., Hangx and Spiers, 2009; Renforth et al., 2013; Kelemen et al., 2020; Rinder and von Hagke, 2021; Bullock et al., 2022). Many of these modified models present partial or complete mineral grain dissolution based on modal mineral abundances in the material, chemical composition of each mineral present, an initial mean grain size, each mineral dissolution (weathering) rate under given conditions, and amount of material present (e.g., annual production). In this study, we utilise a slightly modified version of the shrinking core model utilized by Renforth et al. (2013), later used in Bullock et al. (2022). Here, a theoretical 1 kg of a given material is used, where a range of modal mineralogies (gathered from literature examples; Table SI1) is converted to grams of mineral, with untargeted minerals (e.g., pyrite, magnetite, apatite, quartz) excluded from calculations. The sum for all present mineral phases then gives the overall potential of the material:

$$X(t) = \frac{D_0^3 - (D_0 - 2W_r V_m t)^3}{D_0^3} \quad (8)$$

where  $X$  is the fractional extent of dissolution,  $t$  is dissolution time (s),  $D_0$  is the initial particle diameter (m),  $W_r$  is the average dissolution rate (mol (mineral)/m<sup>2</sup>/s), and  $V_m$  is the molar volume of the mineral (m<sup>3</sup>/mol, converted to one mol Si basis). The maximum CDR capacity of each mineral (in gCO<sub>2</sub>/kg material), required for the shrinking core model, is based on a calculated E<sub>pot</sub> value (alkalinity production) and C<sub>pot</sub> value (for mineral carbonation). Both these values are based on their typical mineral chemistry. The model estimates dissolution extent and CDR (gCO<sub>2</sub>) over a given period of time for each mineral present in the theoretical 1 kg. Cumulative CDR

potential due to alkalinity production (or carbonation) of 1 kg of material  $i$  for a time duration  $t$ , referred to as specific CDR (sCDR), is calculated by:

$$sCDR_i(t) = \sum_j f_{i,j} X_{i,j}(t) E_{pot}^j \quad (9)$$

where  $f_{i,j}$  is the mass fraction of mineral  $j$  in material  $i$ ,  $X_{i,j}$  is the extent of dissolution calculated using the shrinking core model (Eq. (7)) using the kinetics of mineral  $j$  and the initial particle size  $i$ , and  $E_{pot}^j$  is the  $E_{pot}$  for mineral  $j$  (Bullock et al., 2022). For total cumulative CDR (tCDR) of material  $i$  over a given period of time or by a particular year ( $y$ ) within this period, which includes the cumulative contribution from material replenishment in all the years ( $k$ ) up to and including year  $y$ , this is calculated by:

$$tCDR_i(y) = \sum_{k=1}^y sCDR_i(t_k) P_{i,k} \quad (10)$$

where  $t_k$  is the time elapsed from year  $k$  to year  $y$ , and  $P_{i,k}$  is the mass of tailing  $i$  produced in year  $k$ , with  $k = 1$  denoting the first year of weathering (Bullock et al., 2022). The CDR achieved annually (aCDR) of material  $i$  in year  $y$  can then be derived by:

$$aCDR_i(y) = tCDR_i(y) - tCDR_i(y-1) \quad (11)$$

Here, published mineral dissolution rates have been sourced from literature examples (Palandri and Kharaka, 2004 and references therein; Bandstra et al., 2008 and references therein; Gudbrandsson et al., 2011; Stockmann et al., 2011; Thom et al., 2013), where experimentally-derived rates were determined under ambient temperature conditions, atmospheric  $\text{CO}_2$  concentrations and in a starting neutral (pH 6–8) media solution. A starting grain size of 100  $\mu\text{m}$  has also been assumed, consistent with an achieved mean grain size for mined materials aiming to extract precious and base metals from a range of mafic and ultramafic rocks (Bullock et al., 2022). A range of modal mineralogies, sourced from literature examples, are considered for each rock type (Table 3). Calculations also assume that 1 Mt. material can be made available for weathering every year, either through by-product formation from mining and quarrying activities, or by direct means of excavation, crushing and milling specifically for geochemical CDR purposes. CDR has been estimated across a period of 1–70 years (e.g., assuming a possible launch in 2030 after a period of testing, designing and planning, aiming to achieve maximum benefit by 2100), with 1 Mt. per year of material available to weather each year (on top of initial CDR achieved from weathering in year 1, year 2 etc).

For further indication of material geochemical CDR potential, with particular focus on mineral carbonation potential, the saturation indices of each representative modal mineralogy have been computed using PHREEQC (Version 3; Parkhurst and Appelo, 1999), whereby secondary precipitation phases are simulated based on a starting solution composition, experimental conditions and initial solid equilibrium phases. Here, changes in the solution chemistry and the saturation states were modelled with time, the product of variable mineral dissolution, for identification of possible precipitated carbonate phases. Kinetic rate equations and solubility constants were taken from the *MINTEQA2.dat* database. Starting conditions were ambient temperature and pH (7) solution media, at fixed atmospheric pressure, but with enriched  $\text{CO}_2$  (90 %) to deliberately promote simulated carbonation conditions.

### 3. Targetable bedrock

#### 3.1. Mafic and ultramafic rocks

Appropriate silicate lithologies for geochemical CDR implementation purposes include Ca- and Mg-rich mafic and ultramafic rocks (Table 2). Across Spain, these include ultramafic intrusive rocks, mafic extrusive rocks and, to a lesser extent, intrusive mafic rocks and metamorphosed mafic-ultramafic rocks. Suitable mineral assemblages include those that contain reactive Ca- and Mg-rich phases such as brucite (even in small

amounts), talc, wollastonite, serpentine, olivine and smectite. The Mg-hydroxide mineral brucite has been extensively studied for its favourable solubility and reactivity with  $\text{CO}_2$  at ambient temperature conditions for use in geochemical CDR projects (e.g., Pokrovsky et al., 2005; Harrison et al., 2013, 2015; Power et al., 2013, 2014, 2016; Wilson et al., 2014; Zarandi et al., 2016; McCutcheon et al., 2017; Li et al., 2018). Serpentine minerals, typically much more abundant in mafic and ultramafic rocks than brucite, have also been previously targeted due to their high reactivity and high Mg content (Krevor and Lackner, 2011; Oskierski et al., 2013; Lacinska et al., 2017). Smectite-group minerals such as saponite can also provide fast reactivity and cation exchange for CDR purposes (Zeyen et al., 2022). Olivine (Hänchen et al., 2008; Hangx and Spiers, 2009; Schuiling and Krijgsman, 2006; Ten Berge et al., 2012) and wollastonite (Dudhaiya et al., 2019; Haque et al., 2020) have also received attention for their thermodynamic favourability and promising dissolution rates, though hindrances associated with Si-rich layer formation and secondary Mg-Ca-silicate precipitation (in place of carbonates) need to be considered for these and other potentially reactive minerals. Pyroxene, plagioclase, mica and chlorite could also contribute to the required  $\text{Mg}^{2+}$  and  $\text{Ca}^{2+}$  cations for CDR (Meyer, 2014; Marieni et al., 2020; Bullock et al., 2022), although their slower mineral dissolution rates and lower reactivity require deliberate efforts to increase cation release (e.g., changes to pH, temperature,  $\text{CO}_2$  pressure, changes to waste management practices such as better exposure to the atmosphere or water) (Bullock et al., 2022).

Here, potentially suitable bedrock for geochemical CDR is highlighted (Fig. 2, Table 1 and Figs. S11–5 in the supplementary material) based on maps and available data from the 1:1 M Geological Map of Spain (including the Balearic and Canary Islands, produced by the Spanish Geological Survey; IGME, n.d.). This approach follows a similar semi-quantitative method as employed by the US Geological Survey for mapping the mineral resource base for mineral CDR in the conterminous United States (Krevor et al., 2009) but tailored to the specificities of Spain. The overall surface and subsurface mapped extent of targeted rocks give a broad indication of potentially targetable regions for geochemical CDR methods. However, much of these areas are covered by infrastructure, unconsolidated sediments and extensive vegetation, limiting their accessibility (without considerable energy and effort). Therefore, areas of probable exposure, such as regions of mineral excavation, bare rock, scarce vegetation, beaches, dunes, sandbanks and burnt areas, have been identified for potentially targetable surface bedrocks (based on land use classification of the European Environment Agency, n.d.; Fig. 2 and Table 1). National parks and areas of protected land have been excluded here, as extensive geochemical CDR implementation methods may not be permitted or receive public acceptance (though they should not be completely ruled out). Based on these criteria, Spain has up to 1864  $\text{km}^2$  of targetable (probable exposure, unprotected) land for mafic and ultramafic rocks (0.4 % of land coverage; Table 1).

#### 3.1.1. Ultramafic rocks

Ultramafic rocks present across Spain include dunite, harzburgite, lamproite, peridotite, pyroxenite, websterite and wehrlite. The key localities that host ultramafic rocks in Spain are Galicia (NW Iberian Peninsula), the Ronda massif (extending across the southern Iberian Peninsula) and, to a lesser degree of exposure, areas of Extremadura and northern Andalucía (SW Iberian Peninsula), and areas of Almería and Murcia (SE Iberian Peninsula). There are also minor low-volume outcrops in Catalonia and Aragón (Fig. 2).

Galicia hosts ultramafic rocks that include units of dunite, peridotite, pyroxenite and harzburgite, hosted within the Galicia-Trás-os-Montes Zone of the Iberian massif (Farias et al., 1987; Girardeau et al., 1989; Zalduegui et al., 1996; Marcos et al., 2002; Santos et al., 2002). Several outcropping localities occur in the northern peninsula of Cabo Ortegal, where dunite is extracted as a commodity (see Section 3.1). Another extensive area of key interest for geochemical CDR is the Ronda peridotite massif in the Betic Cordillera (S Spain), comprised of ultramafic-mafic intrusives, with large areas (mapped  $\sim 300 \text{ km}^2$ ) of upper mantle rocks extending

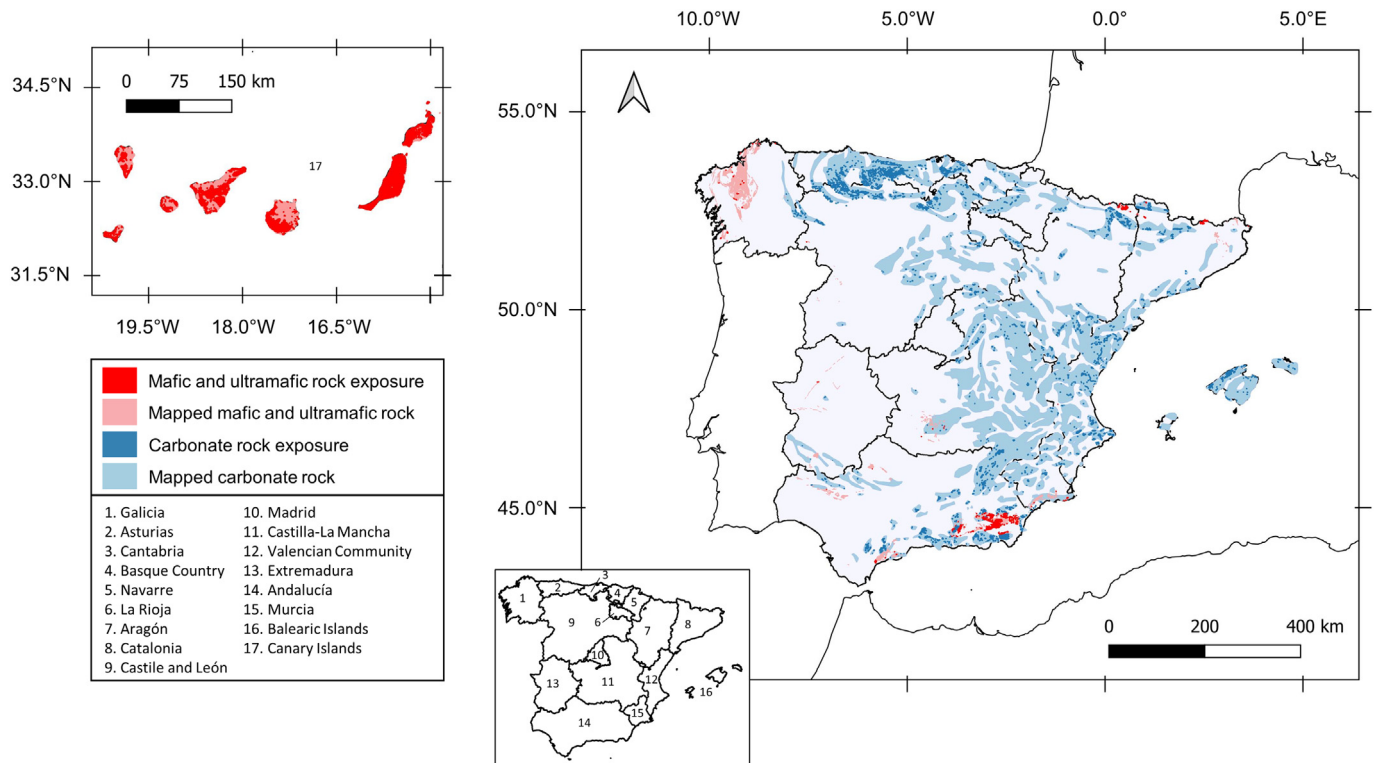


**Fig. 2.** Exposure of the main lithological groups potentially suitable for CDR strategies in Spain (with Canary Islands inset on the top left; autonomous communities of Spain also indicated in bottom middle inset) showing mapped and surface. Areas of probable exposure include mapped mafic, ultramafic and carbonate regions covering areas of mineral excavation, bare rock, scarce vegetation, beaches, dunes, sandbanks and burnt areas (from the land use classification of the [European Environment Agency, n.d.](#)). Lithological information from [IGME \(n.d.\)](#). See supplementary material for detailed regional maps, including areas of exposure and protected lands.

across southern Spain ([Garrido and Bodinier, 1999](#); [Platt et al., 2003](#); [Booth-Rea et al., 2005](#); [Bodinier et al., 2008](#); [Préçigout et al., 2013](#)). The Ronda peridotite massif hosts olivine, serpentine, phlogopite, diopside and accessory brucite. The Mg-carbonate mineral hydromagnesite has also been detected ([Bessi ere et al., 2021](#)), suggesting that some brucite may have already been naturally carbonated. As well as the Ronda peridotite massif, SW Spain hosts harzburgite, part of the brucite-hosting Ossa Morena and South Portuguese Zones.

Areas of Extremadura, including regions of targetable commodities such as the Aguablanca deposit and Tejadillas prospect, host ultramafic

rocks that form part of the magmatic system of the Cortegana Igneous Complex (Aracena massif), containing large sills of olivine-bearing websterite, lherzolite, dunite, pyroxenite and minor harzburgite, troctolite and wehrlite ([Casquet et al., 2001](#); [Tornos et al., 2001, 2006](#); [Pi a et al., 2006, 2012](#)). The ultramafic bodies of Calzadilla de los Barros in the Ossa-Morena Zone (Badajoz, Extremadura) comprise gabbros, highly serpentinized harzburgite, clinopyroxenites and dunites ([Merinero Palomares et al., 2014](#)). The SE Iberian Peninsula (regions of Almer a, Cartagena, Albacete and Murcia) hosts several ultrapotassic and ultramafic units of the SE Volcanic Province ([Venturelli et al., 1984](#); [Contini et al.,](#)

**Table 1**

Suitable bedrock exposure and viable areas for geochemical CDR methods in Spain. Mapped coverage includes surface or near-surface lithologies as classified by [IGME \(n.d.\)](#). Exposed areas include mapped areas that occupy mineral extraction zones, bare rock, spaces with scarce vegetation, burnt areas, beaches, dunes and sandbanks, as classified by the [European Environment Agency \(n.d.\)](#). Unprotected areas include areas outside of national parks ([European Environment Agency, n.d.](#)).

Targetable rock type	Land area covered	Total mapped coverage (including non-exposed areas) (km <sup>2</sup> )	Total coverage in exposed areas (km <sup>2</sup> )	Total coverage in exposed, unprotected areas (km <sup>2</sup> )	Total % of land coverage of exposed, unprotected areas	Targetable area examples (exposed, unprotected areas)
Mafic and ultramafic rock	Mainland	7234	404	146	0.03	La Coru�a and Pontevedra (Galicia), Almer�a, Granada and M�alaga (Andaluc�a), Huesca (Arag�on), Lleida (Catalonia), Ciudad Real (Castilla-La Mancha), Murcia, C�aceres and Badajoz (Extremadura)
	Canary Islands	7560	3357	1718	0.34	All islands, predominant exposed coverage on Fuerteventura
	Spain (Total)	14,794	3761	1864	0.37	Canary Islands, Galicia, Murcia, Andaluc�a and Extremadura
Carbonate rock	Mainland and Balearic Islands	109,475	2228	773	0.15	Oviedo (Asturias), Santander (Cantabria), Gipuzkoa (Basque Country) Burgos (Castile and Le�on), Huesca (Arag�on), Valencia and Alicante (Valencian Community), Almer�a (Andaluc�a)
	Canary Islands	–	–	–	–	–
	Spain (Total)	109,475	2228	773	0.15	Asturias, Cantabria, Valencian Community, Balearic Islands, Basque Country

1993), including peridotites and lamproites, while the Cerro del Almirante ultramafic massif of the Nevado-Filábride Complex (Betic Cordillera) hosts a ~ 200 m thick chlorite harzburgite unit (Marchesi et al., 2013). There are also minor occurrences of peridotite in NE Iberian Peninsula (central-western Pyrenees, from Northeast Catalonia and across northern Aragón).

### 3.1.2. Mafic extrusive rocks

The Canary Islands, an active volcanic ocean island chain approximately 100 km off the west African coast, are dominated by Cenozoic mafic rock occurrences, comprising roughly half (7560 km<sup>2</sup>) of Spain's total mapped coverage of mafic-ultramafic rocks (Table 1). While some intrusive rocks are evident across the islands (wehllites, pyroxenites and gabbros on Fuerteventura, La Gomera and La Palma), most of the suitable rocks are extrusive basaltic (picrite, alkali basalt, tholeiite, basanite, phonolite, nephelinite) lavas (Troll and Carracedo, 2016). The 2021 eruption of Cumbre Vieja in La Palma covered 12 km<sup>2</sup> with new basaltic-basanitic lava in the southwestern part of the island (Castro and Feisel, 2022; Perez-Torrado et al., 2022).

There are other occurrences of mafic extrusive rocks across mainland Spain, predominantly Neogene-Quaternary alkaline basalts in areas such as the NE Volcanic Province, Catalonia (Cebriá et al., 2000), in SE Spain within the Alpine Chains, ahead of the Betic Front, and in central areas of Campo de Calatrava, where the Calatrava Volcanic Province is situated. Neogene-Quaternary alkaline volcanics include basanites, olivine basalts, pyroxenitic basalts, trachybasalts, melilitites, nephelinites and leucitites (Crespo and Lunar, 1997; Hernández et al., 1999; Villaseca et al., 2010; Ancochea and Huertas, 2021). Silurian-Devonian volcanism of the Almadén mining district produced alkali basaltic lava flows, as well as pyroclastic deposits, sills and dykes (Perroud et al., 1991; Hall et al., 1997). There are also minor isolated occurrences of alkaline basalt in vegetated areas of the Valencian Community (in areas north of Ayora within the Valencia Basin) and Andalucía (east of Cádiz).

### 3.1.3. Mafic intrusive rocks

Spatially associated with the locations of the ultramafic rocks detailed above, Galicia, Extremadura and the Ronda peridotite massif also host extensive intrusive mafic rocks, including units of gabbro (e.g., the Monte Castelo Gabbro of Galicia; Abati et al., 2003), anorthosite, gabbrodiorite, gabbronorite, leucogabbro, norite and more intermediate diorite (the latter from the Santa Olalla pluton, Extremadura; Casquet, 1980; Casquet et al., 2001). Areas of Almadén also host shallow intrusive dolerite units (Hernández et al., 1999), the Burguillos del Cerro Plutonic Complex hosts gabbroic-dioritic units (Casquet et al., 2001; García-Lobón et al., 2006; Tornos et al., 2021) and the Betic Cordillera hosts gabbro and dolerite (Rodríguez et al., 2020).

### 3.1.4. Metamorphic rocks of mafic-ultramafic protolith

Prominent serpentinite occurrences are located in areas of Galicia (e.g., Cabo Ortegal; Pereira et al., 2008) and in the Betic Cordillera (e.g., Ronda peridotite massif; Rodríguez et al., 2020; Cerro del Almirante ultramafic massif, Marchesi et al., 2013; SE Volcanic Province; Venturelli et al., 1984; Contini et al., 1993). Metamorphic rocks, which include chlorite schist, metabasalt, metabasite and migmatite, occur in the Alpujarride Complex and Sierra de Baza (Betic Cordillera) and in the Spanish Central System (Extremadura, Castilla-La Mancha and Castile and León).

## 3.2. Carbonate rocks

Though more limited than Mg- and Ca-rich silicate rocks for alkalinity production (Eqs. (1)–(2)) and unable to net remove CO<sub>2</sub> via precipitation steps (mineral carbonation, Eqs. (1) and (3)), carbonate rocks can still provide means of geochemical CDR through ex-situ methods such as ocean alkalinity enhancement, ocean liming and enhanced rock weathering applications for alkalinity production and to counteract the acidification

of oceans (Rau and Caldeira, 1999; Taylor et al., 2016). Such methods may involve the use of CO<sub>2</sub>-enriched gases and activation through calcination (Khesghi, 1995), targeting the separation of CaO, MgO or Ca-Mg-hydroxide (Ca(OH)<sub>2</sub>) (Caserini et al., 2021), which will rapidly dissolve and release alkalinity in seawater (Justnes et al., 2020). Through alkalinity addition in the form of CaO or MgO, ocean pH and resultant CO<sub>2</sub> uptake increase. Between 1.6 and 1.8 mol of CO<sub>2</sub> are absorbed for every 1 mol of added CaO or MgO (Renforth et al., 2013). Limestone and dolostone can provide the source materials for such geochemical CDR approaches. Acceleration of weathering of carbonate rocks in a reaction with water (e.g., seawater) and CO<sub>2</sub>-enriched gas consumes CO<sub>2</sub>, with alkaline bicarbonate water products sent to (or in the case of with seawater usage, returned to) the ocean, neutralizing acidity (Rau and Caldeira, 1999). Such enhanced weathering of carbonate rocks follows the principles of naturally occurring carbonate weathering (Eqs. (1)–(2)), with bicarbonate solutions stabilized by the released solubilized cations (e.g., Ca<sup>2+</sup>, Mg<sup>2+</sup>). There are still uncertainties that need to be considered for geochemical CDR approaches involving the weathering of carbonate rocks, particularly how ecosystems will respond to both the changes in alkalinity and the possible effects of trace element release from the rocks, as well as energy and cost implications for large scale rollout, meaning further scientific assessment is required.

In terms of spatial and volumetric availability, carbonates comprise some of the major lithological units of Spain, with mapped areas covering ~109,475 km<sup>2</sup> (Table 1), accounting for ~22 % of total land coverage (Fig. 2). There are major carbonate outcrops across Spain, with 773 km<sup>2</sup> of targetable (exposed) carbonate rocks across mainland Spain and the Balearic Islands (0.15 % of land coverage; Table 1). Geochemical maps of Ca content of sediments and upper and lower soils generated for the Geochemical Atlas of Spain (Fig. 3; IGME, 2012) define the division between silicate-hosted Paleozoic basement rocks to the W-NW and carbonate rocks prevalent across southern, central and NE Spain, as well as the Balearic Islands. Cambrian carbonates occur in the Ossa Morena Zone (Extremadura) and Lugo (NE Galicia) and Leon (NW Castile and León). Carboniferous carbonates are widespread in Asturias and NW Castile and León, while those of Jurassic-Cretaceous age are abundant in Cantabria, Basque Country, Valencian Community, Murcia and across the Balearic Islands. In Andalucía, thick units of carbonates of Triassic-Jurassic age are hosted in the Betic Cordillera. Carbonate units show variable replacement by dolostone across the hosting regions.

## 4. Industrial sector by-products

Alkaline-rich industrial wastes and by-products have been shown to passively carbonate, while changes to conditions and management practices can accelerate reaction conditions and CDR potential (Khudhur et al., 2022). Spain has historically hosted extensive surface and subsurface mining and prominent raw material consuming (and producing) industrial activities. Main mining activities target metals (e.g., copper, lead-zinc, tin-tungsten, gold and silver), coal, extraction of industrial rocks such as limestone, dolostone, marble, granite and dunite (Fig. 4), and industrial minerals such as bentonite, quartz, magnesite, potash and sepiolite. Additionally, Spain is a historic producer of steel products and metal refining, with sites providing both massive point CO<sub>2</sub> emissions (through fossil fuel consumption) and means of facilitating CDR via waste by-products (e.g., utilizing fly ashes or slags). Spain is also one of the largest users of desalination technologies in the western world and the largest in Europe (Fuentes-Bargues, 2014). Desalinated water is necessary for water-poor regions of the Canary Islands and high-water demanding agricultural regions of the mainland (Palomar and Losada, 2010), with reject brine by-products (of high dissolved salt and cation content) created during the process. These industrial sectors and smaller-scale activities all treat by-products and waste materials that could be targeted for geochemical CDR strategies. The following sub-sections describe the industrial by-products, analysed from a Spain-focused perspective.

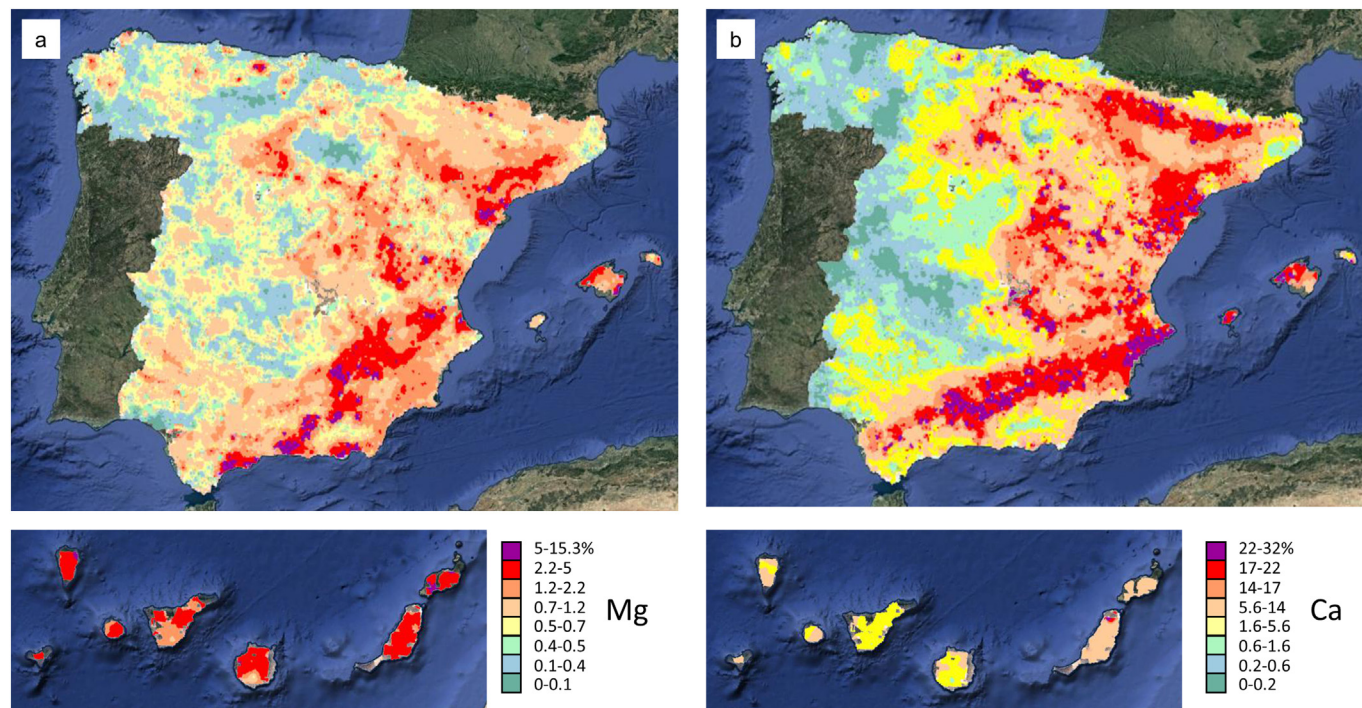


Fig. 3. Geochemical maps of Mg and Ca contents of sediments, upper and lower soils of Spain (Canary Islands inset) (IGME, 2012).

#### 4.1. Silicate mine and quarry wastes

Regarding metal mining from silicate-hosted bedrock and the associated wastes derived from such activities, potential targets for geochemical CDR are limited to areas that exploit mafic and ultramafic rocks. One example of a notable producing region is Aguablanca (Badajoz, Extremadura, SW Spain; Figure S14), exploiting Ni and Cu from breccia hosted within gabbro and gabbro-norite units. The site is currently on care and maintenance at time of writing, though historic tailings are held on site in dams, and production is planned to resume in the near future (Horn et al., 2021). There are few other examples of metallic mines with suitable host rocks for geochemical CDR utilization. The Touro Project (central Galicia, Figure S13) may also offer future opportunities for geochemical CDR strategies. The currently undeveloped project area comprises metabasites of gabbroic protolith (Castiñeiras et al., 2002) with minor lenses of ultramafic rocks. Operational plans include the necessity to strip 35.7 Mt. of overlying bedrock (Mining Data Online, n.d.-b), with an estimated 91 Mt. of tailings projected to be produced across 13 years of operation (Noble, 2018). Though volumetrically low, the Hg-producing region of Almadén in central Spain (Ciudad Real, Figure S13) may have worked intrusive dykes, sills and tuffs of basaltic composition, resulting in unprocessed overburden waste or variably processed tailings, which could be suitable for CDR purposes.

Beyond sporadic examples of CDR from silicate-hosted metal extraction operations, much of the realistic CDR potential from silicate mine wastes in Spain is found in wastes associated with ultramafic dunite extraction. Spain is a key European producer of olivine-bearing dunite rock, produced as a refractory mix for steel making and as raw material for the ceramic and fertiliser industry. Dunite is mined in the La Coruña region of Galicia by Pasek Minerale (Fig. 4a-c), with proven reserves estimated at 600 Mt. (Kremer et al., 2019). The Landoy mine site, which exploits predominant peridotite-harzburgite (containing abundant serpentine, as well as forsterite olivine, diopside, enstatite and hornblende), has produced over 21 Mt. of dunite historically, with a production capacity of 1 Mt. per year (production levels are typically 0.7–0.9 Mt. per year; Pasek Minerale, pers. comms.). For extraction and saleable use, dunite fractions of >3 mm are typically desired, meaning fractions below 3 mm (including a finer

fraction of <63  $\mu\text{m}$ ) are considered waste, stored in landfill or tailings dams (Baragaño et al., 2019). Approximately 80 kilotonnes (kt) of waste is produced each year (40 kt of size fraction 64  $\mu\text{m}$  to 3 mm, 40 kt of sludge <64  $\mu\text{m}$ ). Pasek Minerale have made plans to reduce the amount of waste by ~20%; however, if these finer materials are instead repurposed as a geochemical CDR resource, then the company could exploit dunite specifically for CDR strategies. It has been proposed that the site could double their yearly production level without the need for large investment (Syrett, 2013), so sufficient demand or necessity for materials for CDR purposes could make this a reality. As these materials are already extracted and processed to advantageous grain sizes, there are possibilities for utilization for ex-situ geochemical CDR purposes.

Additional silicate mine and quarry waste sources exist across mainland Spain and the Spanish islands, though details of their activity status and available tonnages are difficult to ascertain. For instance, the Canary Islands host numerous active, inactive and disused basalt quarry mines, with “picón” materials used in construction, agriculture and decorative purposes. The name “picón” is a local word to indicate basaltic, basanitic, and nephelinitic lapilli (fragmented tephra of 2–64 mm grain size), which has been traditionally used as a stone mulch in agriculture, vineyards and gardening to suppress evaporation from the soil, and to absorb and retain moisture (Tejedor et al., 2003; Lomoschitz et al., 2006; Belding, n.d.). Basaltic lapilli is also a common construction material across the islands, with increasing demand and usage over 60 years due to the growing tourism sector, requiring raw materials for concrete and highway construction (Lomoschitz et al., 2006). Quarried mafic lapilli from across the islands generally contain a low fine particle fraction (<5% of material with a diameter <0.06 mm), though the silt and clay fraction can reach up to ~50% in some data examples (Lomoschitz et al., 2006). While finer material is favourable for ex-situ geochemical CDR purposes, the natural porosity of lapilli grains (8.5–33% of interconnected voids; Lomoschitz et al., 2006) means that the reactive surface area is still high, and additional energy-intensive grinding to achieve higher weathering rates for any CDR strategies may not be required. Similar historic basalt quarries exist in the Calatrava Volcanic Province of Ciudad Real, with mining concessions still given for exploitation in volcanic areas of Cerro Gordo (Granátula-

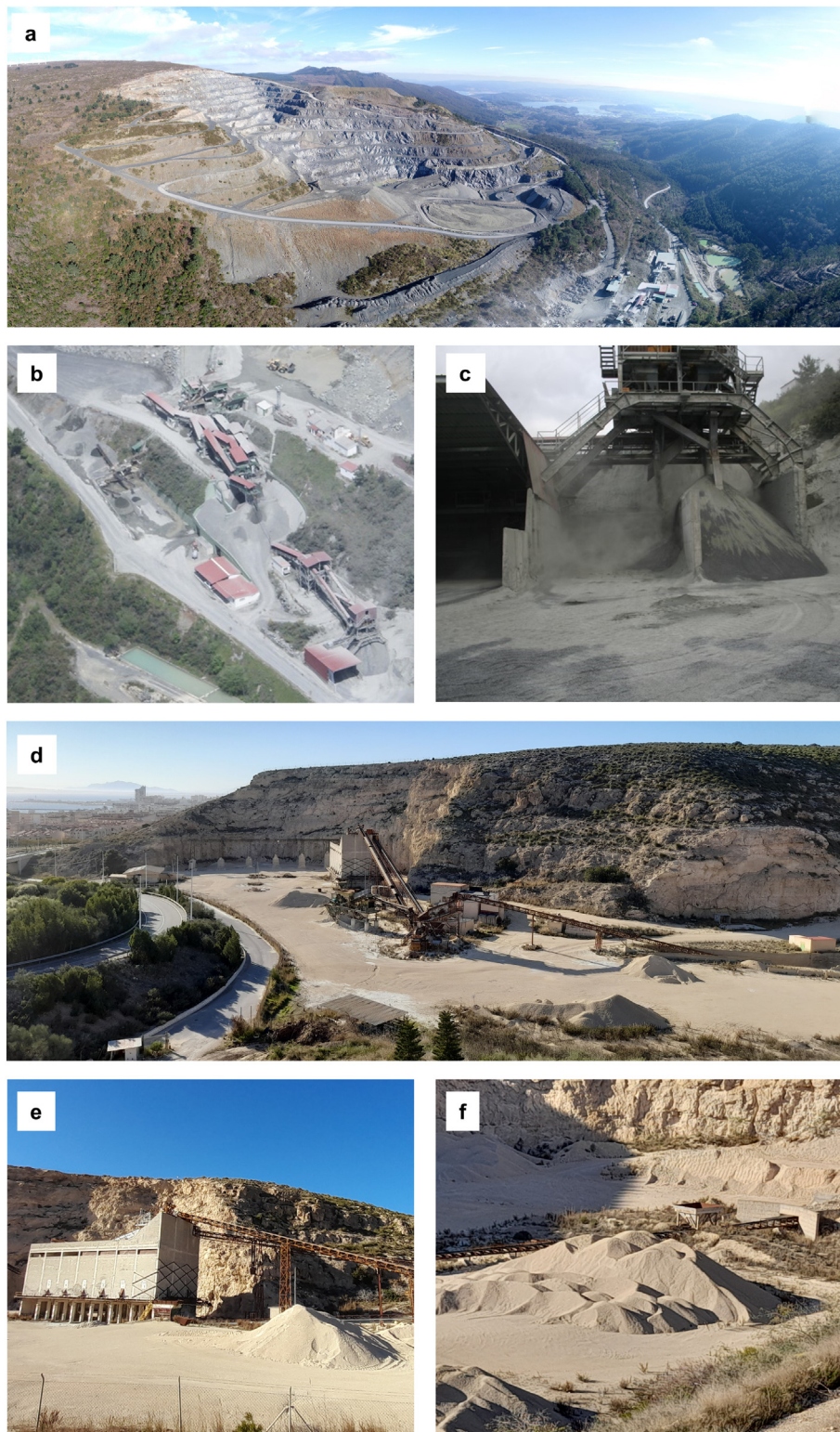


**Fig. 4.** Examples of tailings-producing silicate and carbonate surface mine operations in Spain. (a-c) Dunite mining in Landoy, Galicia, including waste stream facilities shown in (b-c) (photos courtesy of Pasek Minerale); (d-f) Limestone quarrying in Santa Pola, Alicante, with fine grained wastes piled up on-site shown in (f).

Valenzuela), Cabezo Segura (Poblete) or La Yezosa (Almagro) and Arzollar (Virgen de Alarcos) (Becerra-Ramírez et al., 2020).

#### 4.2. Carbonate mine and quarry wastes

Carbonate production and usage is a prominent industry across mainland Spain and the Balearic Islands, with limestone, dolostone, and marble

having been worked for thousands of years as a building material, for concrete and mortar, aggregates, agriculture, glass, in water/soil treatment, for ornamental purposes and many other applications. In 2012, 3 Mt. of limestone, 0.73 Mt. of dolomite and 2.1 Mt. of marble were produced nationally (IGME, 2012). The country hosts one of the largest marble quarries in the world – the Coto Pinoso quarry (Alicante), covering a surface area of approximately 5 km<sup>2</sup>. As well as mines and quarries dedicated to the



extraction of carbonates (e.g., Santa Pola quarry in Alicante; Fig. 4d-f), many metal, mineral and coal mines also exploit from carbonate bedrock (Fig. 5; US Geological Survey, n.d.), requiring the excavation and stockpiling of carbonate materials. For instance, the Reocín Mine (Cantabria, N Spain) is the largest carbonate-hosted Pb-Zn deposit in Spain, and one of the largest Mississippi Valley-type (MVT) deposits worldwide. The Reocín Mine ceased activity in 2003, though there are still multiple active quarries and mines in the area. Fluorite and fluor spar are mined from carbonate host rocks in the neighbouring province of Asturias, including the 140 kt per year capacity producing Mina Ana site in Ribadesella. Active magnesite mining takes place at the Azcárate Quarry (Eugui, Navarre), where 260 kt of magnesite was produced in 2020 (Magnesitas Navarras, n.d.). El Valle Boinás and Carlés gold-copper-silver mines in Asturias host ore deposits within limestone units and associated calcic skarns (Mining Data Online, n.d.-a).

#### 4.3. Slags

There is scope for targeted enhanced weathering and mineral carbonation efforts with metal refinery and iron and steelmaking by-products, collectively known here as slag materials (Huijgen et al., 2005; Mayes et al., 2008, 2018; Renforth et al., 2011; Renforth, 2012, 2019; Vaughan, 2022). Through conventional refining and steelmaking processes, the production of glassy, granular slag by-products can show enrichment of Mg and Ca-rich silicate, oxide and hydroxide minerals (Renforth, 2012). These residues, which include multi-stage developed furnace slags, constitute a low-cost feedstock of potentially high reactivity (due to its glassy nature). Furthermore, they are created in close proximity to massive CO<sub>2</sub> point sources and can be therefore utilized for CDR without the need for additional mining, transportation or consumption of raw materials (Huijgen et al., 2005).

Most major steelmaking operations are located on the northern coast of mainland Spain, particularly with several plants in Basque Country and two large plants in Asturias (Fig. 5). In 2020, Spain produced 11.14 Mt. of crude steel, representing 8 % of the total EU output for the year (EUROFER, n.d.). The Atlantic Copper metallurgical complex (Huelva, Andalucía) is a globally significant producer of copper, molybdenum and gold, and the San Juan de Nieva zinc smelter, one of the world's largest zinc producers, both generate high tonnages of resultant slag by-products during the smelting and concentration processes. Assuming slag residue production represents between 15 and 20 % of total steel production (Frías Rojas

et al., 2002), it is estimated here that approximately 1.7 to 2.2 Mt. of steel slag is produced annually in Spain. Some slag products associated with Spanish coal-fired power plants show a high enrichment of Fe and Al compared to Ca and Mg (e.g., ten slag samples analysed from the Andorra power plant of Teruel province, Aragón, by Querol et al., 1995; Llorens et al., 2001). This composition would likely limit their efficacy for geochemical CDR purposes, though their favourable physical nature, availability and accessibility still make them potentially useful resources for CDR.

#### 4.4. Fly ashes

Similar to other industrial waste products outlined here, fly ashes, derived from thermal power plants (Fig. 5), hold potential for utilization in geochemical CDR strategies (Ecke, 2003; Fernández-Jiménez and Palomo, 2003; Soong et al., 2006; Li et al., 2007; Montes-Hernandez et al., 2009; Muriithi et al., 2013; Dindi et al., 2019; Mustafa et al., 2020; Rausis et al., 2021). Fly ash is produced from coal combustion and is considered an environmental pollutant (Argiz et al., 2015; Querol et al., 1995; Llorens et al., 2001). However, fly ashes share similar favourable CDR properties as other industrial wastes, including a possible enrichment of Mg and Ca (Ecke, 2003; Fernández-Jiménez and Palomo, 2003; Li et al., 2007), and Ca-Mg-rich silicate minerals such as plagioclase, lime (CaO), bredigite (Ca<sub>1.7</sub>Mg<sub>0.3</sub>SiO<sub>4</sub>) and hatrurite (Ca<sub>3</sub>SiO<sub>5</sub>) (Querol et al., 1995). Fly ashes also feature fine grain sizes, including fractions within a range of 10–150 µm (Querol et al., 1995; Nyambura et al., 2011), favourable for higher surface area exposure and faster weathering reactions. Fly ash can also increase the pH of solutions to promote mineral carbonation (Liu and Mercedes Maroto-Valer, 2013).

Reported figures for annual fly ash generation from the energy sector of Spain from 2010 onwards range 2–5 Mt. (Argiz et al., 2015). At time of writing, there are still four active coal-fired power plants across Spain (Aboño, Soto de Ribera, Alcudia, and As Pontes; Fig. 5), with at least 17 more having ceased operations in the last decade to meet decarbonation targets (MITECO, 2020a). Those that still operate continue to produce fly ash, and even after closure and demolition, most former plant sites may have retained historic stockpiles of fly ashes accumulated over years of operation. The majority of operations (active, dormant or ceased) are concentrated on the coal mining regions of Asturias and northern Castile and León, with other plants are located in the northern regions of Galicia, Aragón, Cantabria and Basque Country (Fig. 5).

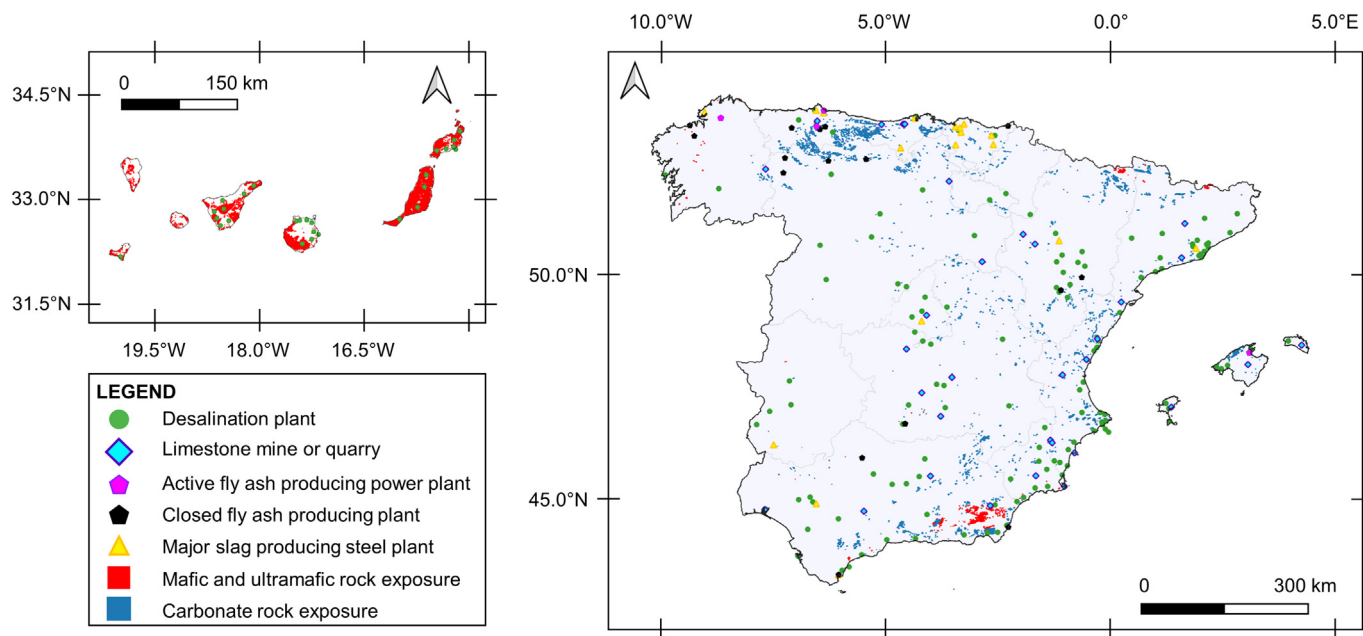


Fig. 5. Map of major by-product and waste-producing industrial sites and plants in Spain (data from EMODnet, n.d.; US Geological Survey, n.d.). Currently active fly ash producing power plants as of July 2022 (Aboño, Soto de Ribera, Alcudia, and As Pontes) are indicated.

#### 4.5. Ceramic wastes

Construction by-products include ceramic wastes generated by the tile producing sector in Spain, one of the largest European and global producers (Reig et al., 2014). Almost all of the ceramic tile industry of Spain is centred in the Castellón province of the Valencian Community. Ceramic waste may constitute up to 54 % of construction wastes, which totalled 32.7 Mt. in 2011 (Reig et al., 2014). An example of diopside-bearing ceramic tile waste, analysed by Mas et al. (2016), has a chemical composition including up to 12 wt% total MgO, CaO, Na<sub>2</sub>O and K<sub>2</sub>O.

#### 4.6. Desalination reject brines

Much like solid by-products generated from various extraction and processing operations, liquid desalination reject brines, the saline effluent by-product formed from seawater (and brackish water) separation at desalination plants, have been typically perceived as waste products of limited value. Attention has been paid to their detrimental effects to the local environment and ecological systems (Fernández-Torquemada et al., 2005; Zhou et al., 2013; Kossoff et al., 2014; García-Giménez and Jiménez-Ballesta, 2017). However, due to their alkaline-rich chemistry, waste reject brines can offer a substrate for CDR. One approach is to react Mg chloride in brines with CO<sub>2</sub> in the presence of ammonia to produce Mg-carbonates and additional ammonium chloride by-products. Another approach, through electrochemical, nanofiltration and multiple effect distillation processes, is to hydrolyse Mg and Ca chloride complexes to form MgO and CaO (with alkalinity returned to seawater), with hydrochloric acid (HCl) produced and separated (acidity removed). This separation of alkalinity and acidity promotes additional oceanic CO<sub>2</sub> drawdown. The HCl product can either be sold as an inorganic chemical commodity or neutralized via geological disposal for safe return to the ocean. The process may incorporate suitable geological materials such as peridotite, basalt and limestone to neutralise acidic by-products (House et al., 2007; Rau, 2008; Davies, 2015; Ihsanullah et al., 2021; Mourad et al., 2022; Mustafa et al., 2020). Pathways of geological disposal may include in-situ injection or circulation in favourable bedrock (Section 2) or in controlled ex-situ reaction settings with crushed and processed rocks and materials (Sections 3.1–3.5). Any excess alkalinity produced and released in the ocean could lead to additional CO<sub>2</sub> drawdown.

Spain hosts 5.7 % of total global desalination plants, more than half of all plants in Europe (Jones et al., 2019; Zarza and Novo, n.d.). The industry as a whole is expected to intensify in the future, with desalination outputs rising at a rate of ~10 % each year (Davies, 2015), while in Spain, increases in population, tourism and agriculture have led to the national growth of the sector (Hernández-Sánchez et al., 2017). Across 765 desalination plants (key localities shown in Fig. 5; EMODnet Data Services), Spain produces approximately 5 million m<sup>3</sup>/day of desalinated water for human supply, irrigation, and industrial use (Aedyr, n.d.). The resulting hypersaline reject brine effluents are typically disposed of in the ocean. According to the study by Jones et al. (2019), Spain produces 1.01 million m<sup>3</sup> of reject brine per day or 369 million m<sup>3</sup>/year. Assuming 10 % output growth each year (Davies, 2015) and equal growth of waste brine production, this may have increased to ~534 million m<sup>3</sup>/year by 2022. In terms of geographic distribution, Spanish desalination plants are heavily concentrated along the Mediterranean coast of the mainland, particularly in areas of Barcelona, Valencia, Alicante and Murcia, and on the Canary Islands of Tenerife, Gran Canaria, Fuerteventura and Lanzarote (Fig. 5). There are comparatively fewer plants near the northern mainland coast.

### 5. Preliminary assessment of geochemical CDR potential

#### 5.1. Silicate rocks and industrial materials

Overall, the average E<sub>pot</sub> value across all data points of Spain is 395 g CO<sub>2</sub>/kg, and C<sub>pot</sub> 244 g CO<sub>2</sub>/kg (n = 373; Fig. 6). The highest rock values are attributed to peridotites, harzburgites and serpentinites of Galicia, the Ronda peridotite massif and Cerro del Almiraz ultramafic massif. Due to

the generally high (>30 wt%) MgO contents, ultramafic rocks show high E<sub>pot</sub> and C<sub>pot</sub> values, with an average E<sub>pot</sub> of 543 kgCO<sub>2</sub>/t (C<sub>pot</sub> average 350 kgCO<sub>2</sub>/t) (n = 91; geochemical data derived from Chi-Yeung, 1972; Crespo and Lunar, 1997; Contini et al., 1993; Santos et al., 2002; Piña et al., 2006, 2012; Tornos et al., 2006; Marchesi et al., 2013). The highest values correspond to peridotites from the Ronda peridotite massif (Chi-Yeung, 1972) and harzburgites from the Cerro del Almiraz ultramafic massif (Marchesi et al., 2013), both in southern Spain, with other notably high values for dunites and harzburgites of Cabo Ortegal, Galicia (Santos et al., 2002). Serpentine E<sub>pot</sub> values range from 594 to 688 kgCO<sub>2</sub>/t, with an average value of 627 kgCO<sub>2</sub>/t (C<sub>pot</sub> range: 395–457 kgCO<sub>2</sub>/t; C<sub>pot</sub> average: 417 kgCO<sub>2</sub>/t; n = 29; data from Pereira et al., 2008; Marchesi et al., 2013). By contrast, metamorphic rocks of mafic protoliths and more variable grades show an E<sub>pot</sub> value range of 140 to 394 kgCO<sub>2</sub>/t (average 237 kgCO<sub>2</sub>/t) and C<sub>pot</sub> range of 31–262 kgCO<sub>2</sub>/t (average: 136 kgCO<sub>2</sub>/t; n = 29; data from Hobson et al., 1998; Barbero and Villaseca, 2000; Esteban et al., 2007; Rodríguez et al., 2020).

The calculated E<sub>pot</sub> and C<sub>pot</sub> values (Fig. 6) provide a theoretical indication of total maximum potential of rocks and solid waste materials suitable for geochemical CDR; however, these values do not account for mineral kinetics, which govern the timescales on which mineral dissolution can be achieved. The shrinking core model applied in this study aims to account for variations in modal mineralogy and across rock types selected based on (1) their considered geochemical potential and (2) their volumetric abundance across Spain (Table 3 and Fig. 7). Results here give a baseline indicator of how variations within and across rocks can affect achievable CDR (Fig. 7).

While chemical potential indicated by E<sub>pot</sub> and C<sub>pot</sub> values may be high for the selected rock types, only a fraction of the maximum CDR can realistically be realized under ambient or non-optimized reaction conditions for CDR (Fig. 7, Table 3 and Table S11). For the first year of weathering, all rocks with favourable geochemistry and mineralogy generally achieve αCDR of <1 kt of CO<sub>2</sub> (ktCO<sub>2</sub>) as alkalinity generation and mineral carbonation, with the exception of Ronda peridotite rocks which may remove 1.4–2.5 ktCO<sub>2</sub> as alkalinity, or 0.9–1.6 ktCO<sub>2</sub> as carbonate precipitation (Table 3). This represents <0.5 % of the maximum capacity indicated by E<sub>pot</sub> and C<sub>pot</sub> values. Ronda peridotites, along with Nevado-Filábride Complex serpentinites, show the highest potential for geochemical CDR, reaching 166–288 ktCO<sub>2</sub> (αCDR) over 70 years of weathering as alkalinity (up to 40 % of maximum achievable CDR, with variations relating to differences in modal mineralogy within peridotites; Fig. 7 and Tables S11–3), or 120–193 ktCO<sub>2</sub> via carbonation for Ronda peridotite, and 40–175 ktCO<sub>2</sub> as alkalinity (up to 27 % of maximum achievable CDR; Fig. 7) and 27–117 ktCO<sub>2</sub> via carbonation for serpentinites. These ultramafic rocks generally contain more serpentine, olivine (forsterite), talc and clinopyroxene (augite, diopside) than more mafic rocks such as pyroxenites, gabbros and basalts, which contain more orthopyroxene (enstatite), clinocllore, amphibole (hornblende, tremolite-actinolite) and plagioclase (anorthite, albite). The majority of targetable rocks show >1 Mt. tCDR potential over 70 years of weathering of accumulated weathered material (i.e., with 1 Mt. feedstock added each year). In the case of the Ronda peridotite, this value is as high as 11 Mt. for alkalinity generation.

As an additional indicator of geochemical CDR (in this case, specifically mineral carbonation) potential of each material, PHREEQC modelling has been applied to suggest which, if any, carbonates could precipitate from a CO<sub>2</sub>-rich (90 %) solution, based on the range of modal mineralogies for each rock type used in the shrinking core model. Once again, Ronda peridotites are shown to be highly promising for geochemical CDR via carbonation, potentially precipitating aragonite (CaCO<sub>3</sub>), calcite (CaCO<sub>3</sub>), dolomite (CaMg(CO<sub>3</sub>)<sub>2</sub>), huntite (CaMg<sub>3</sub>(CO<sub>3</sub>)<sub>4</sub>), hydromagnesite (Mg<sub>5</sub>(CO<sub>3</sub>)<sub>4</sub>(OH)<sub>2</sub>·4(H<sub>2</sub>O)), magnesite (MgCO<sub>3</sub>) and nesquehonite (Mg(HCO<sub>3</sub>)(OH)·2(H<sub>2</sub>O)) across the modal mineralogical variations. Basalts have more limited carbonation potential, with no carbonates predicted to precipitate, suggesting alkalinity generation would be the most viable option for pursuit with these materials as a feedstock. Fly ashes and slags containing low amounts of Ca- and Mg-bearing minerals from Spanish power stations and refineries show similar limited abilities to produce carbonates, though

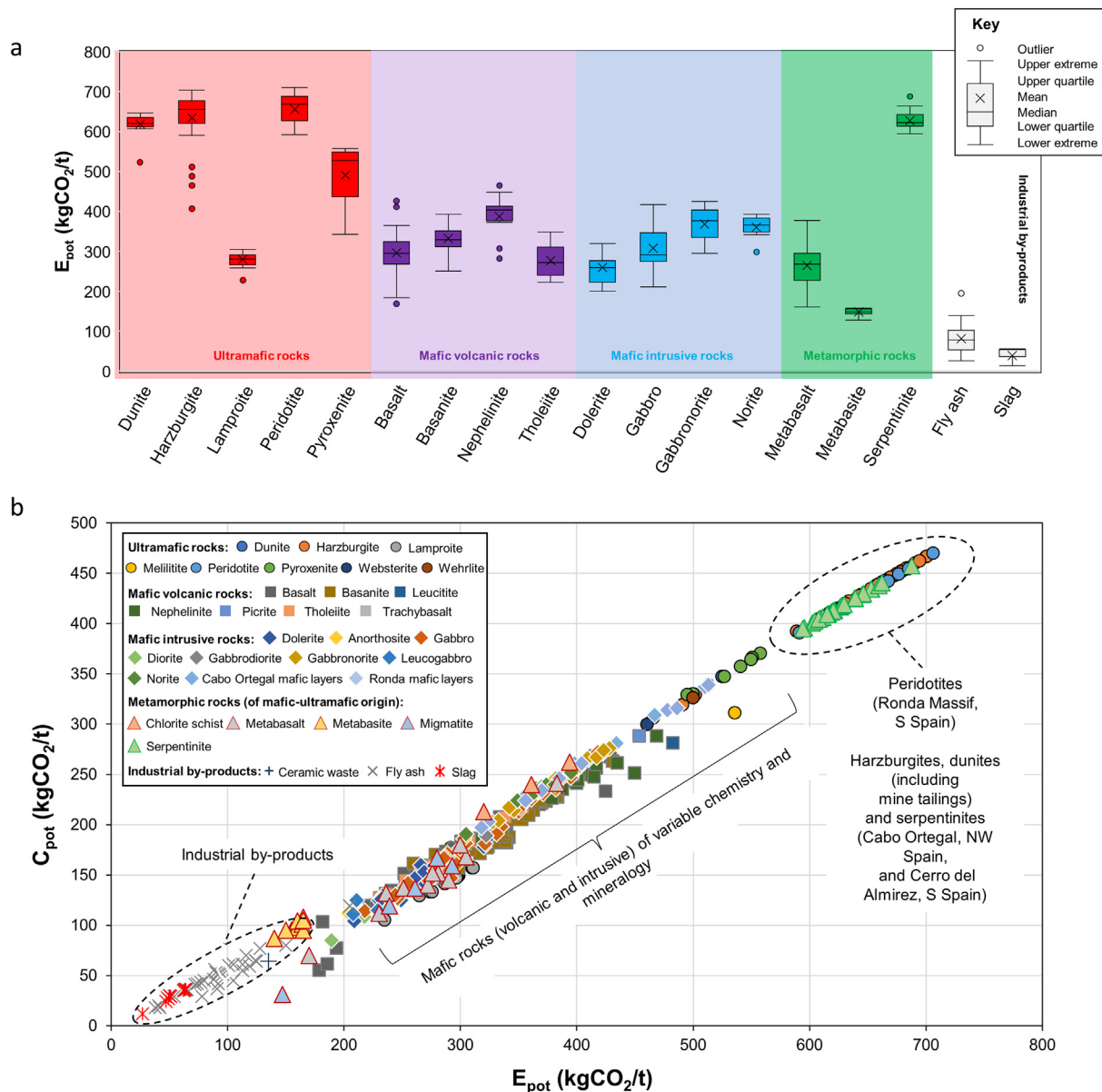


Fig. 6. Enhanced weathering potential ( $E_{pot}$ ) of (a) select grouped suitable (mafic and ultramafic rocks) rocks, derived mine wastes and other industrial by-products present in Spain, and (b)  $E_{pot}$  and mineral carbonation potential ( $C_{pot}$ ) of different mafic and ultramafic rocks and industrial by-products hosted across Spain. Data for calculations derived from sources presented in Table S11.

literature examples of Polish, Chinese and Australian fly ashes (Jaschik et al., 2016; Ji et al., 2019), which may contain trace amounts of plagioclase, lime, portlandite, periclase, clinopyroxene and brucite, do indicate potential for carbonate precipitation. Phases such as brucite ( $Mg(OH)_2$ ), periclase ( $MgO$ ), portlandite ( $Ca(OH)_2$ ) and lime ( $CaO$ ) can act as alkalinity sources (Roadcap et al., 2006, 2015; Riley and Mayes, 2015; Khudhur et al., 2022), and can undergo 100 % dissolution in less than a decade, even under ambient or near-ambient conditions. The presence of these reactive Mg- and Ca-bearing phases is vital for fly ash and slag CDR suitability, as these materials generally contain abundant unreactive phases (with respect to  $CO_2$ ), or are predominantly comprised of amorphous glass of variable reactivity depending on the composition (for instance, these may typically be aluminosilicate glass, and thus not highly appropriate for CDR).

### 5.2. Carbonate rocks and industrial materials

It has been proposed that to remove 1 Gt  $CO_2$  from the atmosphere, ~1.8 Gt of limestone is required to produce ~0.7 Gt of lime, with

consideration paid to energy expenses from mining, grinding and distribution (Renforth et al., 2013). Applying this conversion with the same excavation assumptions as Section 2.1 (depth 5 m, density  $2.5 t/m^3$ ), up to 137 Gt of limestone extraction would achieve a maximum of 76 Gt of CDR in Spain. In reality, carbonate availability for any proposed geochemical CDR scheme is unlikely to be the limiting factor for large-scale implementation due to the widespread occurrences of carbonates across Spain. Though the societal, energetic and engineering constraints make this theoretical maximum unobtainable, if even a fraction of this potential can be realized, the contribution would be substantial. Assuming that 1.8 t of carbonate can sequester 1 t of  $CO_2$  (Renforth et al., 2013), this equates to a maximum of ~0.7 Mt $CO_2$  per year from carbonate mine waste fines produced in Spain. As previously stated, carbonate mine wastes are similarly voluminous, likely beyond estimations made here based on available data. Spain hosts hundreds of active, inactive and historic limestone and dolostone quarries, though publicly available information on their localities and current/previous production figures is generally lacking.

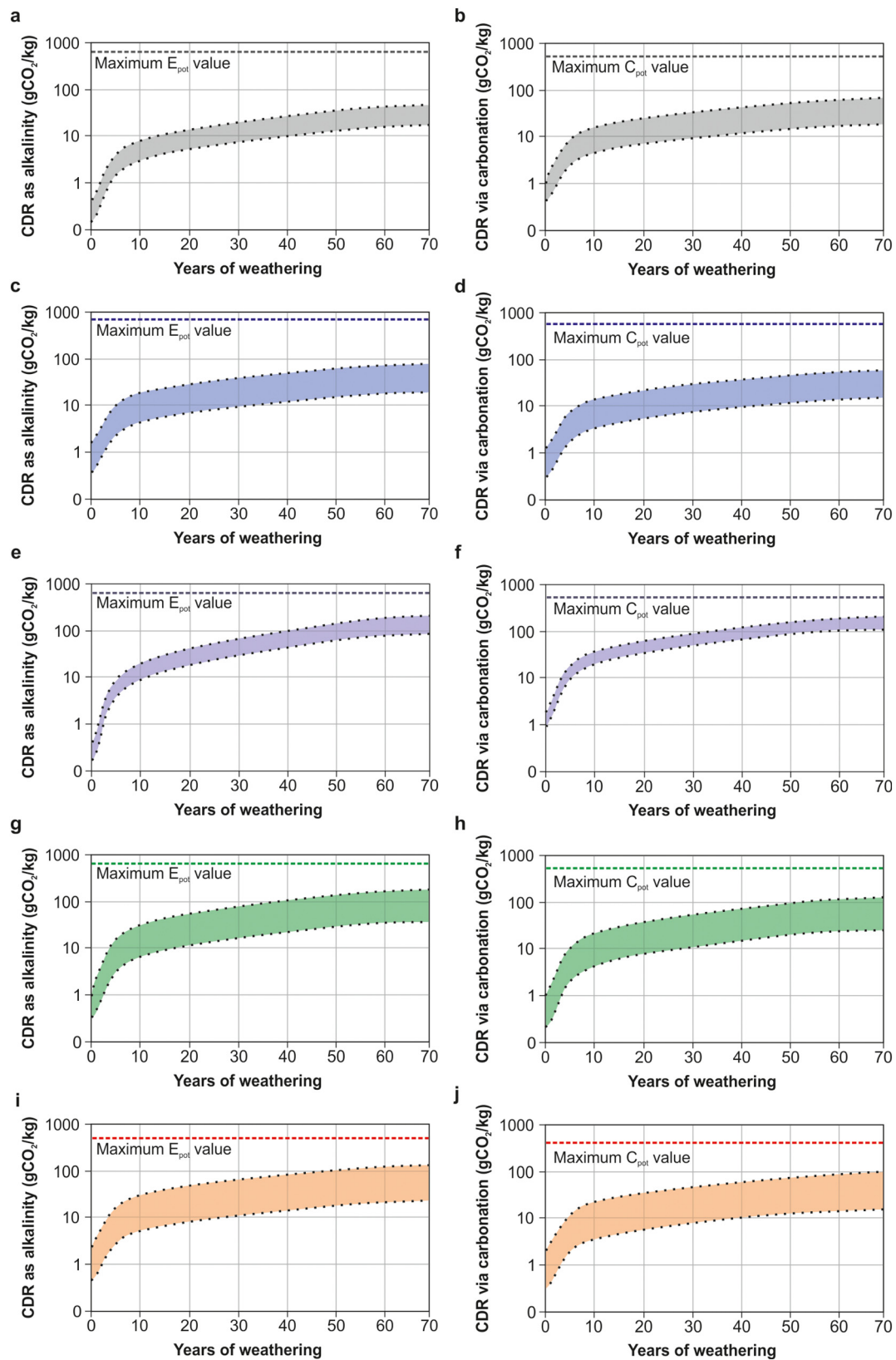


Fig. 7. Cumulative CDR potential (sCDR) by alkalinity production and carbonation of 1 kg of a given material for a weathering time duration between 0 and 70 years for select rock types in Spain: (a-b) dunites of Galicia, (c-d) pyroxenites of Galicia, (e-f) serpentinites of the Nevado-Filábride Complex, and (g-h) serpentinites of the Nevado-Filábride Complex, and (i-j) basalts of the Canary Islands. Maximum  $E_{pot}$  and  $C_{pot}$  values also shown by dashed lines. Shaded areas between dotted lines indicate variations in sCDR relating to variations in modal mineralogies for a given rock type. Sources from Table S11; see Table S12–3 for data.

### 5.3. Desalination brines

There are numerous studies that present concentrations of elements of CDR interest (i.e.,  $\text{Ca}^{2+}$ ,  $\text{Mg}^{2+}$ ,  $\text{K}^+$ ,  $\text{Na}^+$ ) in desalination reject brines collected within Spain (e.g., Casas et al., 2011, 2012, 2014; Reig et al., 2014, 2016b, a; Mountadar et al., 2017; Sanmartino Rodríguez, 2018; Sola et al., 2020; Jiménez-Arias et al., 2022), as well as global studies (e.g., Mabrook, 1994; Ahmed et al., 2003; Korngold et al., 2009; Martinetti et al., 2009; Hajbi et al., 2010; Ji et al., 2010; Macedonio et al., 2011; Kasedde et al., 2014; Katal et al., 2016; Pramanik et al., 2017; Dong et al., 2018; Mohammad et al., 2019). From these available datasets, an average concentration (in mg/L) can be derived for both Spain ( $n = 17$ ) and the rest of the world ( $n = 60$ ). On average, Spanish reject brines generally contain more  $\text{Ca}^{2+}$  (866 mg/L),  $\text{Mg}^{2+}$  (2300 mg/L),  $\text{K}^+$  (2259 mg/L) and  $\text{Na}^+$  (24,365 mg/L) concentrations than average global values (842, 1423, 1225 and 14,300 mg/L respectively, averaged across data from references given above), with an overall average of 29,780 mg/L total elements of interest compared to 17,789 mg/L. Samples from Almería and Valencia (the latter derived from brackish waters) contain notably high  $\text{Ca}^{2+}$ , up to 1828 mg/L (Pérez-González et al., 2015) and 1250 mg/L (Mountadar et al., 2017) respectively. Samples from Barcelona show high  $\text{Mg}^{2+}$  (up to 5490 mg/L),  $\text{K}^+$  (up to 14,970 mg/L) and  $\text{Na}^+$  (up to 88,660 mg/L; Casas et al., 2014).

Using these average concentrations as representative for Spanish brines and assuming an annual brine production of 369 million  $\text{m}^3/\text{year}$  (Jones et al., 2019), it is possible to estimate how much Mg and Ca are theoretically produced in reject brines per year. These values would produce ~848 million kg of Mg and ~319 million kg of Ca annually. In oxide form, this constitutes ~1.5 Mt. MgO and ~0.5 Mt. CaO. Assuming that 1 kg of MgO can react with 1.1 kg of  $\text{CO}_2$  to form solid magnesite (Mg-carbonate;  $\text{MgCO}_3$ ), and 1 kg of CaO can react with 0.79 kg of  $\text{CO}_2$  to form calcite ( $\text{CaCO}_3$ ) (Tomsich et al., 2015), these tonnages could remove a maximum of 1.7 Mt $\text{CO}_2$  in the form  $\text{MgCO}_3$ , and 0.4 Mt $\text{CO}_2$  in  $\text{CaCO}_3$ , giving a total maximum CDR of 2.1 Mt $\text{CO}_2$ . As this is in the solid carbonate form, it assumes that some of the  $\text{CO}_2$  were returned during precipitation (Eq. (3)). If products are in the alkalinity form, ~2.3 Mt $\text{CO}_2$  could be removed as Mg-bicarbonate ( $\text{Mg}(\text{HCO}_3)_2$ ), and ~0.6 Mt. as Ca-bicarbonate ( $\text{Ca}(\text{HCO}_3)_2$ ), giving ~3.1 Mt $\text{CO}_2$ . These CDR estimates may be higher by including  $\text{Na}^+$  and  $\text{K}^+$  as possible bicarbonate and carbonate producers with  $\text{CO}_2$ . Considering kinetics and reaction times, the deliberate production of magnesium hydroxide ( $\text{Mg}(\text{OH})_2$ ) and calcic equivalents in place of MgO and CaO from reject brines may be a favoured route to pursue geochemical CDR. This feature is because these phases require less time and energy for processing/recovery and also for subsequent reaction times with  $\text{CO}_2$  to produce bicarbonate and carbonate, as  $\text{Mg}(\text{OH})_2$  and  $\text{Ca}(\text{OH})_2$  (synthesized or in their natural forms, brucite and portlandite respectively) are faster reactants than their oxide equivalents (Fagerlund and Zevenhoven, 2011; Scott et al., 2021).

## 6. Discussion

### 6.1. Geochemical CDR potential in Spain

Ultramafic rocks such as dunite, harzburgite, peridotite, serpentinite and pyroxenite, and mafic rocks such as gabbro and basalt, all hosted across Spain, are considered the most viable material options for use in targeted geochemical CDR strategies. Furthermore, carbonate rocks could also be targeted for specific alkalinity generation strategies. For both silicate and carbonate rocks, their industrial waste derivatives, such as mine tailings, fly ashes and slag materials, can also be targeted, particularly due to their generally fine-grained nature, ideal for ex-situ CDR strategies. Desalination brines may also offer a CDR route in coast-proximal areas.

Estimates made in this work suggest that a maximum of 7.7 Mt. of  $\text{CO}_2$  per year could be removed from annually produced industrial alkaline wastes and by-products across Spain (Table 2). There is also a possible 6.03 Mt $\text{CO}_2$  that could be removed from available stockpiled materials,

giving a total maximum geochemical CDR capacity of 13.04 Mt. from the utilization of by-products, roughly equivalent to all GHGs emitted by the waste management sector of Spain (Tiseo, 2022). The national annual  $\text{CO}_2$  emissions as of 2020 for Spain were 209 Mt. (Ritchie et al., 2020), meaning this maximum capacity would have the potential to offset ~6 % of Spanish emissions. However, these calculations do not consider the kinetic properties of the materials that are being subject to weathering, meaning only a fraction (on average, roughly 12 % over 70 years of weathering) of the overall potential could be achieved without efforts to speed up dissolution and  $\text{CO}_2$  reactions. Shrinking core modelling highlights the importance of optimizing the grain size of the feedstock, and exploring methods to increase the dissolution rates of Ca- and Mg-containing minerals for cation release and reactions with  $\text{CO}_2$ . This is particularly pertinent for rocks containing abundant plagioclase and pyroxene, such as basalt, gabbro and gabbro-norite, which are generally slower to react compared to serpentine and olivine-rich dunites, peridotites and serpentinites (Gadikota et al., 2020; Kelemen et al., 2011, 2020). Methods to improve the dissolution rate, such as promoting reactions in lower pH solutions, coupled with grinding materials to smaller particle size, may greatly increase CDR for geochemically-suitable materials such as mafic and ultramafic rocks (Bullock et al., 2022). For energy intensive and costly approaches such as material grinding, the addition of renewable energy sources to limit costs and additional GHG emissions would be greatly beneficial to Spain. In 2021, Spain generated the second highest amount of electricity using wind and solar power, including photovoltaic and thermal power, in Europe according to European association for the cooperation of transmission system operators (ENTSO-E1) data, suggesting the country is well positioned to incorporate such energy sources into any future CDR strategies.

Though rocks such as basalt are slower reacting, and therefore less susceptible to undergo complete or near-complete dissolution on sufficient timescales at near-ambient conditions, they are not ruled out for CDR purposes, as they have proven to be suitable feedstocks for ex-situ enhanced weathering (alkalinity generation) approaches such as agricultural spreading of crushed materials (Taylor et al., 2016; Andrews and Taylor, 2019; Beerling et al., 2020; Kelland et al., 2020; Smet et al., 2021; Cipolla et al., 2022; Table 4). Some basalts may also contain abundant amorphous glassy phases, which may react similarly to, or even more rapidly than, olivine (Gislason and Oelkers, 2003; Kelemen et al., 2011, 2020). This approach is also likely to achieve co-benefits such as increased crop yields, lower agricultural lime usage (thus reducing lime-associated  $\text{CO}_2$  emissions), reduction in toxicity associated through increased silicon accumulation and K, P and Ca uptake (Gillman et al., 2002; Rinder and von Hagke, 2021). These added benefits, coupled with the reduced safety risk with basalt usage compared to potential asbestos, Ni and Cr-hosting rocks such as dunites and serpentinites, can also aid with public acceptance for implementation, particularly as field spreading would likely not impose any additional physical footprint on the land. Discrepancies between laboratory-derived and field-derived dissolution rates and CDR (e.g., Gruber et al., 2014; Buckingham et al., 2022), particularly with multiphase materials such as basalt, mean that further field experiments are needed to elucidate the effects of local soil systems,  $\text{SiO}_2$  polymerization, water flux and secondary mineral formation (Buckingham et al., 2022).

Simulations of dissolution and precipitation in  $\text{CO}_2$ -rich solutions also indicate the potential for carbonate mineral precipitation in the majority of the identified mafic and ultramafic rocks of Spain, particularly in peridotites (e.g., of the Ronda Massif), serpentinites (e.g., of the Nevado-Filábride Complex), dunites (e.g., of Cabo Ortegal, Galicia) and wehrlites (e.g., of Aguablanca, Badajoz). Therefore, these rocks may be highly suitable for in-situ and ex-situ approaches that target mineral carbonation. However, it should be considered that precipitation of some carbonates is kinetically inhibited at the Earth's surface (Hänchen et al., 2008; Saldi et al., 2010, 2012; Haug et al., 2011; Power et al., 2013; Li et al., 2018). This may not be an issue for in-situ approaches, where fluids can be trapped and maintained for reactions to take place over long time periods, but may not be suitable for ex-situ approaches under ambient conditions. As such, feedstocks may require additional support to permit mineral carbonation in a

**Table 2**  
Potentially suitable rocks and materials for geochemical CDR strategies in Spain, their key localities, maximum removal potential and evaluation of their possible methods and applications.

Material targeted	Key localities	Coverage or availability of materials	Targetable method examples for CDR	Assumptions and considerations for implementation
Mafic and ultramafic bedrock	Canary Islands; Galicia; Murcia; Andalucía; Extremadura Key targets may include Ronda peridotite massif of southern Spain, Cabo Ortegal (Galicia) and basaltic lavas of the Canary Islands	13,744 km <sup>2</sup> of land coverage	In-situ mineralization – injection of CO <sub>2</sub> -rich gas or fluid into bedrock for CO <sub>2</sub> mineralization (mineral carbonation) Ex-situ enhanced weathering and mineral carbonation – field-based spreading or reactor-based techniques	Variable extent of alteration, whole rock geochemistry and mineralogy within and across units needs to be investigated for any site of interest Any extraction could require blasting, crushing, grinding and additional energy-intensive processing methods Utilization of natural bedrock may lack public support and acceptance Induced seismicity requires stringent monitoring Rock requires extraction and pre-treatment for suitable ocean liming approaches
Carbonate bedrock	Asturias; Cantabria; Basque Country; Catalonia; Valencian Community; Murcia; Castilla-La Mancha; Balearic Islands	109,474 km <sup>2</sup> of land coverage	Ocean liming and ocean alkalinity enhancement – spreading or reacting material with seawater to increase alkalinity Enhanced weathering – field-based spreading or reactor-based techniques	Carbonation needs to be suppressed to eliminate risk of CO <sub>2</sub> return to atmosphere and no net intake Any additional crushing, grinding or milling, and transport and distribution, must be considered for net CDR evaluation Based only on limited site examples of publicly available production tonnages Does not assume any contribution from basalt quarry wastes, as these additional tonnages from basalt mining are difficult to ascertain Methods to speed up dissolution kinetics of minerals may be required Liberation of other elements to the environment needs to be monitored Alkalinity release into rivers and ocean requires further fundamental understanding, as well as monitoring and regulations Any additional crushing, grinding or milling, and transport and distribution, must be considered for net CDR evaluation Based only on limited public information for limestone, dolomite and marble production (2012 production figure; IGME, 2012). Available tonnages likely to be much higher.
Silicate mine tailings	Galicia; Andalucía; Extremadura; Canary Islands	10's of Mt. produced annually	Enhanced weathering and mineral carbonation – field-based spreading or reactor-based techniques	Rock pre-treatment (calcination) may be required for suitable ocean liming approaches Limited spatial flux of alkalinity, lower CDR and fewer added benefits compared to silicate rocks and wastes for enhanced weathering Alkalinity release into ocean requires further study Any additional crushing, grinding or milling, and transport and distribution, must be considered for net CDR evaluation Based on 11.14 Mt. crude steel production (EUROFER, n.d.), with slag representing 15–20 % of total steel production (Frías Rojas et al., 2002) Potentially low Ca and Mg content in some slags May require additional grinding (financial and energy/CO <sub>2</sub> emission penalties) Liberation of other elements to the environment needs to be monitored Any additional crushing, grinding or milling, and transport and distribution, must be considered for net CDR evaluation Based on fly ash production of 2–5 Mt. per year, and uses cited geochemical data from 18 power plants as a proxy for all fly ashes (Argiz et al., 2015) Potentially low Ca and Mg content in some fly ashes Liberation of other elements to the environment needs to be monitored Any additional crushing, grinding or milling, and transport and distribution, must be considered for net CDR evaluation Potentially low Ca and Mg content May require additional grinding. Liberation of other elements to the environment needs to be monitored Any additional crushing, grinding or milling, and transport and distribution, must be considered for net CDR evaluation Based on 369 million m <sup>3</sup> reject brine production per year, with annual 10 % output growth (Davies, 2015; Jones et al., 2019) HCl by-product requires storage (for re-use or sale) or treatment (e.g., neutralization with alkaline-rich materials such as tailings, slags, or fly ashes) Chlorine production without cation bonds needs to be avoided to prevent CO <sub>2</sub> outgassing
Carbonate mine tailings	Asturias; Cantabria; Basque Country; Valencian Community; Murcia; Catalonia; Balearic Islands	10's of Mt. produced annually	Ocean liming and ocean alkalinity enhancement – spreading or reacting material with seawater to increase alkalinity Enhanced weathering – field-based spreading or reactor-based techniques	
Slag by-products	Basque Country; Asturias	Up to ~3 Mt. produced per year	Enhanced weathering and mineral carbonation – field-based spreading or reactor-based techniques	
Fly ashes	Asturias; Galicia; Aragón	Up to ~5 Mt. produced per year	Enhanced weathering and mineral carbonation – field-based spreading or reactor-based techniques	
Ceramic wastes	Valencian Community	Up to ~20 Mt. produced per year	Enhanced weathering and mineral carbonation – field-based spreading or reactor-based techniques	
Desalination brines	Canary Islands; Valencian Community; Murcia; Catalonia	Up ~300–500 million m <sup>3</sup> produced per year	Electrochemical, nanofiltration and multiple effect distillation processes – seawater splitting to yield MgO and CaO to increase alkalinity	

given reaction setting, if carbonation is hindered. This may be the case for Mg-carbonates (e.g., magnesite), whereby precipitation can be 4 to 6 orders of magnitude slower than precipitation of Ca-carbonates (e.g., calcite) at 25 °C (Giammar et al., 2005; Morse et al., 2007; Hänchen et al., 2008; Saldi et al., 2009; Power et al., 2013). Feedstocks such as dunites and harzburgites in Galicia and Aguablanca are predicted to only precipitate magnesite, huntite and dolomite. The formation of these Mg-carbonates from their respective feedstocks may require additional conditions, such as increasing temperature, pH, presence of ligands and microbial mediation (Power et al., 2013; Li et al., 2018).

By contrast, metastable hydrated Mg-carbonate minerals may still precipitate at ambient temperatures and pressures, particularly associated with brucite and serpentine mineral weathering processes (O'Neil and Barnes, 1971; Wilson et al., 2009; Power et al., 2014). For instance, Li et al. (2018) state that kinetic reactions are fast enough that there is generally no need for acceleration, particularly for nesquehonite. Hydromagnesite has also been shown to precipitate in ambient settings such as at the Woodsreef asbestos mine (Oskierski et al., 2013) and Mount Keith nickel mine (Wilson et al., 2014) in Australia, considered to be triggered by significant evaporation in the natural environment. Similar observations were also made at the Diavik diamond mine and Clinton Creek asbestos mine, Canada (Power et al., 2013).

Should induced mineral carbonation be required, it has been suggested that mineral buffering under high  $p\text{CO}_2$  conditions can allow for carbonate precipitation (Power et al., 2013, also indicated here by PHREEQC modelling). Elevated dissolved inorganic carbon (DIC) may also promote carbonate precipitation (Harrison et al., 2013), while increasing the temperature has also been shown to speed up precipitation (Giammar et al., 2005; Morse et al., 2007; Sipilä et al., 2008; Casas et al., 2011; Harrison et al., 2013; Power et al., 2013). One method with particular relevance to possible future ex-situ methods in Spain, where increased  $p\text{CO}_2$ , DIC and temperature may not be achievable without significant associated costs and emissions, is precipitation acceleration through microbial mediation. The aforementioned examples of secondary carbonate precipitation at various Ni, asbestos and diamond mines are typically associated with microbialites that naturally thrive at these sites (Power et al., 2013; Li et al., 2018). Such a biological approach may be utilized at low cost and low energy, and by-products such as biomass can be harvested as biofuel (Li et al., 2018). These may prove viable options for any implemented ex-situ CDR schemes at sites in Spain such as Landoy and Aguablanca.

## 6.2. In-situ and ex-situ CDR implementation opportunities

As stressed throughout this study, only a fraction of this total CDR potential may be realistically achieved through any implemented measures. The aim here is to highlight the areas of the highest potential, both through chemical (high Ca and Mg), mineralogical (kinetically-favourable) and physical suitability (high surface areas, capability to mobilise materials), and high practicality (accessibility) of available materials. In terms of chemical favourability for optimal removal capacity, areas of extensive ultramafic rocks, serpentinites and mafic extrusive rocks provide the best opportunities for successful CDR implementation. These rocks outcrop across areas of Galicia, Canary Islands, Murcia and Andalucía (Fig. 8), with promising preliminary results demonstrated for the Ronda peridotite massif, the Nevado-Filábride Complex, the mining regions of Cabo Ortegal, Galicia, and extensive lava exposures of the Canary Islands. Fine grained (crushed) rocks such as those produced from mine sites in Galicia and Extremadura, and industrial by-products generated across regions of northern mainland Spain (Asturias, Cantabria and Basque Country; Fig. 8), have inherently favourable physical properties for CDR, with greater availability of reactive surface areas for faster reaction rates than in-situ bedrock (Bullock et al., 2022). These areas can be considered the highest priority in geochemical CDR potential and should be the primary targets in future CDR implementation projects. As well as suitability of feedstock, for each targeted in-situ and ex-situ method and implementation site, considerations need to be paid to both the energy penalty (and associated  $\text{CO}_2$  emissions)

and financial cost. If, following a life cycle analysis (LCA), a method is not considered financially viable, with costs far outweighing any potential carbon value or additional financial benefits achieved, or potential GHG emissions produced make the CDR achieved through geochemical methods negligible or net positive, other approaches need to be considered. Any LCA should be made on a site-by-site basis and include the cost and energy penalty associated with mining, crushing, and grinding, transport, distribution and method execution, and the possibilities to incorporate renewable energy sources into any proposed methods of implementation.

Based on the suitable materials hosted and the national (and global) necessity for large-scale CDR, two of the more straightforward routes for CDR implementation in Spain arise (Table 2): (1) projects and strategies aimed at geochemical CDR through the use of readily available and physically favourable mine tailings and other industrial alkaline wastes, and (2) projects and strategies aimed at improving understanding of the potential for in-situ and ex-situ strategies with suitable undisturbed rock formations.

### 6.2.1. Mine wastes and other industrial by-products for ex-situ CDR

Using ground-down alkaline wastes offers a promising “low-hanging fruit” option for Spain in terms of rapid implementation (practical accessibility), relatively low cost, low energy requirements, the potential for co-benefits and multiple available strategies to pursue. This scenario is appropriate for mine tailings derived from mafic and ultramafic rocks, which exhibit variably reactive minerals, such as olivine, serpentine and sporadic brucite. Compared to bedrock, mine tailings, typically finer than 200  $\mu\text{m}$  in mean grain size (Bullock et al., 2022), exhibit high reactive surface areas, reducing or removing the need for energy-intensive excavation and crushing and grinding. An additional benefit to using mine tailings includes their production on sites that are well-equipped to convey, transport and store high tonnages of these materials continuously. Such systems may be utilized for CDR strategies that could be adapted to fit within conventional mine tailings management and site wastewater treatment works. Carbonate-derived tailings, fly ashes, slags and ceramic wastes offer similar promise, with geochemical CDR routes by way of alkalinity production through enhanced weathering, mineral carbonation (excluding carbonate wastes) and ocean liming.

With those benefits in mind, the best opportunities for Spain to implement geochemical CDR strategies with mine tailings are in the mining regions of Galicia (Figs. 4-5 and 8), such as annually produced and historic stockpiles associated with olivine dunite extraction at the Landoy mine site, and proposed production (including overburden and tailings production) at the Touro copper project. Additionally, it may be possible to utilise annually produced and historic mine tailings associated with basalt quarrying across the Canary Islands. Similar potential may exist for using fly ash samples generated at coal-fired power plants in Asturias, which may produce high Ca and Mg contents. This is also the case for iron and steelmaking-generated slag by-products and ceramic waste materials. The glassy nature of slags is of particular interest, as the material may be susceptible to higher dissolution rates than crystalline equivalents due to inherent disruption to chemical bonds, reducing the effects of Si-rich layer development to hinder cation release (Perez et al., 2019). Glassy slags are produced across Spain (Fig. 5), but Asturias and Basque Country industrial regions likely provide abundant materials sources. Ceramic waste production is centred in the Valencian Community, where numerous carbonate quarries can also provide suitable materials for geochemical CDR. Coastal regions of Asturias, Cantabria, Valencian Community, Balearic Islands and Basque Country also host several active, inactive and abandoned limestone, dolostone and marble quarries (Figs. 4-5) containing significant tonnages of crushed up carbonate material for ocean alkalinity enhancement, ocean liming and enhanced weathering approaches.

### 6.2.2. Priority ex-situ implementation areas

The added benefit of utilizing alkaline wastes and industrial by-products in Spain is that key national land uses are highly suitable for launching strategies such as enhanced weathering and mineral carbonation on a rapid timescale (e.g., testing, planning and execution for

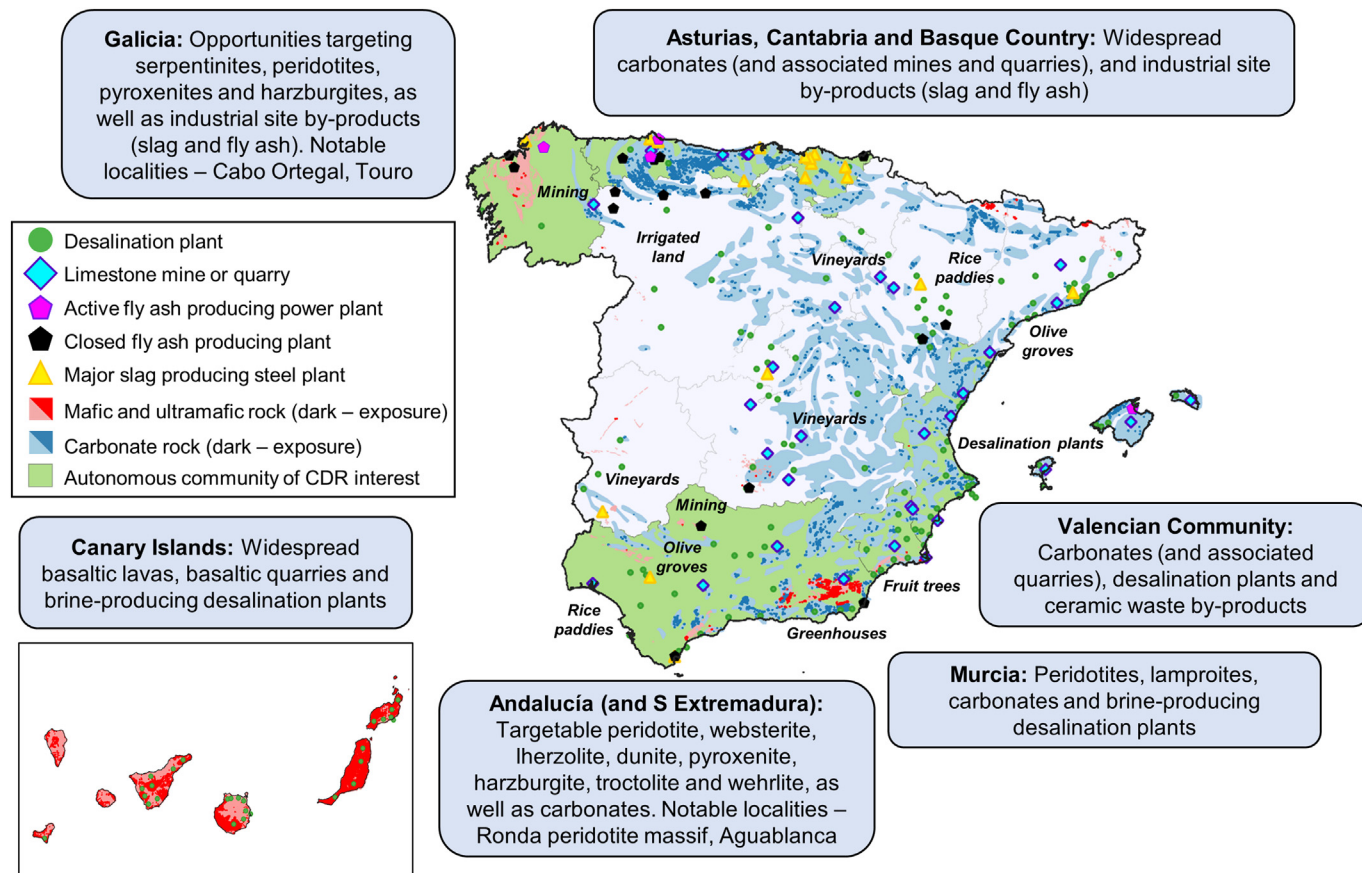


**Fig. 8.** Map highlighting targetable areas for geochemical CDR projects and approaches in Spain. Possible complementary land uses for ex-situ approaches (e.g., material spreading) are also highlighted.

commencement by 2030). For field-based methods of enhanced weathering and mineral carbonation, Spain has widespread areas of natural, industrial and agricultural land uses that could be adapted to host material spreading strategies (Table 4). Areas of routinely irrigated agricultural land, such as select croplands, rice fields, vineyards, olive trees and fruit plantations, hold the advantage of requiring the repetitive additions of water, which would also be a requirement to promote sufficiently fast  $\text{CO}_2$ -material reaction rates. Industrial areas such as mineral extraction sites could provide opportunities for both reactor-based and field-based approaches, with additional benefits to mine companies trying to achieve their own internal CDR targets, as well as positive impacts on waste management systems and public perception. Natural areas such as forests, grasslands, beaches, dunes and sandbanks may permit natural alkalinity generation and mineral carbonation. Still, reaction rates may be slow, verification of CDR may be challenging to obtain regularly, and consideration of environmental, economic, infrastructural and public health issues needs to be paid.

Spain's vast areas of agricultural and forested land are highly appropriate for strategies aimed at spreading fine materials for enhanced weathering, such as those being undertaken using powdered silicate rocks (typically basalt) applied over other global cropland localities (Taylor et al., 2016; Andrews and Taylor, 2019; Beerling et al., 2020; Kelland et al., 2020; Smet et al., 2021; Cipolla et al., 2022; Table 4). >52 % of Spain is occupied by agricultural land (265,666  $\text{km}^2$ ; WorldData.info, n.d.), with the only areas of limited agricultural land restricted to mountainous and desert regions. Approximately 20 % of total land use is occupied by non-irrigated arable land, with ~20 % taken by permanently irrigated land, olive groves, complex cultivation patterns and agroforestry areas (Table 4). Alkaline powders, such as crushed rock, mine tailings, and fly ashes, could be deployed on proximal (e.g., within mapped regions of suitable rock or close to industrial centres) croplands and amended with soils as a

geochemical CDR strategy, with reactions accelerated by the presence of plant roots and soil microbes.

Rocks and associated soils of mafic-ultramafic compositions are generally considered beneficial for fruit plantations, rice paddies, olive groves and vineyards globally due to their heat retention, promoting ripening, and high Fe, Mg and Ca contents. Silica release can also provide additional resistance to pests and diseases, improve water-use efficiency and increase crop yields (Edwards et al., 2017; Vicca et al., 2022). These cases demonstrate that geochemical CDR strategies within croplands can act either without hindrance or even deliver co-benefits to land use. While agricultural land is widespread across the country, areas of specific land use could also be utilized for spreading, such as greenhouses in Almería, covering ~720  $\text{km}^2$  of land. This means of containment may be advantageous for CDR purposes, as such environments can maintain high relative humidity, a requirement for CDR by direct  $\text{CO}_2$  mineralization (Sharma et al., 2002; Smith et al., 2014; Longo et al., 2015). Optimal greenhouse conditions could be achieved to maintain heat (30 °C) and relative humidity of 90 % using trays of water-saturated salt, fans, tiered airflow and a solar photovoltaic system, as suggested as an option for CDR using natural rocks in Japan (Myers and Nakagaki, 2020). Indeed, seasonally high temperatures, high humidity and high precipitation in some regions of Spain, including high seasonal rainfall in areas such as Galicia, Asturias and Basque Country, generally provide their benefits for speeding up reactions compared to countries with cooler, drier climates.

An additional option available to Spain as a spreading area is the expansive coastline, including the Atlantic (Cantabrian) and Mediterranean coasts of mainland Spain, Canary and Balearic Islands coastlines, and inland dune and sandbank areas (Table 4). The total coastline length of Spain is 4964 km, the ninth longest in Europe (WorldData.info, n.d.). Coastal weathering of suitable materials (e.g., olivine) has been proposed as an



option for ocean alkalinity enhancement and ocean liming under ambient conditions (Hangx and Spiers, 2009), whereby materials are spread along large parts of the coastline above the wave base to promote alkalinity production. The availability of coast-proximal olivine-rich materials, particularly in Galicia and across the Ronda Massif of southern Spain, makes this an option that could be further explored, although no natural olivine-rich beaches occur in Spain. Railway lines and parallel pathways have been investigated as a hosting site for CDR spreading activities in the Netherlands (Movares, 2012), though conditions for sufficiently fast reactions may be limited to areas of high precipitation within Spain, or require regular treatment and monitoring.

Finally, it is important to consider the possibilities of desalination brines for CDR, as there may be an inherent link to the use of crushed alkaline rocks and industrial by-products. Here, the source of the cations is the seawater reject brine itself, rather than any solid rock or waste product. As HCl is produced as a by-product of the conversion process, there may still be a need for solid materials for geological disposal of produced acids for neutralization or possibly for additional alkalinity production. The HCl by-product is effectively reacted with minerals or crushed up rocks (e.g., olivine dunite mine tailings) before its release into the ocean. Here, the products from the reaction are benign  $\text{SiO}_2$ , water and Mg or Ca chlorides. There is a requirement to produce  $\text{MgCl}_2$  and  $\text{CaCl}_2$ , as without the cations, chlorine will cause  $\text{CO}_2$  to degas, meaning such processes must be strictly regulated. By following this approach under planned conditions and settings (e.g., implemented reactor system, heap leaching pond), there is a degree of control over the reaction conditions, including the distribution of the solid and liquid materials, as well as easier monitoring of reactants and products. It is also likely that there would be a broader social acceptance of such processes if they occur in an industrial setting instead of directly into natural bedrock in soils or across coastal settings.

### 6.2.3. In-situ opportunities within suitable bedrock

A key benefit of in-situ approaches compared to ex-situ approaches is that through deep underground injection, the necessity for rapid reactions and mineralization is not inevitably required, assuming that leakage cannot occur and  $\text{CO}_2$  can reside within units for sufficient time (Bide et al., 2014; Alcalde et al., 2018a; White et al., 2020; Holliman et al., 2021). These approaches also negate the need for excavation, crushing, grinding and transportation of materials, eliminating financial costs and energy requirements associated with these activities. The evaluation carried out in this study serves as a broad indicator of the potential for suitable materials, though thorough assessments of specific locations, areas, and rock units would be required for more detailed constraints, including exposure and accessibility assessments. Despite covering a much smaller area of land, mafic-ultramafic rock units offer higher CDR potential per tonne of rock than carbonates, and more opportunities to implement methods that do not necessarily require excavation, pre-treatment (e.g., calcination) or suppression of carbonate precipitation (all likely to be encountered with carbonate rock CDR methods). There are also options to use reactant solutions such as seawater (due to being saturated with calcite, surface seawater would need to be enriched with  $\text{CO}_2$  above atmospheric levels for effective reactions with carbonate materials; Darton et al., 2022).

Suitable rock units offer a substrate for in-situ mineralization schemes, whereby  $\text{CO}_2$ -laden fluids and gases are injected into the bedrock for circulation and reactions with Mg- and Ca-rich minerals (Matter and Kelemen, 2009; Gislason et al., 2010; Matter et al., 2016). The resultant product is alkalinity, particularly if there is an eventual pathway out of the rock to the ocean, and secondary carbonate precipitates (if the rock is adequately sealed). Through deep injection processes, mineral carbonation may be accelerated by higher temperatures, with carbonation rates up to 76 times higher than surface exposed rocks (Paukert et al., 2012).

### 6.2.4. In-situ implementation areas

Accessible mafic and ultramafic rocks of Galicia, Murcia and Andalucía, such as peridotites, serpentinites, dunites, harzburgites and basalts, offer the best opportunities for in-situ CDR approaches for mainland Spain

(Figs. 6–8). At the same time, extensive basaltic-basanitic lava units that comprise much of the Canary Islands also offer a possible geological storage rock or spreading material. Ultramafic rocks such as peridotite and serpentinite present the highest reactivity of the rocks available, owing to their high olivine and serpentine (and minor brucite) contents, meaning formations such as the Ronda massif would be desirable for this approach. While of lower chemical favourability, basaltic rocks of the Canary Islands also offer a notable prospect for CDR strategies due to their greater spatial extent and volumetric abundances across islands compared to mainland exposures, their young age and freshness (younger emplaced flows have had less time to alter), the glassy nature of some of the rocks (may react faster than crystalline equivalents) and their porosity (in unaltered rocks), with resulting high reactive surface areas and fluid flow pathways for reactions and precipitation to occur.

Such an approach whereby  $\text{CO}_2$ -rich solutions or gases are injected into the bedrock would feasibly require a proximal  $\text{CO}_2$  source emitter, such as coal-fired power plants, smelters and cement works (Bide et al., 2014). Large-scale emitters that sit on top of, or in close proximity to, mafic and ultramafic rocks include several plants in northeast Galicia (e.g., the thermal power plants of Sabón and the Narón steelmaking plant), the Carboneras C.T. Litoral power plant in Almería, the Puertollano power plant in Ciudad Real and the Puente Nuevo plant north of Córdoba. Smaller local plants and works may also provide point sources for  $\text{CO}_2$  in promising areas, such as those in the Canary Islands. Hybrid DAC-mineralization methods could also provide  $\text{CO}_2$ -enrichment in implemented airflow or solution (Kelemen et al., 2020). In the absence of natural porosity, which will be the case in fully crystalline intrusive rocks, a means of gas or fluid flow pathway needs to be identified, such as natural fractures, planes of weakness and faults and fractures within the rock. Without sufficient natural pathways, such a network would need to be purposefully engineered, either through borehole drilling and direct injection or by other cracking methods (Kelemen and Hirth, 2012; Sohn, 2013; Evans et al., 2020).

## 6.3. Challenges

Though the potential for geochemical CDR strategies has been identified for Spain, a number of caveats, challenges, and limitations exist which must be considered if any full-scale implementation is to occur, relating to maximum CDR capacity, methods of implementation, incentives to act and public acceptance (Tables 2–3).

### 6.3.1. CDR capacity

It is noted that the calculated  $\text{CO}_2$  offsets for ex-situ methods presented here represent ~6–15 % of national emissions. While the total capacity only represents a fraction of the theoretical total to achieve net zero or net negative emissions, this is still a practical contribution to an overall shift to utilizing means of lowering  $\text{CO}_2$  emissions. Climate and energy legislation for 2030 implemented by the EU means that Spain will further adopt national energy and climate plans, including increasing the country's commitment to energy transition with greater deployment of wind and solar power (IEA, 2019). Spain has committed to reducing non-Emission Trading Scheme emissions (e.g., transport, agriculture, waste, industrial emissions) by at least 26 % by 2030 and generating energy efficiency improvements by over 39 % (European Union, 2021). As  $\text{CO}_2$  emissions decrease, the importance of utilizing geochemical CDR approaches (for removal of diffuse or residual emissions) increases. The maximum theoretical CDR surpasses all required emission offsets to reach net zero, though this upper threshold is not feasibly targetable due to spatial and technological limitations (among other factors). However, assuming in-situ methods in mafic-ultramafic rocks have a maximum CDR capacity of 1.8 Gt, achieving approximately 10 % of this potential could help to reach national net zero emissions. This would require ~296–686 Mt. of mafic-ultramafic feedstock (based on 1.6–3.7 t feedstock required for 1 t  $\text{CO}_2$ ; Lackner et al., 1995; IPCC, 2005; Bide et al., 2014). Extraction of such an amount every year is infeasible (this would represent >100 times the annual national

**Table 3**

Estimated CDR achieved annually, based on annual replenishment of 1 Mt. feedstock (aCDR) and total cumulative CDR (tCDR) as alkalinity generation and via carbonation, based on whole rock geochemistry and modal mineralogy (shrinking core modelling) of a range of possible targetable rocks in Spain over 1 to 70 years of execution. Possible secondary carbonate precipitates from a CO<sub>2</sub>-rich solution reaction for each material also shown.

Material	Region	Brief description of mineralogy	CDR achieved by x years of weathering (aCDR as alkalinity, kt)				CDR achieved for the x year of weathering (aCDR via carbonation, kt)				Total (t)CDR over entire period from all tailings made available (Mt)		Carbonates that may precipitate in CO <sub>2</sub> -rich solution (PHREEQC modelling)
			1 yr	10 yrs	50 yrs	70 yrs	1 yr	10 yrs	50 yrs	70 yrs	Alkalinity generation	Carbonation	
Dunite	Cabo Ortegal, Galicia	Srp and hbl-rich	0.4	7.5	34.6	46.4	0.3	5.0	23.2	31.1	1.73	1.16	Mag
Dunite	Cabo Ortegal, Galicia	Srp and hbl-rich	0.3	6.1	27.9	37.1	0.2	4.1	21.8	24.8	1.40	0.93	Mag
Dunite	Cabo Ortegal, Galicia	Srp and chl-rich	0.02	0.4	2.1	2.9	0.01	0.3	1.4	2.0	0.10	0.07	Hun, mag
Dunite	Cabo Ortegal, Galicia	Srp-rich	0.3	6.4	29.0	38.6	0.2	4.3	19.4	25.9	1.45	0.97	Hun, mag
Harzburgite	Cabo Ortegal, Galicia	Srp and ol-rich	0.7	13.3	60.1	79.9	0.5	8.9	40.1	53.4	3.01	2.01	Mag
Harzburgite	Cabo Ortegal, Galicia	Srp and hbl-rich	0.4	7.1	32.3	43.1	0.2	4.8	21.6	28.8	1.62	1.08	Mag
Pyroxenite	Cabo Ortegal, Galicia	Cpx, hbl and opx-rich	0.3	6.7	30.7	41.2	0.2	4.5	20.7	27.8	1.54	1.03	Ara, cal, dol, hun, mag, nes
Pyroxenite	Cabo Ortegal, Galicia	Cpx and opx-rich	0.07	1.4	6.7	9.4	0.05	0.9	4.7	6.6	0.33	0.23	Ara, cal, dol
Pyroxenite	Cabo Ortegal, Galicia	Cpx and opx-rich	0.06	1.1	5.7	7.9	0.04	0.8	4.0	5.5	0.28	0.2	Ara, cal, dol
Pyroxenite	Cabo Ortegal, Galicia	Cpx and opx-rich	0.08	1.5	7.6	10.6	0.05	1.0	5.2	7.2	0.38	0.26	Ara, cal, dol
Pyroxenite	Cabo Ortegal, Galicia	Cpx-rich	0.07	1.3	6.5	9.1	0.04	0.9	4.4	6.2	0.32	0.22	Ara, cal, dol
Pyroxenite	Cabo Ortegal, Galicia	Cpx, hbl and opx-rich	0.06	1.3	6.3	8.8	0.04	0.9	4.4	6.1	0.31	0.22	Ara, cal, dol
Pyroxenite	Cabo Ortegal, Galicia	Cpx-rich	0.2	3.7	17.4	23.7	0.1	2.5	11.7	15.9	0.87	0.58	Ara, cal, dol
Pyroxenite	Cabo Ortegal, Galicia	Opx-rich	0.1	1.9	9.0	12.1	0.07	1.4	6.6	8.9	0.45	0.33	Mag
Peridotite	Ronda Massif	Ol-rich	2.5	48.1	217	288	1.6	32.1	145	193	10.88	7.26	Ara, cal, dol, hun, hyd, mag, nes
Peridotite	Ronda Massif	Ol-rich	2.5	48.0	217	288	1.6	32.0	145	192	10.87	7.25	Ara, cal, dol, hun, mag, nes
Peridotite	Ronda Massif	Ol and srp-rich	1.4	27.6	125	166	0.9	18.4	83.2	111	6.25	4.17	Dol, hun, mag, nes
Peridotite	Ronda Massif	Ol and opx-rich	2.1	41.5	188	249	1.4	27.7	125	166	9.40	6.27	Ara, cal, dol, hun, mag, nes
Peridotite	Ronda Massif	Ol and opx-rich	1.6	31.9	144	192	1.1	21.3	96.3	128	7.23	4.83	Ara, cal, dol, hun, hyd, mag, nes
Peridotite	Ronda Massif	Ol and srp-rich	2.3	45.3	205	272	1.6	30.2	136	181	10.25	6.84	Ara, cal, dol, hun, hyd, mag, nes
Dunite	Aguablanca, Badajoz	Ol-rich	1.5	29.9	135	180	1.0	19.9	90.0	120	6.78	4.51	Ara, cal, dol, hun, hyd, mag, nes
Werhlite	Aguablanca, Badajoz	Ol and cpx-rich	2.0	38.9	176	234	1.3	25.9	117	156	8.82	5.87	Ara, cal, dol, hun, hyd, mag, nes
Harzburgite	Aguablanca, Badajoz	Opx-rich	0.03	0.6	3.0	4.1	0.03	0.5	2.6	3.6	0.15	0.13	Mag
Pyroxenite	Aguablanca, Badajoz	Cpx-rich	0.1	2.0	10.0	13.9	0.07	1.3	6.5	9.1	0.50	0.32	Ara, cal, dol
Pyroxenite	Aguablanca, Badajoz	Cpx and pl-rich	0.07	1.4	7.2	10.1	0.05	0.9	4.5	6.3	0.36	0.23	Ara, cal, dol, hun, mag
Gabbro	Aguablanca, Badajoz	Cpx and pl-rich	0.07	1.5	7.3	10.1	0.05	0.9	4.5	6.3	0.36	0.23	Ara, cal, dol
Gabbro	Aguablanca, Badajoz	Pl and cpx-rich	0.04	0.8	3.9	5.5	0.02	0.5	2.3	3.2	0.20	0.11	Ara, cal, dol, hun, mag
Gabbro	Aguablanca, Badajoz	Pl and hbl-rich	0.03	0.5	2.6	3.7	0.01	0.3	1.3	1.8	0.13	0.06	Hyd, mag, nes
Gabbro	Aguablanca, Badajoz	Pl-rich	0.04	0.8	4.1	5.7	0.02	0.4	2.0	2.8	0.20	0.10	Mag
Serpentinite	Cerro del Almirez,												
Serpentinite	Nevado-Filábride Complex	Srp and talc-rich	0.3	6.7	30.4	40.6	0.2	4.5	20.3	27.1	1.52	1.02	Ara, cal, dol, hun, hyd, mag, nes
Serpentinite	Cerro del Almirez,												
Serpentinite	Nevado-Filábride Complex	Srp and opx-rich	0.3	6.6	29.8	39.7	0.2	4.4	20.0	26.7	1.49	1.00	Mag
Serpentinite	Cerro del Almirez,												
Serpentinite	Nevado-Filábride Complex	Srp and chl-rich	0.5	9.5	43.1	57.4	0.3	6.3	28.7	38.3	2.16	1.44	Ara, cal, dol, hun, hyd, mag, nes
Serpentinite	Cerro del Almirez,												
Serpentinite	Nevado-Filábride Complex	Srp and chl-rich	0.5	9.4	42.5	56.6	0.3	6.2	28.3	37.7	2.13	1.42	Mag
Serpentinite	Cerro del Almirez,												
Serpentinite	Nevado-Filábride Complex	Ol and opx-rich	1.5	28.5	129	171	1.0	19.0	86.0	114	6.45	4.31	Hun, hyd, mag, nes
Serpentinite	Cerro del Almirez,												
Serpentinite	Nevado-Filábride Complex	Ol and opx-rich	1.4	26.5	120	160	0.9	17.7	80.2	107	6.01	4.02	Hun, hyd, mag, nes
Serpentinite	Cerro del Almirez,												
Serpentinite	Nevado-Filábride Complex	Ol and opx-rich	1.5	29.2	132	175	1.0	19.5	88.1	117	6.61	4.42	Hun, hyd, mag, nes
Serpentinite	Cerro del Almirez,												
Serpentinite	Nevado-Filábride Complex	Ol and opx-rich	1.1	21.7	98.1	131	0.7	14.5	65.7	87.4	4.92	3.29	Hyd, mag, nes
Basalt	Canary Islands	Glass, ol and cpx-rich	0.6	12.2	57.5	78.3	0.4	8.1	38.2	52.0	2.87	1.91	-
Basalt	Canary Islands	Glass, ol and cpx-rich	0.3	6.2	29.3	39.9	0.2	4.1	19.4	26.4	1.46	0.97	-
Basalt	Canary Islands	Glass, cpx and pl-rich	0.07	1.4	6.7	9.3	0.04	0.8	4.0	5.6	0.33	0.20	-
Basalt	Canary Islands	Glass, ol and cpx-rich	0.3	6.7	31.9	43.6	0.2	4.5	21.2	28.9	1.59	1.06	-
Basalt	Canary Islands	Cpx-rich	0.3	5.3	25.2	34.5	0.2	3.5	16.6	22.7	1.26	0.83	-
Basalt	Canary Islands	Glass, ol and cpx-rich	0.6	11.9	56.3	76.7	0.4	7.9	37.4	50.9	2.81	1.87	-
Basalt	Canary Islands	Glass, ol and cpx-rich	0.3	5.6	26.4	36.0	0.2	3.7	17.9	23.9	1.32	0.87	-
Basalt	Canary Islands	Glass, ol and cpx-rich	0.4	8.8	41.6	56.8	0.3	5.8	27.7	37.7	2.08	1.38	-
Basalt	Canary Islands	Glass, ol, pl and cpx-rich	0.4	8.9	42.1	57.5	0.3	5.8	27.6	37.6	2.10	1.38	-

Ara = Aragonite, cal = calcite, dol = dolomite, hun = huntite, hyd = hydromagnesite, mag = magnesite, nes = nesquehonite. Hyphen (-) indicates absence of carbonates in PHREEQC modelling results.

extraction of more volumetrically abundant carbonate rocks). However, any in- or ex-situ methods could still provide significant offset contributions.

### 6.3.2. Implementing geochemical CDR strategies

Despite academic advancements on the subject of geochemical CDR strategies since the start of the century and the onset of commercial and industrial pilot schemes in the last decade (e.g., Gíslason et al., 2018;

Holliman et al., 2021), gaps remain in the current knowledge relating to geochemical CDR processes in a broad sense, as well as intricate details of potential targets within Spain. Without numerous pilot trials occurring on an industrial scale (for tonnes of CDR) and over several years of monitoring, it is challenging to implore companies and governing bodies to implement schemes that may or may not achieve calculated targets, particularly when some methods come at a financial cost, requiring significant energy inputs and dedicated workforces. Questions regarding environmental implications

of the different geochemical CDR strategies, such as alkalinity effects on local river and ocean ecosystems and management of potentially toxic, liberated trace elements, are also a key determinant in future regulation and monitoring of large-scale systems.

There are other important questions relating to geochemical CDR research, but these topics have been subject to rigorous studies and are still being actively investigated for further elucidation. In reality, large-scale pilot studies can only fully answer many of these questions. One of the challenges is to improve associations between academia, industrial operators, governmental bodies and other sectors of interest (e.g., charities and non-profit organizations) for a joint responsibility to tackle these questions as a new research and development sector. New incentives to deploy multi-sector large-scale schemes are now being initiated, such as the Carbon XPRIZE competition, a global grant which has committed \$100 million to tackle climate change, with the conversion of CO<sub>2</sub> into valuable products at the forefront of the research pursuit (Extavour, 2021; Sleep et al., 2021). The National Academies of Sciences Engineering Medicine has also called for investments of up to \$1 billion over 10–20 years to advance CDR deployment strategies on a scale of Mt-GtCO<sub>2</sub> per year (NASEM, 2019). There is a challenge for the EU to match or better these actions through their implementation of engineered CDR strategies (Galán-Martín et al., 2021), for which geochemical CDR approaches in Spain could be highly relevant. Research and development and demonstrator funding schemes launched by the EU include the Innovation Fund (€25 billion) for investigating breakthrough technologies in carbon capture and storage (CCS) and Horizon Europe funding for research, pilots and small-scale demonstration projects related to CCS and CDR, such as the DETAILS Project being undertaken by authors of this study (European Commission, n.d.).

### 6.3.3. Motivations to pursue CDR strategies

While key fundamental questions are being tackled through ongoing research and development, other drawbacks remain regarding a reluctance to commit to such strategies without adequate enticements and co-benefits financially. In-situ and ex-situ approaches to CDR on a Gt-scale can cost upwards of \$500–1000 per t CO<sub>2</sub>, or even higher for approaches such as air capture in peridotite (Kelemen et al., 2019). Approaches to improve the economic feasibility of CDR strategies for the industry include (1) targeted carbon prices, taxes and credit systems, and (2) implementation of strategies that deliver co-benefits to the operator. Regulated EU tax credits and incentives, with legal frameworks and certified measures for CDR and storage timescales, would provide countries like Spain with a financial incentive to pursue geochemical CDR strategies, specifically for large-scale industrial operators in steel, energy, mining, agricultural landowners and even “niche” sectors of the wine, olive, rice and ceramics industry. The EU has stated a need to step up CDR, and as of December 2021, the Commission stated its intent to explore the possibility of developing an EU certification system for carbon removal (European Union, 2022).

As an alternative incentive, the prospect of generating secondary revenue or higher productivity, or reducing costs associated with the primary activities of an operator hosting CDR strategies, may entice financial commitment or reduce associated risks. Beyond carbon pricing incentives, there are limited co-benefits to in-situ approaches that could be realized, although there is a possibility to utilise wastewater as the injection solution (Phan et al., 2018), while the scale of operations could provide an employment transition from diminishing fossil fuels industries. Ex-situ methods likely afford several possible co-benefits, such as increased crop yields and plant growth associated with enhanced weathering and spreading in soils, as well as remediation of toxic metal contamination, reversal of soil acidification and replenishment of macro and micronutrients (Leonardos et al., 1987; Hartmann et al., 2013; Anda et al., 2015; Renforth et al., 2013; Beerling et al., 2018, 2020; Kelland et al., 2020; Buckingham et al., 2022). Using appropriate materials for CDR in soils can also reduce the usage of fertilizers and pesticides (Haque et al., 2020; Kantola et al., 2017; Beerling et al., 2018, 2020). Spain is the fourth largest agri-food producer in Europe and tenth in the world, and the industry is the main national manufacturing activity (ICEX, 2020). The agricultural sector,

including food products, olive oil and wine, and encompassing the covered produce hosted within greenhouses of Almería, could highly benefit from these additional benefits to crop yields and lower consumption of agricultural additives, particularly in cropland areas proximal to material sources such as in Galicia (mine sites, power plants and steelmaking plants) and the Canary Islands (abundant loose basalt materials at active and formerly worked quarries). There may also be opportunities to seize economic returns on mineral carbonation by-products such as silica and carbonates, which hold several possible applications for aggregates, cements, neutralizing acidic waters and backfill.

### 6.3.4. Challenges ahead for Spain

One of the key challenges to geochemical CDR implementation for any localized or regional system is to develop a comprehensive understanding of the rocks or materials that are intended to be utilized. Geological units, and their derivative industrial wastes, are inherently heterogeneous in terms of their mineralogy (including zones of alteration and natural carbonation), geochemistry and physical coarseness. A thorough evaluation of the physical, mineral and chemical properties of any targeted materials is required prior to testing and development, and accurate reactivity potential for optimized performance needs to be determined on a site-by-site basis (Holloway, 2007; Wilkin and Digiulio, 2010; Gomes et al., 2016; Power et al., 2014; Jones et al., 2019; Bullock et al., 2022). Further studies are also required to determine the true extent of rock and material volume availability, particularly for the true depth and morphology of in-situ bedrock units beyond information based on mapped surface extent only. The responsibility for the production of these detailed assessment lies with the interested parties, such as academic and public research institutions, universities, governmental bodies and industrial companies from the mining, steelmaking, energy and agricultural sectors, or where possible, through collaboration across several interested parties and sectors.

It may be concluded that areas of CDR promise require further material testing under controlled conditions, determination of possible links to point sources, the need for additional mining, processing and transport, and adequate monitoring of potential environmental threats. One major challenge for Spain as a collective entity seeking to implement geochemical CDR strategies is to generate public acceptance through stakeholder engagement, communication and education efforts. Public perception of CCS technologies has previously included a mixture of positive engagement and support for developments, a passive interest, a reluctance to support projects that may incur public costs or loss of land, misconceptions about the methods or targeted outcomes, or strong rejection of developments relating to risks, with a preference for renewable energies or perception of limited CCS contributions to solving climate issues (L'Orange Seigo et al., 2014; Braun, 2017; Pind Aradóttir and Hjálmarsson, 2018; Bertram and Merk, 2020). Factors that invoke an adverse reaction to such methods include the possibilities of induced seismicity, increased mining activities, controllability of processes, potential environmental impacts, material containment, CO<sub>2</sub> storage permanence and hesitation to live close to any implemented systems.

The key to ensuring public acceptance is as high as possible is to provide clear, transparent communications with affected communities, encouraging feedback from stakeholders and incorporating outcomes from such discussions into the planning and development stages. A high proportion of Spanish citizens (67 %) expect that governmental bodies take responsibility for tackling climate change (European Union, 2021), with a high level of concern related to first-hand experience with drought (Upham and Roberts, 2011). There is a general positive attitude towards CCS implementation in Spain from experts with a professional interest in CCS. Public consultation also confirmed that people believe that CCS has a crucial role as a mitigation option (Sala and Oltra, 2011). Clear communications from experts and operators to local communities and the general populace regarding environmental risk management of geochemical CDR approaches, the permanence of geological storage, the co-benefits of implementing such systems, and the high CDR potential across Spain could help to ensure public acceptance for development of strategies going forward. It could be

Table 4

Possible spreading areas in Spain (based on land use classification of the [European Environment Agency, n.d.](#)). Here, coverage proximal to suitable rock types indicates designated land use covering any mapped area of mafic, ultramafic or carbonate rock.

Designated land use	Land coverage (km <sup>2</sup> )	% of total land use	Coverage proximal to suitable rock types (km <sup>2</sup> )	Example localities	Considerations
Mineral extraction sites	806	0.2	63	La Coruña and Pontevedra (Galicia); Ciudad Real (Castilla-La Mancha); Almería (Andalucía); Badajoz (Extremadura); Murcia; Tenerife and Gran Canaria (Canary Islands)	Appropriate space and infrastructure for reactor-based and spreading methods, including possible incorporation into existing concentrator plants and tailings dams. May be controlled and operated by mine companies for internal CDR targets
Non-irrigated arable land	102,279	20.2	6038	La Coruña and Pontevedra (Galicia); Ciudad Real (Castilla-La Mancha); Almería, Córdoba, Sevilla and Málaga (Andalucía); Murcia; Badajoz and Cáceres (Extremadura); Zamora (Castile and León); Girona (Catalonia); Tenerife and Fuerteventura (Canary Islands)	Limited cultivation and rainfall will hinder reaction times, reducing efficiency and annually achievable CDR. May be operated by farmers or co-operated with public or private sectors
Permanently irrigated land	31,453	6.2	6332	Ciudad Real (Castilla-La Mancha); Murcia; Tenerife, Gran Canaria and Lanzarote (Canary Islands)	Permanent infrastructure for wetting and draining to promote reactions, with sufficient monitoring and control for methodological evaluation and adaption
Rice fields	1386	0.3	375	Valencia (Valencian Community); Tarragona (Catalonia); Albacete (Castilla-La Mancha)	Flooded paddy fields can promote reactions. Silica release by enhanced weathering can help confer resistance to pests and diseases, improve water-use efficiency and increase yields ( <a href="#">Edwards et al., 2017</a> ; <a href="#">Vicca et al., 2022</a> ). Variable reported effects on CH <sub>4</sub> , N <sub>2</sub> O and CO <sub>2</sub> emissions ( <a href="#">Vicca et al., 2022</a> )
Vineyards	12,042	2.4	7687	Ciudad Real (Castilla-La Mancha); Tenerife, La Palma and Lanzarote (Canary Islands)	Permanently irrigated system. Some appropriate rocks can help to maintain heat and moisture, which may act to positively impact the grape ( <a href="#">Stephen, 2013</a> ; <a href="#">Tejedor et al., 2003</a> ; <a href="#">Lomoschitz et al., 2006</a> )
Fruit trees and berry plantations	11,995	2.4	7259	Almería, Córdoba, Sevilla and Málaga (Andalucía); Murcia; Tenerife, La Palma, El Hierro and Gran Canaria (Canary Islands)	Permanently irrigated system, permanent trunks, branches and roots for long term CDR, though efficiency is variably affected by growth and development patterns, biomass accumulation and environmental factors ( <a href="#">Sharma et al., 2002</a> )
Olive groves	23,289	4.6	13,540	Ciudad Real (Castilla-La Mancha); Almería, Córdoba, Sevilla and Málaga (Andalucía); Badajoz, Cáceres and Salamanca (Extremadura); Zamora (Castile and León)	Similar long-term properties, characteristics, benefits and limitations to fruit trees and berry plantations
Pastures, meadows and other permanent agricultural grasslands	11,825	2.3	4429	La Coruña and Pontevedra (Galicia); Almería, Córdoba, Sevilla and Málaga (Andalucía); Murcia, Badajoz, Cáceres and Salamanca (Extremadura); Zamora (Castile and León); Tenerife, Lanzarote and Gran Canaria (Canary Islands)	Land may be periodically or regularly disturbed, with limited exposure to atmosphere due to growth of vegetation and grasslands, and the use of farm infrastructure
Annual and permanent crops	187	<0.1	54	Majorca (Balearic Islands); Zaragoza (Aragón); El Hierro (Canary Islands)	Mixed-use land with similar properties, characteristics, benefits and limitations to fruit trees, berry plantations and olive groves
Complex cultivation patterns	19,162	3.8	8972	La Coruña and Pontevedra (Galicia); Ciudad Real (Castilla-La Mancha); Almería (Andalucía); Murcia; all Canary Islands	Mixed-use land with similar properties, characteristics, benefits and limitations to fruit trees, berry plantations, olive groves and annual crops associated with permanent crops
Agriculture and natural vegetation	14,397	2.8	4761	La Coruña and Pontevedra (Galicia); Ciudad Real (Castilla-La Mancha); Almería (Andalucía); Murcia; Zamora (Castile and León); Girona (Catalonia); all Canary Islands	Mixed-use land with similar properties, characteristics, benefits and limitations to fruit trees, berry plantations, olive groves, annual crops associated with permanent crops and complex cultivation patterns
Agroforestry areas	23,771	4.7	11,396	Ciudad Real and Albacete (Castilla-La Mancha); Almería, Granada, Jaén, Córdoba, Sevilla and Málaga (Andalucía); Badajoz, Cáceres and Salamanca (Extremadura); Zamora (Castile and León)	Spreading can reduce forested land's acidity and improve soil quality ( <a href="#">Schuiling and Krijgsman, 2006</a> ). Long-term systems, retention of moisture in shaded zones. Protected lands, public access and non-dedicated operators may limit application, monitoring and verification
Beaches, dunes and sandbanks	246	<0.1	182	Beaches in all coastal areas of mainland Spain and Spanish islands; dunes and sandbanks in Alicante (Valencian Community); Lanzarote (Canary Islands)	Beach weathering promotes natural alkalinity production and ocean alkalization and can be integrated into existing coastal management technologies ( <a href="#">Meysman and Montserrat, 2017</a> ). Requires preparation and transport and may invoke economic, infrastructural and public health issues ( <a href="#">Hangx and Spiers, 2009</a> ). Water addition may be limited to water marks, rivers, lagoonal and lacustrine areas. Protected lands, public access and non-dedicated operators may limit application, monitoring and verification
Bare rock	1932	0.4	1864	Almería and Granada (Andalucía); Asturias; Huesca (Aragón); Lleida (Catalonia); Málaga (Andalucía); Tenerife, La Palma, La Gomera, Fuerteventura and Lanzarote (Canary Islands)	Possible direct extraction sites or sites for in-situ injection schemes (for suitable rock types only and subject to greater understanding of geochemistry and mineralogy of rocks)
Spaces with scarce vegetation	5424	1.1	6002	Almería, Jaén and Granada (Andalucía); Murcia; Huesca (Aragón); Asturias, Cantabria; León, Palencia and Burgos (Castile and León); Alicante and Castellón (Valencian Community); Teruel (Aragón); all Canary Islands, particularly Fuerteventura	Possible means to access rocks (with low energy input) for extraction or in-situ injection schemes (for suitable rock types) or areas for spreading (requires land permission, monitoring and maintenance)
Burnt areas	294	0.1	106	Alicante, Valencia and Castellón (Valencian Community); Albacete and Cuenca (Castilla-La Mancha); Asturias; Tenerife (Canary Islands)	Possible means to access rocks for extraction or in-situ injection schemes (for suitable rock types) or areas for spreading (requires land permission, monitoring and maintenance)
Major railway lines	337	0.1	233	Major rail network across all regions of mainland Spain and Majorca (Balearic Islands)	Suitable rocks may replace existing aggregates used in railway lines and inspection paths as ballast or grit ( <a href="#">Movares, 2012</a> ). Requires preparation and transport and may invoke economic, infrastructural and public health issues

important to stress the current state of research and development of these approaches to alleviate some concerns, with limited testing under controlled conditions still holding a priority ahead of implementation at a large scale.

## 7. Conclusions

This study provides the first overview assessment of CDR potential specifically aimed at geochemical approaches for Spain. The work focuses on the potential to utilise suitable rocks and industrial by-products, which are in high abundance in Spain and could be implemented in systems and settings specific to the country. Spain plays host to chemically and mineralogically suitable surface exposed mafic, ultramafic, and carbonate rock units (rich in Mg and Ca) and is a producer of alkaline industrial wastes such as mine and quarry fine tailings, glassy slags, fly ashes, ceramic wastes and desalination brines, all of variable volumetric abundance, chemical composition, physical nature and CDR suitability. The objectives and methods implemented in this study may also form an applicable strategy for other countries and regions for general assessments of their hosted geochemical CDR potential.

Methods of in-situ injection, ex-situ enhanced weathering, mineral carbonation, ocean liming, and electrochemical processes are theoretically applicable for these hosted rocks and materials, and the wide spread of agricultural land, coastlines and greenhouses could make highly appropriate settings for strategies to be deployed. Materials are distributed across the mainland and islands, with particularly high potential for Galicia, Andalucía, Murcia and the Canary Islands regions. Overall, there is the maximum potential to achieve up to 8 MtCO<sub>2</sub> through available and annually produced waste materials, but with potentially greater-scale removal if suitable rock units can be excavated for ex-situ approaches or exploited in-situ for CDR purposes. The key is to target the best opportunities for initial trials and to test to achieve the highest possible amount of the overall maximum potential.

Spain's challenges are developing structured approaches and dedicated associations to tackle key fundamental questions relating to material kinetics, regional mineral and chemical heterogeneity, exploitable abundances, environmental considerations, resource usage and public acceptance. Collaborative efforts from academia, industry, government and other sectors could help to address these matters and steer the nation towards pilot studies and full-scale deployment of geochemical CDR methods. Such an approach requires dedicated time and funding from all sectors of interest, but the rewards, including several co-benefits beyond CDR, could be considerable as Spain and the EU continue to move towards net zero and net negative emissions throughout the century.

## Funding

LB and JLFT are funded under H2020-EU.1.3.2. (DETAILS Project, grant agreement ID: 101018312). JA is funded by MCIN through the Juan de la Cierva Incorporación fellowship (IJC 2018-036074-I), supported by MCIN/AEI /10.13039/501100011033.

## CRediT authorship contribution statement

**Liam A. Bullock:** Conceptualization, Methodology, Formal analysis, Investigation, Data curation, Writing – original draft, Visualization, Funding acquisition. **Juan Alcalde:** Methodology, Validation, Formal analysis, Investigation, Writing – review & editing, Visualization. **Fernando Tornos:** Validation, Formal analysis, Resources, Data curation, Writing – review & editing. **Jose-Luis Fernandez-Turiel:** Methodology, Validation, Resources, Data curation, Writing – review & editing, Supervision, Project administration, Funding acquisition.

## Data availability

Data will be made available on request.

## Declaration of Competing Interest

The authors have no competing interests to declare.

## Acknowledgements

The authors wish to thank Pamela Díaz García (Pasek Minerale) for her advice and contributions. The authors appreciate the comments of the anonymous reviewers, and the editorial work of Prof. Dan Tsang, that helped to improve the manuscript.

## Appendix A. Supplementary data

Supplementary data to this article can be found online at <https://doi.org/10.1016/j.scitotenv.2022.161287>.

## References

- Abati, J., Arenas, R., Martínez Catalán, J.R., Díaz García, F., 2003. Anticlockwise P-T path of granulites from the Monte Castelo Gabbro (Ordénes complex, NW Spain). *J. Petrol.* 44 (2), 305–327. <https://doi.org/10.1093/ptrology/44.2.305>.
- Aedyr, . Technical Seminar: Valorisation in desalination product and energy recovery (November 2022) <https://aedyr.com/en/> last access: 2 June 2022.
- Ahmed, M., Arakel, A., Hoey, D., Thumarukudy, M.R., Goosen, M.F.A., Al-Haddabi, M., Al-Belushi, A., 2003. Feasibility of salt production from inland RO desalination plant reject brine: a case study. *Desalination* 158, 109–117. [https://doi.org/10.1016/S0011-9164\(03\)00441-7](https://doi.org/10.1016/S0011-9164(03)00441-7).
- Alcalde, J., Flude, S., Wilkinson, M., Johnson, G., Edlmann, K., Bond, C.E., Scott, V., Gilfillan, S.M.V., Ogaya, X., Stuart Haszeldine, R., 2018a. Estimating geological CO<sub>2</sub> storage security to deliver on climate mitigation. *Nat. Commun.* 9. <https://doi.org/10.1038/s41467-018-04423-1>.
- Alcalde, J., Smith, P., Haszeldine, R.S., Bond, C.E., 2018b. The potential for implementation of Negative Emission Technologies in Scotland. *Int. J. Greenh. Gas Control* 76, 85–91. <https://doi.org/10.1016/j.ijggc.2018.06.021>.
- Ancochea, E., Huertas, M.J., 2021. Radiometric ages and time–space distribution of volcanism in the Campo de Calatrava Volcanic Field (Iberian Peninsula). *J. Iber. Geol.* 47 (1), 209–223. <https://doi.org/10.1007/s41513-021-00167-y>.
- Anda, M., Shamsuddin, J., Fauziah, C.I., 2015. Improving chemical properties of a highly weathered soil using finely ground basalt rocks. *Catena* 124, 147–161. <https://doi.org/10.1016/j.catena.2014.09.012>.
- Andrews, M.G., Taylor, L.L., 2019. Combating climate change through enhanced weathering of agricultural soils. *Elements* 15, 253–258. <https://doi.org/10.2138/gselements.15.4.253>.
- Argiz, C., Menéndez, E., Moragues, A., Sanjuán, M.A., 2015. Fly ash characteristics of spanish coal-fired power plants. *Afinidad* 572, 269–277.
- Bandstra, J.Z., Buss, H.L., Campen, R.K., Liermann, L.J., Moore, J., Hausrath, E.M., 2008. Appendix: compilation of mineral dissolution rates. In: Brantley, S.L., Kubicki, J.D., White, A.F. (Eds.), *Kinetics of Water-rock Interaction*. Springer, New York, pp. 737–823.
- Baragaño, D., Forján, R., Aguado, J.M.M., Martino, M.C., García, P.D., Rubio, J.M., Rueda, J.J. Á., Gallego, J.L.R., 2019. Reuse of dunite mining waste and sub-products for the stabilization of metal(oid)s in polluted soils. *Minerals* 9, 1–11. <https://doi.org/10.3390/min9080481>.
- Barbero, L., Villaseca, C., 2000. Eclogite facies relics in metabasites from the Sierra de Guadarrama (Spanish Central System): P-T estimations and implications for the Hercynian evolution. *Mineral. Mag.* 64, 815–836. <https://doi.org/10.1180/002646100549814>.
- Becerra-Ramírez, R., Gosálvez, R.U., Escobar, E., González, E., Serrano-Patón, M., Guevara, D., 2020. Characterization and geotourist resources of the Campo de Calatrava Volcanic Region (Ciudad Real, Castilla-La Mancha, Spain) to develop a UNESCO global geopark project. *Geosciences* 10 (11), 441. <https://doi.org/10.3390/geosciences10110441>.
- Beerling, D.J., Leake, J.R., Long, S.P., Scholes, J.D., Ton, J., Nelson, P.N., Bird, M., Kantzas, E., Taylor, L.L., Sarkar, B., Kelland, M., DeLucia, E., Kantola, I., Müller, C., Rau, G., Hansen, J., 2018. Farming with crops and rocks to address global climate, food and soil security. *Nat. Plants* 4, 138–147. <https://doi.org/10.1038/s41477-018-0108-y>.
- Beerling, D.J., Kantzas, E.P., Lomas, M.R., Wade, P., Eufrazio, R.M., Renforth, P., Sarkar, B., Andrews, M.G., James, R.H., Pearce, C.R., Mercure, J.F., Pollitt, H., Holden, P.B., Edwards, N.R., Khanna, M., Koh, L., Quegan, S., Pidgeon, N.F., Janssens, I.A., Hansen, J., Banwart, S.A., 2020. Potential for large-scale CO<sub>2</sub> removal via enhanced rock weathering with croplands. *Nature* 583, 242–248. <https://doi.org/10.1038/s41586-020-2448-9>.
- Belding, W., . Wine Review Online - The Dark Side of Volcanic Rocks: Basaltic Basics <http://www.winereviewonline.com/printArticle.cfm?articleID=1758>.
- Bertram, C., Merk, C., 2020. Public perceptions of ocean-based carbon dioxide removal: the nature-engineering divide? *Front. Clim.* 2, 1–8. <https://doi.org/10.3389/fclim.2020.594194>.
- Bessière, E., Augier, R., Jolivet, L., Précigout, J., Romagny, A., 2021. Exhumation of the Ronda peridotite during hyper-extension: new structural and thermal constraints from the Nieves Unit (Western Betic Cordillera, Spain). *Tectonics* 40, 1–39. <https://doi.org/10.1029/2020TC006271>.

- Bide, T.P., Styles, M.T., Naden, J., 2014. An assessment of global resources of rocks as suitable raw materials for carbon capture and storage by mineralisation. *Trans. Inst. Min. Metall. Sect. B Appl. Earth Sci.* 123, 179–195. <https://doi.org/10.1179/1743275814Y.0000000057>.
- Bodinier, J.L., Garrido, C.J., Chanefo, I., Bruguié, O., Gervilla, F., 2008. Origin of pyroxenite-peridotite veined mantle by refertilization reactions: evidence from the Ronda peridotite (Southern Spain). *J. Petrol.* 49, 999–1025. <https://doi.org/10.1093/petrology/egn014>.
- Booth-Rea, G., Azañón, J.M., Martínez-Martínez, J.M., Vidal, O., García-Dueñas, V., 2005. Contrasting structural and P-T evolution of tectonic units in the southeastern Betics: key for understanding the exhumation of the Alboran Domain HP/LT crustal rocks (western Mediterranean). *Tectonics* 24, 1–23. <https://doi.org/10.1029/2004TC001640>.
- Braun, C., 2017. Not in my backyard: CCS sites and public perception of CCS. *Risk Anal.* 37, 2264–2275. <https://doi.org/10.1111/risa.12793>.
- Buckingham, F., Henderson, G.M., Holdship, P., Renforth, P., 2022. Soil core study indicates limited CO<sub>2</sub> removal by enhanced weathering in dry croplands in the UK. *Appl. Geochem.* 105482. <https://doi.org/10.1016/j.apgeochem.2022.105482>.
- Bullock, L.A., James, R.H., Matter, J., Renforth, P., Teagle, D.A.H., 2021. Global carbon dioxide removal potential of waste materials from metal and diamond mining. *Front. Clim.* 3, 1–12. <https://doi.org/10.3389/fclim.2021.694175>.
- Bullock, L.A., Yang, A., Darton, R.C., 2022. Kinetics-informed global assessment of mine tailings for CO<sub>2</sub> removal. *Sci. Total Environ.* 808, 152111. <https://doi.org/10.1016/j.scitotenv.2021.152111>.
- Campbell, J.S., Foteinis, S., Furey, V., Hawrot, O., Pike, D., Aeschlimann, S., Maesano, C.N., Reginato, P.L., Goodwin, D.R., Looger, L.L., Boyden, E.S., Renforth, P., 2022. Geochemical negative emissions technologies: part I. Review. *Front. Clim.* 4, 133. <https://doi.org/10.3389/fclim.2022.879133>.
- Canadell, J.G., Monteiro, P.M.S., Costa, M.H., Cotrim da Cunha, L., Cox, P.M., Eliseev, A.V., Henson, S., Ishii, M., Jaccard, S., Koven, C., Lohila, A., Patra, P.K., Piao, S., Rogelj, J., Syampungani, S., Zaehle, S., Zickfeld, K., 2021. Global carbon and other biogeochemical cycles and feedbacks. In: Masson-Delmotte (Ed.), *Climate Change 2021: The Physical Science Basis. Contribution of Working Group I to the Sixth Assessment Report of the Intergovernmental Panel on Climate Change*. Cambridge University Press, Cambridge, United Kingdom and New York, NY, USA, pp. 673–816. <https://doi.org/10.1017/9781009157896.007>.
- Casas, S., Bonet, N., Aladjem, C., Cortina, J.L., Larrotcha, E., Cremades, L.V., 2011. Modelling sodium chloride concentration from seawater reverse osmosis brine by electro-dialysis: preliminary results. *Solvent Extr. Ion Exch.* 29, 488–508. <https://doi.org/10.1080/07366299.2011.573451>.
- Casas, S., Aladjem, C., Cortina, J.L., Larrotcha, E., Cremades, L.V., 2012. Seawater reverse osmosis brines as a new salt source for the chlor-alkali industry: integration of NaCl concentration by electro-dialysis. *Solvent Extr. Ion Exch.* 30, 322–332. <https://doi.org/10.1080/07366299.2012.686849>.
- Casas, S., Aladjem, C., Larrotcha, E., Gibert, O., Valderrama, C., Cortina, J.L., 2014. Valorisation of Ca and Mg by-products from mining and seawater desalination brines for water treatment applications. *J. Chem. Technol. Biotechnol.* 89, 872–883. <https://doi.org/10.1002/jctb.4326>.
- Caserini, S., Pagano, D., Campo, F., Abbà, A., De Marco, S., Righi, D., Renforth, P., Grosso, M., 2021. Potential of maritime transport for ocean liming and atmospheric CO<sub>2</sub> removal. *Front. Clim.* 3, 1–18. <https://doi.org/10.3389/fclim.2021.575900>.
- Casquet, C., 1980. *Fenómenos de endomorfismo, metamorfismo y metasomatismo de contacto en los mármoles de Rivera de Cala (Sierra Morena)*. Complutense University Doctoral Thesis.
- Casquet, C., Galindo, C., Tornos, F., Velasco, F., 2001. The Aguablanca Cu–Ni ore deposit (Extremadura, Spain), a case of synorogenic orthomagmatic mineralization: isotope composition of magmas (Sr, Nd) and ore (S). *Ore Geol. Rev.* 18, 237–250. [https://doi.org/10.1016/S0169-1368\(01\)00033-6](https://doi.org/10.1016/S0169-1368(01)00033-6).
- Castiñeiras, P., Gómez Barreiro, J., Martínez Catalán, J.R., Arenas, R., 2002. Nueva interpretación petrológica y tectónica de las anfíbolitas pobres en calcio del antiformal de Arinteiro (NO del Macizo Ibérico). I: Descripción de las anfíbolitas pobres en calcio y rocas asociadas.
- Castro, J.M., Feisel, Y., 2022. Eruption of ultralow-viscosity basanite magma at Cumbre Vieja, La Palma, Canary Islands. *Nat. Commun.* 13, 3174. <https://doi.org/10.1038/s41467-022-30905-4>.
- Cebriá, J.M., López-Ruiz, J., Doblas, M., Oyarzun, R., Hertogen, J., Benito, R., 2000. Geochemistry of the Quaternary alkali basalts of Garrotxa (NE Volcanic Province, Spain): a case of double enrichment of the mantle lithosphere. *J. Volcanol. Geotherm. Res.* 102, 217–235. [https://doi.org/10.1016/S0377-0273\(00\)00189-X](https://doi.org/10.1016/S0377-0273(00)00189-X).
- Chi-Yeung, J.S., 1972. *Geochemistry of peridotites and associated mafic rocks. Ronda Ultramafic Complex, Spain*. McGill University Doctoral Thesis.
- Cipolla, G., Calabrese, S., Porporato, A., Noto, L., 2022. Effects of precipitation seasonality, vegetation cycle, and irrigation on enhanced weathering. *EGU sphere* 1–29. <https://doi.org/10.5194/egusphere-2022-196>.
- Climate Analytics, 2021. *Spain Scenario Analysis, Country Factsheet: 1.5°C Pathways for Europe*, pp. 1–8.
- Contini, S., Venturelli, G., Toscani, L., Capedri, S., Barbieri, M., 1993. Cr–Zr–armalcolite-bearing lamproites of Cancarix, SE Spain. *Mineral. Mag.* 57, 203–216. <https://doi.org/10.1180/minmag.1993.057.387.02>.
- Crespo, A., Lunar, R., 1997. Terrestrial hot-spring Co-rich Mn mineralization in the Pliocene–Quaternary Calatrava Region (central Spain). *Geol. Soc. Spec. Publ.* 119 (1), 253–264. <https://doi.org/10.1144/GSL.SP.1997.119.01.16>.
- Darton, R.C., Yang, A., Xing, L., Bullock, L., 2022. Carbon Dioxide Removal from the atmosphere by weathering minerals in a gas-liquid-solid contactor. The 12th International Conference Distillation & Absorption 2022. 1202 last access: 2 June 2022.
- Daval, D., Martínez, I., Corvisier, J., Findling, N., Goffé, B., Guyot, F., 2009. Carbonation of Ca-bearing silicates, the case of wollastonite: experimental investigations and kinetic modeling. *Chem. Geol.* 265, 63–78. <https://doi.org/10.1016/J.CHEMGEO.2009.01.022>.
- Davies, P.A., 2015. Solar thermal decomposition of desalination reject brine for carbon dioxide removal and neutralisation of ocean acidity. *Environ. Sci. Water Res. Technol.* 1, 131–137. <https://doi.org/10.1039/c4ew00058g>.
- Dindi, A., Quang, D.V., Vega, L.F., Nashef, E., Abu-Zahra, M.R.M., 2019. Applications of fly ash for CO<sub>2</sub> capture, utilization, and storage. *J. CO<sub>2</sub> Util.* 29, 82–102. <https://doi.org/10.1016/j.jcou.2018.11.011>.
- Dong, H., Unluer, C., Yang, E.H., Al-Tabbaa, A., 2018. Recovery of reactive MgO from reject brine via the addition of NaOH. *Desalination* 429, 88–95. <https://doi.org/10.1016/j.desal.2017.12.021>.
- Dudhaiya, A., Haque, F., Fantucci, H., Santos, R.M., 2019. Characterization of physically fractionated wollastonite-amended agricultural soils. *Minerals* 9 (10), 635.
- Ecke, H., 2003. Sequestration of metals in carbonated municipal solid waste incineration (MSWI) fly ash. *Waste Manag.* 23, 631–640. [https://doi.org/10.1016/S0956-053X\(03\)00095-3](https://doi.org/10.1016/S0956-053X(03)00095-3).
- Edwards, D.P., Lim, F., James, R.H., Pearce, C.R., Scholes, J., Freckleton, R.P., Beerling, D.J., 2017. Climate change mitigation: potential benefits and pitfalls of enhanced rock weathering in tropical agriculture. *Biol. Lett.* 13. <https://doi.org/10.1098/rsbl.2016.0715>.
- EMODnet, .. Data services <https://www.emodnet-humanactivities.eu/search-results.php?dataname=Desalination+plant+locations> last access: 2 June 2022.
- Energy Futures Initiative, .. Clearing the air: a federal RD&D Initiative and Management Plan for CO<sub>2</sub> removal technologies. Report. Available online at <https://www.ourenergypolicy.org/resources/clearing-the-air-a-federal-rdd-initiative/> last access: 2 June 2022.
- Esteban, J.J., Cuevas, J., Tubía, J.M., Liati, A., Seward, D., Gebauer, D., 2007. Timing and origin of zircon-bearing chlorite schists in the Ronda peridotites (Betic cordilleras, Southern Spain). *Lithos* 99, 121–135. <https://doi.org/10.1016/j.lithos.2007.06.006>.
- EUROFER, .. Where is steel made in Europe? <https://www.eurofer.eu/about-steel/learn-about-steel/where-is-steel-made-in-europe/> last access: 2 June 2022.
- European Commission, 2021. *Climate Change: Climate Change Consequences*. Eur. Comm., pp. 1–19.
- European Commission, .. Developing enhanced weathering methods in mine tailings for CO<sub>2</sub> sequestration Horizon 2020 Fact Sheet <https://cordis.europa.eu/project/id/101018312> last access: 2 June 2022.
- European Environment Agency, n.. EEA Glossary <http://esa.un.org/unsd/envmnt/default.asp> last access: 2 June 2022.
- European Union, 2021. *Climate action in Spain - latest state of play*. EU Prog. Clim. Action - How Member States Are Doing.
- European Union, 2022. *Call for evidence for an impact assessment - certification of carbon removals-EU rules. Proposal for a Regulation*.
- Evans, O., Spiegelman, M., Kelemen, P.B., 2020. Phase-field modeling of reaction-driven cracking: determining conditions for extensive olivine serpentinization. *J. Geophys. Res. Solid Earth* 125, 1–21. <https://doi.org/10.1029/2019JB018614>.
- Extavour, M., 2021. Editorial: NRG COSIA carbon XPRIZE in context. *Clean Energy* 5, 551–552. <https://doi.org/10.1093/ce/zbak044>.
- Fagerlund, J., Zevenhoven, R., 2011. An experimental study of Mg(OH)<sub>2</sub> carbonation. *Int. J. Greenh. Gas Control* 5, 1406–1412. <https://doi.org/10.1016/j.ijggc.2011.05.039>.
- Fariás, P., Gallastegui, G., González Lodeiro, F., Marquín, J., Martín Parra, L.M., Martínez Catalán, J.R., de Pablo, J.G., Rodríguez Fernández, L.R., 1987. *Aportaciones al conocimiento de la litoestratigrafía y estructura de Galicia Central. Memórias da Faculdade de Ciências. I. Universidade do Porto*, pp. 411–431.
- Fernández-Jiménez, A., Palomo, A., 2003. Characterisation of fly ashes. Potential reactivity as alkaline cements. *Fuel* 82, 2259–2265. [https://doi.org/10.1016/S0016-2361\(03\)00194-7](https://doi.org/10.1016/S0016-2361(03)00194-7).
- Fernández-Torquemada, Y., Sánchez-Lizaso, J.L., González-Correa, J.M., 2005. Preliminary results of the monitoring of the brine discharge produced by the SWRO desalination plant of Alicante (SE Spain). *Desalination* 182, 395–402. <https://doi.org/10.1016/j.desal.2005.03.023>.
- Frías Rojas, M., Sánchez De Rojas, M.I., Uría, A., 2002. Estudio de la inestabilidad en escorias negras de hierro de arco eléctrico. *Mater. Constr.*, 79–83 <https://doi.org/10.3989/mc.2002.v52.i267.328>.
- Fuentes-Bargues, J.L., 2014. Analysis of the process of environmental impact assessment for seawater desalination plants in Spain. *Desalination* 347, 166–174. <https://doi.org/10.1016/j.desal.2014.05.032>.
- Gadikota, G., Matter, J., Kelemen, P., Brady, P.V., Park, A.H.A., 2020. Elucidating the differences in the carbon mineralization behaviors of calcium and magnesium bearing aluminosilicates and magnesium silicates for CO<sub>2</sub> storage. *Fuel* 277, 117900. <https://doi.org/10.1016/j.fuel.2020.117900>.
- Galán-Martín, Á., Vázquez, D., Cobo, S., Mac Dowell, N., Caballero, J.A., Guillén-Gosálbez, G., 2021. Delaying carbon dioxide removal in the European Union puts climate targets at risk. *Nat. Commun.* 12, 1–12. <https://doi.org/10.1038/s41467-021-26680-3>.
- García-Giménez, R., Jiménez-Ballesta, R., 2017. Mine tailings influencing soil contamination by potentially toxic elements. *Environ. Earth Sci.* 76. <https://doi.org/10.1007/s12665-016-6376-9>.
- García-Lobón, J.L., Rey-Moral, C., Ayala, C., 2006. Comprehensive petrophysics of rocks from the Monesterio antiformal (Ossa Morena zone, SW Spain). *J. Appl. Geophys.* 59 (3), 190–204. <https://doi.org/10.1016/j.jappgeo.2005.10.005>.
- Garrido, C.J., Bodinier, J., 1999. Diversity of mafic rocks in the Ronda peridotite: evidence for pervasive melt–rock reaction during heating of subcontinental lithosphere by upwelling asthenosphere. *J. Petrol.* 40, 729–754. <https://doi.org/10.1093/petroj/40.5.729>.
- Giammar, D.E., Bruant, R.G., Peters, C.A., 2005. Forsterite dissolution and magnesite precipitation at conditions relevant for deep saline aquifer storage and sequestration of carbon dioxide. *Chem. Geol.* 217, 257–276. <https://doi.org/10.1016/j.chemgeo.2004.12.013>.
- Gillman, G.P., Burkett, D.C., Coventry, R.J., 2002. Amending highly weathered soils with finely ground basalt rock. *Appl. Geochem.* 17 (8), 987–1001. [https://doi.org/10.1016/S0883-2927\(02\)00078-1](https://doi.org/10.1016/S0883-2927(02)00078-1).

- Girardeau, J., Ibarra, J.G., Jamaa, N.B., 1989. Evidence for a heterogeneous upper mantle in the Cabo Ortegal Complex, Spain. *Science* 245 (4923), 1231–1233. <https://doi.org/10.1126/science.245.4923.1231>.
- Gislason, S.R., Oelkers, E.H., 2003. Mechanism, rates, and consequences of basaltic glass dissolution: II. An experimental study of the dissolution rates of basaltic glass as a function of pH and temperature. *Geochim. Cosmochim. Acta* 67 (20), 3817–3832. [https://doi.org/10.1016/S0016-7037\(03\)00176-5](https://doi.org/10.1016/S0016-7037(03)00176-5).
- Gislason, S.R., Wolff-Boenisch, D., Stefansson, A., Oelkers, E.H., Gunnlaugsson, E., Sigurdardottir, H., Sigfusson, B., Broecker, W.S., Matter, J.M., Stute, M., Axelsson, G., Fridriksson, T., 2010. Mineral sequestration of carbon dioxide in basalt: a pre-injection overview of the CarbFix project. *Int. J. Greenh. Gas Control* 4, 537–545. <https://doi.org/10.1016/j.ijggc.2009.07.001>.
- Gislason, S.R., Sigurdardottir, H., Aradóttir, E.S., Oelkers, E.H., 2018. A brief history of CarbFix: challenges and victories of the project's pilot phase. *Energy Procedia* 146, 103–114. <https://doi.org/10.1016/j.egypro.2018.07.014>.
- Gomes, H.I., Mayes, W.M., Rogerson, M., Stewart, D.I., Burked, I.T., 2016. Alkaline residues and the environment: a review of impacts, management practices and opportunities. *J. Clean. Prod.* 112, 3571–3582. <https://doi.org/10.1016/j.jclepro.2015.09.111>.
- Gruber, C., Zhu, C., Georg, R.B., Zakon, Y., Ganor, J., 2014. Resolving the gap between laboratory and field rates of feldspar weathering. *Geochim. Cosmochim. Acta* 147, 90–106. <https://doi.org/10.1016/j.gca.2014.10.013>.
- Gudbrandsson, S., Wolff-Boenisch, D., Gislason, S.R., Oelkers, E.H., 2011. An experimental study of crystalline basalt dissolution from 2 pH and temperatures from 5 to 75 °C. *Geochim. Cosmochim. Acta* 75 (19), 5496–5509. <https://doi.org/10.1016/j.gca.2011.06.035>.
- Hajbi, F., Hammi, H., M'Nif, A., 2010. Reuse of RO desalination plant reject brine. *J. Phase Equilibria Diffus.* 31, 341–347. <https://doi.org/10.1007/s11669-010-9727-3>.
- Hall, C.M., Higuera, P.L., Kesler, S.E., Lunar, R., Dong, H., Halliday, A.N., 1997. Dating of alteration episodes related to mercury mineralization in the Almadén district, Spain. *Earth Planet. Sci. Lett.* 148 (1–2), 287–298. [https://doi.org/10.1016/S0012-821X\(97\)00041-1](https://doi.org/10.1016/S0012-821X(97)00041-1).
- Hänchen, M., Prigobbe, V., Baciocchi, R., Mazzotti, M., 2008. Precipitation in the Mg carbonate system - effects of temperature and CO<sub>2</sub> pressure. *Chem. Eng. Sci.* 63, 1012–1028. <https://doi.org/10.1016/j.ces.2007.09.052>.
- Hangx, S.J.T., Spiers, C.J., 2009. Coastal spreading of olivine to control atmospheric CO<sub>2</sub> concentrations: a critical analysis of viability. *Int. J. Greenh. Gas Control* 3, 757–767. <https://doi.org/10.1016/j.ijggc.2009.07.001>.
- Haque, F., Santos, R.M., Chiang, Y.W., 2020. CO<sub>2</sub> sequestration by wollastonite-amended agricultural soils - an Ontario field study. *Int. J. Greenh. Gas Control* 97, 103017. <https://doi.org/10.1016/j.ijggc.2020.103017>.
- Harrison, A.L., Power, I.M., Dipple, G.M., 2013. Accelerated carbonation of brucite in mine tailings for carbon sequestration. *Environ. Sci. Technol.* 47, 126–134. <https://doi.org/10.1021/es3012854>.
- Harrison, A.L., Dipple, G.M., Power, I.M., Mayer, K.U., 2015. Influence of surface passivation and water content on mineral reactions in unsaturated porous media: implications for brucite carbonation and CO<sub>2</sub> sequestration. *Geochim. Cosmochim. Acta* 148, 477–495. <https://doi.org/10.1016/j.gca.2014.10.020>.
- Hartmann, J., West, A.J., Renforth, P., Köhler, P., De La Rocha, C.L., Wolf-Gladrow, D.A., Dürr, H.H., Scheffran, J., 2013. Enhanced chemical weathering as a geoengineering strategy to reduce atmospheric carbon dioxide, supply nutrients, and mitigate ocean acidification. *Rev. Geophys.* 51, 113–149. <https://doi.org/10.1002/rog.20004>.
- Haug, T.A., Munz, I.A., Kleiv, R.A., 2011. Importance of dissolution and precipitation kinetics for mineral carbonation. *Energy Procedia* 4, 5029–5036. <https://doi.org/10.1016/j.egypro.2011.02.475>.
- Hernández, A., Jébrak, M., Higuera, P., Oyarzun, R., Morata, D., Munhá, J., 1999. The Almadén mercury mining district, Spain. *Mineral. Deposita* 34, 539–548. <https://doi.org/10.1007/s001260050219>.
- Hernández-Sánchez, J.C., Boluda-Botella, N., Sánchez-Lizaso, J.L., 2017. The role of desalination in water management in southeast Spain. *Desalin. Water Treat.* 76, 71–76. <https://doi.org/10.5004/dwt.2017.20657>.
- Hietkamp, S., 2005. The potential for sequestration of carbon dioxide in South Africa. Carbon capture and storage in South Africa. 6665 <http://playpen.meraka.csir.co.za/~acd/education/CSIR%20conference%202008/Proceedings/CPO-0027.pdf> 2005.
- Hitch, M., Ballantyne, S.M., Hindle, S.R., 2010. Revaluing mine waste rock for carbon capture and storage. *Int. J. Min. Reclam. Environ.* 24, 64–79. <https://doi.org/10.1080/17480930902843102>.
- Hobson, A., Bussy, F., Hernandez, J., 1998. Shallow-level migmatization of gabbros in a metamorphic contact aureole, Fuerteventura basal complex, Canary Islands. *J. Petrol.* 39, 1025–1037. <https://doi.org/10.1093/ptro/39.5.1025>.
- Holliman, J., Schaefer, T., Miller, Q.R.S., Horner, J., McGrail, B.P., Polites, E., 2021. Sidewall Core Characterization - Wallula Pilot Project Carbon Sequestration in Basalts. AGU Fall Meeting.
- Holloway, S., 2007. Carbon dioxide capture and geological storage. *Philos. Trans. R. Soc. A* 365, 1095–1107. <https://doi.org/10.1098/rsta.2006.1953>.
- Horn, S., Gunn, A.G., Petavratzi, E., Shaw, R.A., Eilu, P., Törmänen, T., Bjerkgård, T., Sandstad, J.S., Jonsson, E., Koumoutrellis, S., Wall, F., 2021. Cobalt resources in Europe and the potential for new discoveries. *Ore Geol. Rev.* 130, 103915. <https://doi.org/10.1016/j.oregeorev.2020.103915>.
- House, K.Z., House, C.H., Schrag, D.P., Aziz, M.J., 2007. Electrochemical acceleration of chemical weathering as an energetically feasible approach to mitigating anthropogenic climate change. *Environ. Sci. Technol.* 41, 8464–8470. <https://doi.org/10.1021/es0701816>.
- Huijgen, W.J.J., Witkamp, G.J., Comans, R.N.J., 2005. Mineral CO<sub>2</sub> sequestration by steel slag carbonation. *Environ. Sci. Technol.* 39, 9676–9682. <https://doi.org/10.1021/es050795f>.
- ICEX, 2020. Trade and Investment: Agri-Food industry - a strong, resilient industry. <https://www.investinspain.org/content/icex-invest/en/sectors/agrifood.html#> last access: 2 June 2022.
- IEA, 2019. Energy Policy Review Spain 2021. Int. Energy Agency.
- IGME, 2012. Mining in Spain 2012 - summary. <https://www.igme.es/panoramaminero/MINING%20IN%20SPAIN%20SUMMARY-2012.pdf>.
- IGME, 2022. Spanish Geological Survey maps: MAGNA 50 - Geological map of Spain, scale 1: 50,000 <https://info.igme.es/cartografiadigital/geologica/Magna50.aspx?language=en#info> last access: 2 June 2022.
- Ihsanullah, I., Atieh, M.A., Sajid, M., Nazal, M.K., 2021. Desalination and environment: a critical analysis of impacts, mitigation strategies, and greener desalination technologies. *Sci. Total Environ.* 780, 146585. <https://doi.org/10.1016/j.scitotenv.2021.146585>.
- IPCC, 2005. IPCC special report on carbon dioxide capture and storage. Prepared by Working Group III of the Intergovernmental Panel on Climate Change. Cambridge, New York.
- IPCC, 2022. Climate Change 2022 - Impacts, Adaptation And Vulnerability - Summary for Policymakers 37 pp.
- Jaschik, J., Jaschik, M., Warmuziński, K., 2016. The utilisation of fly ash in CO<sub>2</sub> mineral carbonation. *Chem. Process. Eng.* 37 (1), 29–39. <https://doi.org/10.1515/cpe-2016-0004>.
- Ji, X., Curcio, E., Al Obaidani, S., Di Profo, G., Fontananova, E., Drioli, E., 2010. Membrane distillation-crystallization of seawater reverse osmosis brines. *Sep. Purif. Technol.* 71, 76–82. <https://doi.org/10.1016/j.seppur.2009.11.004>.
- Ji, L., Yu, H., Zhang, R., French, D., Grigore, M., Yu, B., Wang, X., Yu, J., Zhao, S., 2019. Effects of fly ash properties on carbonation efficiency in CO<sub>2</sub> mineralisation. *Fuel Process. Technol.* 188, 79–88. <https://doi.org/10.1016/j.fuproc.2019.01.015>.
- Jiménez-Arias, D., Sierra, S.M., García-Machado, F.J., García-García, A.L., Borges, A.A., Luis, J.C., 2022. Exploring the agricultural reutilisation of desalination reject brine from reverse osmosis technology. *Desalination* 529, 115644. <https://doi.org/10.1016/j.desal.2022.115644>.
- Jones, E., Qadir, M., van Vliet, M.T.H., Smakhtin, V., Kang, S.M., 2019. The state of desalination and brine production: a global outlook. *Sci. Total Environ.* 657, 1343–1356. <https://doi.org/10.1016/j.scitotenv.2018.12.076>.
- Justnes, H., Escudero-Oñate, C., Garmo, Ø.A., Mengede, M., 2020. Transformation kinetics of burnt lime in freshwater and sea water. *Materials* 13 (21), 4926. <https://doi.org/10.3390/ma13214926>.
- Kantola, I.B., Masters, M.D., Beerling, D.J., Long, S.P., DeLucia, E.H., 2017. Potential of global croplands and bioenergy crops for climate change mitigation through deployment for enhanced weathering. *Biol. Lett.* 13. <https://doi.org/10.1098/rsbl.2016.0714>.
- Kantzas, E.P., Val Martin, M., Lomas, M.R., Eufrazio, R.M., Renforth, P., Lewis, A.L., Taylor, L.L., Mecure, J., Pollitt, H., Vercoulen, P.V., Vakilifard, N., Holden, P.B., Edwards, N.R., Koh, L., Pidgeon, N.F., Banwart, S.A., Beerling, D.J., 2022. Substantial carbon drawdown potential from enhanced rock weathering in the United Kingdom. *Nat. Geosci.* 15, 382–389. <https://doi.org/10.1038/s41561-022-00925-2>.
- Kasedde, H., Kirabira, J.B., Bähler, M.U., Tilliander, A., Jonsson, S., 2014. Characterization of brines and evaporites of Lake katwe, Uganda. *J. Afr. Earth Sci.* 91, 55–65. <https://doi.org/10.1016/j.jafrearsci.2013.12.004>.
- Katal, R., Shen, T.Y., Jafari, I., Masudy-Panah, S., Farahani, M.H.D.A., 2016. An overview on the treatment and management of the desalination brine solution. *Desalination* 11, 13.
- Kelemen, P.B., Hirth, G., 2012. Reaction-driven cracking during retrograde metamorphism: olivine hydration and carbonation. *Earth Planet. Sci. Lett.* 345–348, 81–89. <https://doi.org/10.1016/j.epsl.2012.06.018>.
- Kelemen, P.B., Matter, J., Streit, E.E., Rudge, J.F., Curry, W.B., Blusztajn, J., 2011. Rates and mechanisms of mineral carbonation in peridotite: natural processes and recipes for enhanced, in situ CO<sub>2</sub> capture and storage. *Annu. Rev. Earth Planet. Sci.* 39 (1), 545–576. <https://doi.org/10.1146/annurev-earth-092010-152509>.
- Kelemen, P., Benson, S.M., Pilorgé, H., Psarras, P., Wilcox, J., 2019. An overview of the status and challenges of CO<sub>2</sub> storage in minerals and geological formations. *Front. Clim.* 1, 1–20. <https://doi.org/10.3389/fclim.2019.00009>.
- Kelemen, P.B., McQueen, N., Wilcox, J., Renforth, P., Dipple, G., Vankeuren, A.P., 2020. Engineered carbon mineralization in ultramafic rocks for CO<sub>2</sub> removal from air: review and new insights. *Chem. Geol.* 550, 119628. <https://doi.org/10.1016/j.chemgeo.2020.119628>.
- Kelland, M.E., Wade, P.W., Lewis, A.L., Taylor, L.L., Sarkar, B., Andrews, M.G., Lomas, M.R., Cotton, T.E.A., Kemp, S.J., James, R.H., Pearce, C.R., Hartley, S.E., Hodson, M.E., Leake, J.R., Banwart, S.A., Beerling, D.J., 2020. Increased yield and CO<sub>2</sub> sequestration potential with the C4 cereal Sorghum bicolor cultivated in basaltic rock dust-amended agricultural soil. *Glob. Chang. Biol.* 26, 3658–3676. <https://doi.org/10.1111/gcb.15089>.
- Kheshgi, H.S., 1995. Sequestering atmospheric carbon dioxide by increasing ocean alkalinity. *Energy* 20, 915–922. [https://doi.org/10.1016/0360-5442\(95\)00035-F](https://doi.org/10.1016/0360-5442(95)00035-F).
- Khudhur, F.W.K., MacDonald, J.M., Macente, A., Daly, L., 2022. The utilization of alkaline wastes in passive carbon capture and sequestration: promises, challenges and environmental aspects. *Sci. Total Environ.* 823, 153553. <https://doi.org/10.1016/j.scitotenv.2022.153553>.
- Korngold, E., Aronov, L., Daltrophe, N., 2009. Electrodialysis of brine solutions discharged from an RO plant. *Desalination* 242, 215–227. <https://doi.org/10.1016/j.desal.2008.04.008>.
- Kossoff, D., Dubbin, W.E., Alfredsson, M., Edwards, S.J., Macklin, M.G., Hudson-Edwards, K.A., 2014. Mine tailings dams: characteristics, failure, environmental impacts, and remediation. *Appl. Geochem.* 51, 229–245. <https://doi.org/10.1016/j.apgeochem.2014.09.010>.
- Kremer, D., Eitzold, S., Boldt, J., Blaum, P., Hahn, K.M., Wotruba, H., Telle, R., 2019. Geological mapping and characterization of possible primary input materials for the mineral sequestration of carbon dioxide in Europe. *Minerals* 9 (8), 485. <https://doi.org/10.3390/min9080485>.
- Krevor, S.C.M., Lackner, K.S., 2011. Enhancing serpentine dissolution kinetics for mineral carbon dioxide sequestration. *Int. J. Greenh. Gas Control* 5, 1073–1080. <https://doi.org/10.1016/j.ijggc.2011.01.006>.
- Krevor, S., Graves, C., Van Gosen, B., McCafferty, A., (US), G.S., 2009. Mapping the mineral resource base for mineral carbon-dioxide sequestration in the conterminous United States. US Geological Survey.

- L'Orange Seigo, S., Arvai, J., Dohle, S., Siegrist, M., 2014. Predictors of risk and benefit perception of carbon capture and storage (CCS) in regions with different stages of deployment. *Int. J. Greenh. Gas Control* 25, 23–32. <https://doi.org/10.1016/j.ijggc.2014.03.007>.
- Lacinska, A.M., Styles, M.T., Bateman, K., Hall, M., Brown, P.D., 2017. An experimental study of the carbonation of serpentinite and partially serpentinised peridotites. *Front. Earth Sci.* 5, 37.
- Lackner, K.S., Wendt, C.H., Butt, D.P., Joyce, E.L., Sharp, D.H., 1995. Carbon dioxide disposal in carbonate minerals. *Energy* 20, 1153–1170. [https://doi.org/10.1016/0360-5442\(95\)00071-N](https://doi.org/10.1016/0360-5442(95)00071-N).
- Leonardos, O.H., Fyfe, W.S., Kronberg, B.L., 1987. The use of ground rocks in laterite systems: an improvement to the use of conventional soluble fertilizers? *Chem. Geol.* 60, 361–370. [https://doi.org/10.1016/0009-2541\(87\)90143-4](https://doi.org/10.1016/0009-2541(87)90143-4).
- Li, X., Bertos, M.F., Hills, C.D., Carey, P.J., Simon, S., 2007. Accelerated carbonation of municipal solid waste incineration fly ashes. *Waste Manag.* 27, 1200–1206. <https://doi.org/10.1016/j.wasman.2006.06.011>.
- Li, J., Hitch, M., Power, I.M., Pan, Y., 2018. Integrated mineral carbonation of ultramafic mine deposits—a review. *Minerals* 8, 1–18. <https://doi.org/10.3390/min8040147>.
- Liu, Q., Mercedes Maroto-Valer, M., 2013. Experimental studies on mineral sequestration of CO<sub>2</sub> with buffer solution and fly ash in brines. *Energy Procedia* 37, 5870–5874. <https://doi.org/10.1016/j.egypro.2013.06.511>.
- Llorens, J.F., Fernández-Turiel, J.L., Querol, X., 2001. The fate of trace elements in a large coal-fired power plant. *Environ. Geol.* 40, 409–416. <https://doi.org/10.1007/s002540000191>.
- Lomoschitz, A., Jiménez, J.R., Yepes, J., Pérez-Luzardo, J.M., Macías-MacHín, A., Socorro, M., Hernández, L.E., Rodríguez, J.A., Olalla, C., 2006. Basaltic lapilli used for construction purposes in the Canary Islands, Spain. *Environ. Eng. Geosci.* 12, 327–336. <https://doi.org/10.2113/gsegeosci.12.4.327>.
- Longo, R.C., Cho, K., Bruner, P., Welle, A., Gerdes, A., Thissen, P., 2015. Carbonation of wollastonite(001) competing hydration: microscopic insights from ion spectroscopy and density functional theory. *ACS Appl. Mater. Interfaces* 7, 4706–4712. <https://doi.org/10.1021/am508313g>.
- Mabrook, B., 1994. Environmental impact of waste brine disposal of desalination plants, Red Sea, Egypt. *Desalination* 97, 453–465. [https://doi.org/10.1016/0011-9164\(94\)00108-1](https://doi.org/10.1016/0011-9164(94)00108-1).
- Macedonio, F., Katzir, L., Geisma, N., Simone, S., Drioli, E., Gilron, J., 2011. Wind-Aided Intensified eVaporation (WAIv) and Membrane Crystallizer (MCR) integrated brackish water desalination process: advantages and drawbacks. *Desalination* 273, 127–135. <https://doi.org/10.1016/j.desal.2010.12.002>.
- Magnesitas Navarras, .. Mining process <https://www.magnesitasnavarras.es/> last access: 22 July 2022.
- Marchesi, C., Garrido, C.J., Padron-Navarta, J.A., Sánchez-Vizcaíno, V.L., Gómez-Pugnaire, M.T., 2013. Element mobility from seafloor serpentinization to high-pressure dehydration of antigorite in subducted serpentinite: insights from the Cerro del Almirez ultramafic massif (southern Spain). *Lithos* 178, 128–142. <https://doi.org/10.1016/j.lithos.2012.11.025>.
- Marcos, A., Fariás, P., Galán, G., Fernández, F.J., Llana-Fúnez, S., 2002. Tectonic framework of the Cabo Ortegal Complex: a slab of lower crust exhumed in the Variscan orogen (north-western Iberian Peninsula). *Geol. Soc. Am. Spec. Pap.* 364, 143–162. <https://doi.org/10.1130/0-8137-2364-7.143>.
- Marieni, C., Matter, J.M., Teagle, D.A., 2020. Experimental study on mafic rock dissolution rates within CO<sub>2</sub>-seawater-rock systems. *Geochim. Cosmochim. Acta* 272, 259–275. <https://doi.org/10.1016/j.gca.2020.01.004>.
- Martinetti, C.R., Childress, A.E., Cath, T.Y., 2009. High recovery of concentrated RO brines using forward osmosis and membrane distillation. *J. Membr. Sci.* 331, 31–39. <https://doi.org/10.1016/j.memsci.2009.01.003>.
- Mas, M.A., Monzó, J., Payá, J., Reig, L., Borrachero, M.V., 2016. Ceramic tiles waste as replacement material in Portland cement. *Adv. Cem. Res.* 28 (4), 221–232. <https://doi.org/10.1680/adcr.15.00021>.
- Matter, J.M., Kelemen, P.B., 2009. Permanent storage of carbon dioxide in geological reservoirs by mineral carbonation. *Nat. Geosci.* 2, 837–841. <https://doi.org/10.1038/ngeo683>.
- Matter, J.M., Stute, M., Snæbjörnsdóttir, S., Oelkers, E.H., Gislason, S.R., Aradóttir, E.S., Sigfusson, B., Gunnarsson, I., Sigurdardóttir, H., Gunnlaugsson, E., Axelsson, G., Alfredsson, H.A., Wolff-Boenisch, D., Mesfin, K., Taya, D.F.D.L.R., Hall, J., Dideriksen, K., Broecker, W.S., 2016. Rapid carbon mineralization for permanent disposal of anthropogenic carbon dioxide emissions. *Science* 352 (6291), 1312–1314. <https://doi.org/10.1126/science.aad8132>.
- Mayes, W.M., Younger, P.L., Aumônier, J., 2008. Hydrogeochemistry of alkaline steel slag leachates in the UK. *Water Air Soil Pollut.* 195, 35–50. <https://doi.org/10.1007/s11270-008-9725-9>.
- Mayes, W.M., Riley, A.L., Gomes, H.L., Brabham, P., Hamlyn, J., Pullin, H., Renforth, P., 2018. Atmospheric CO<sub>2</sub> sequestration in iron and steel slag: Consett, County Durham, United Kingdom. *Environ. Sci. Technol.* 52, 7892–7900. <https://doi.org/10.1021/acs.est.8b01883>.
- McCutcheon, J., Turvey, C.C., Wilson, S.A., Hamilton, J.L., Southam, G., 2017. Experimental deployment of microbial mineral carbonation at an asbestos mine: potential applications to carbon storage and tailings stabilization. *Minerals* 7, 15–18. <https://doi.org/10.3390/min7100191>.
- Merinero Palomares, R., Lunar Hernández, R., Ortega Menor, L., Piña García, R., Monterrubio Pérez, S., Gervilla, F., 2014. Zoned chromite records multiple metamorphic episodes in the Calzadilla de los Barros ultramafic bodies (SW Iberian peninsula). *Eur. J. Mineral.* 26 (6), 757–770. <https://doi.org/10.1127/ejm/2014/0026-2406>.
- Meyer, N.A., 2014. An Investigation Into the Dissolution of Pyroxene: A Precursor to Mineral Carbonation of PGM Tailings in South Africa. University of Cape Town Doctoral Thesis.
- Meyer, N.A., Vögeli, J.U., Becker, M., Broadhurst, J.L., Reid, D.L., Franzidis, J.P., 2014. Mineral carbonation of PGM mine tailings for CO<sub>2</sub> storage in South Africa: a case study. *Miner. Eng.* 59, 45–51. <https://doi.org/10.1016/j.mineng.2013.10.014>.
- Meysman, F.J., Montserrat, F., 2017. Negative CO<sub>2</sub> emissions via enhanced silicate weathering in coastal environments. *Biol. Lett.* 13 (4), 20160905.
- Mining Data Online, .. Major Mines & Projects | OroValle/El Valle Operation <https://miningdataonline.com/property/1204/OroValle-El-Valle-Operation.aspx> last access: 2 June 2022.
- Mining Data Online, .. Major Mines & Projects | Touro Project <https://miningdataonline.com/property/3446/Touro-Project.aspx#Production> last access: 2 June 2022.
- MITECO, 2020a. Acuerdo por una transición energética justa para centrales térmicas en cierre: el empleo, la industria y los territorios, Minist. Para La Transic. Ecológica y El Reto Demográfico.
- MITECO, 2020b. Estrategia De Descarbonización a Largo Plazo 2050. 73 37 pp.
- Mohammad, A.F., El-Naas, M.H., Al-Marzouqi, A.H., Suleiman, M.I., Al Musharfy, M., 2019. Optimization of magnesium recovery from reject brine for reuse in desalination post-treatment. *J. Water Process Eng.* 31, 1–8. <https://doi.org/10.1016/j.jwpe.2019.100810>.
- Montes-Hernandez, G., Pérez-López, R., Renard, F., Nieto, J.M., Charlet, L., 2009. Mineral sequestration of CO<sub>2</sub> by aqueous carbonation of coal combustion fly-ash. *J. Hazard. Mater.* 161, 1347–1354. <https://doi.org/10.1016/j.jhazmat.2008.04.104>.
- Morse, J.W., Arvidson, R.S., Lüttge, A., 2007. Calcium carbonate formation and dissolution. *Chem. Rev.* 107 (2), 342–381. <https://doi.org/10.1021/cr050358j>.
- Mountadar, S., Carbonell-Alcaina, C., Luján-Facundo, M.J., Ferrer-Polonio, E., Soler-Cabezas, J.L., Mendoza-Roca, J.A., Tahiri, S., 2017. Desalination of brackish water and reverse osmotic retentate using nanofiltration membranes: effects of TMP and feed concentration on the treatment. *Desalin. Water Treat.* 87, 68–75. <https://doi.org/10.5004/dwt.2017.21312>.
- Mourad, A.A.H.I., Mohammad, A.F., Al-Marzouqi, A.H., El-Naas, M.H., Al-Marzouqi, M.H., Altarawneh, M., 2022. CO<sub>2</sub> capture and ions removal through reaction with potassium hydroxide in desalination reject brine: statistical optimization. *Chem. Eng. Process. Intensif.* 170. <https://doi.org/10.1016/j.cep.2021.108722>.
- Movares, 2012. Het Groene Schouwpad Het Groene Schouwpad. <https://movares.nl/projecten/het-groene-schouwpad/>.
- Muriithi, G.N., Petrik, L.F., Fatoba, O., Gitari, W.M., Doucet, F.J., Nel, J., Nyale, S.M., Chuks, P.E., 2013. Comparison of CO<sub>2</sub> capture by ex-situ accelerated carbonation and in situ naturally weathered coal fly ash. *J. Environ. Manag.* 127, 212–220. <https://doi.org/10.1016/j.jenvman.2013.05.027>.
- Mustafa, J., Mourad, A.A.H.I., Al-Marzouqi, A.H., El-Naas, M.H., 2020. Simultaneous treatment of reject brine and capture of carbon dioxide: a comprehensive review. *Desalination* 483. <https://doi.org/10.1016/j.desal.2020.114386>.
- Myers, C., Nakagaki, T., 2020. Direct mineralization of atmospheric CO<sub>2</sub> using natural rocks in Japan. *Environ. Res. Lett.* 15. <https://doi.org/10.1088/1748-9326/abc217>.
- NASEM: National Academies of Sciences, Engineering, and Medicine, 2019. Negative Emissions Technologies and Reliable Sequestration: A Research Agenda. The National Academies Press, Washington, DC <https://doi.org/10.17226/25259>.
- NECP, 2020. Plan de Energía Nacional Integrada y Climática de España, pp. 1–262.
- Noble, A.C., 2018. Technical report on the mineral resources and reserves of the Touro Copper Project. Prepared for Atalaya Mining, Report NI-43-101 <https://atalayamining.com/wp-content/uploads/2020/01/NI-43-101-Technical-Report-for-Proyecto-Touro.pdf>.
- Nyambura, M.G., Muger, G.W., Felicia, P.L., Gathura, N.P., 2011. Carbonation of brine impacted fractionated coal fly ash: implications for CO<sub>2</sub> sequestration. *J. Environ. Manag.* 92, 655–664. <https://doi.org/10.1016/j.jenvman.2010.10.008>.
- O'Neil, J.R., Barnes, I., 1971. C13 and O18 compositions in some fresh-water carbonates associated with ultramafic rocks and serpentinites: western United States. *Geochim. Cosmochim. Acta* 35 (7), 687–697. [https://doi.org/10.1016/0016-7037\(71\)90067-6](https://doi.org/10.1016/0016-7037(71)90067-6).
- Oskierski, H.C., Dlugogorski, B.Z., Jacobsen, G., 2013. Sequestration of atmospheric CO<sub>2</sub> in chrysotile mine tailings of the Woodsreef Asbestos Mine, Australia: quantitative mineralogy, isotopic fingerprinting and carbonation rates. *Chem. Geol.* 358, 156–169. <https://doi.org/10.1016/j.chemgeo.2013.09.001>.
- Palandri, J.L., Kharaka, Y.K., 2004. A compilation of rate parameters of water-mineral interaction kinetics for application to geochemical modeling. Geological Survey Menlo Park CA.
- Palomar, P., Losada, I.J., 2010. Desalination in Spain: recent developments and recommendations. *Desalination* 255, 97–106. <https://doi.org/10.1016/j.desal.2010.01.008>.
- Parkhurst, D.L., Appelo, C.A.J., 1999. User's guide to PHREEQC (Version 2): a computer program for speciation, batch-reaction, one-dimensional transport, and inverse geochemical calculations. *Water-Resources Investigations Report* 99(4259), p. 312.
- Paukert, A.N., Matter, J.M., Kelemen, P.B., Shock, E.L., Havig, J.R., 2012. Reaction path modeling of enhanced in situ CO<sub>2</sub> mineralization for carbon sequestration in the peridotite of the Samail Ophiolite, Sultanate of Oman. *Chem. Geol.* 330–331, 86–100. <https://doi.org/10.1016/j.chemgeo.2012.08.013>.
- Pereira, M.D., Peinado, M., Blanco, J.A., Yenes, M., 2008. Geochemical characterization of serpentinites at Cabo Ortegal, northwestern Spain. *Canad. Mineral.* 46 (2), 317–327. <https://doi.org/10.3749/canmin.46.2.317>.
- Perez, A., Daval, D., Fournier, M., Vital, M., Delaye, J.M., Gin, S., 2019. Comparing the reactivity of glasses with their crystalline equivalents: the case study of plagioclase feldspar. *Geochim. Cosmochim. Acta* 254, 122–141. <https://doi.org/10.1016/j.gca.2019.03.030>.
- Pérez-González, A., Ibáñez, R., Gómez, P., Urtiaga, A.M., Ortiz, I., Irabien, J.A., 2015. Recovery of desalination brines: separation of calcium, magnesium and sulfate as a pre-treatment step. *Desalin. Water Treat.* 56, 3617–3625. <https://doi.org/10.1080/19443994.2014.973454>.
- Perez-Torrado, F.J., Rodríguez González, A., Moreno-Medina, C.L., Cabrera, M.D.L., Carracedo-Gomez, J.C., Díaz-Rodríguez, S., Fernandez-Turiel, J.L., Criado Hernández, C., Aulinas, M., Prieto-Torrell, C., 2022. Digitalisación “Volcanes en movimiento: El Hierro y La Palma”. <https://doi.org/10.20350/exposic%2F14494>.
- Perroud, H., Calza, F., Khattach, D., 1991. Paleomagnetism of the Silurian volcanism at Almaden, southern Spain. *J. Geophys. Res. Solid Earth* 96 (B2), 1949–1962. <https://doi.org/10.1029/90JB02226>.





- Aguablanca, Spain. Mineral. Deposita 36 (7), 700–706. <https://doi.org/10.1007/s001260100204>.
- Tornos, F., Galindo, C., Casquet, C., Rodríguez Pevida, L., Martínez, C., Martínez, E., Velasco, F., Iriondo, A., 2006. The Aguablanca Ni–(Cu) sulfide deposit, SW Spain: geologic and geochemical controls and the relationship with a midcrustal layered mafic complex. Mineral. Deposita 41 (8), 737–769. <https://doi.org/10.1007/s00126-006-0090-6>.
- Tornos, F., Galindo, C., Darbyshire, F., Casquet, C., Noble, S.R., 2021. Isotope geochemistry, age, and origin of the magnetite-vonsenite mineralization of the Monchi Mine, SW Iberia. J. Iber. Geol. 47 (1), 65–84. <https://doi.org/10.1007/s41513-020-00159-4>.
- Troll, V.R., Carracedo, J.C., 2016. The Canary Islands: an introduction. The Geology of the Canary Islands, pp. 1–41. <https://doi.org/10.1016/b978-0-12-809663-5.00001-3>.
- Upham, P., Roberts, T., 2011. Public perceptions of CCS in context: results of NearCO2 focus groups in the UK, Belgium, the Netherlands, Germany, Spain and Poland. Energy Procedia 4, 6338–6344. <https://doi.org/10.1016/j.egypro.2011.02.650>.
- US Geological Survey, .. Mineral resources online spatial data <https://mrdata.usgs.gov/general/map-global.html>.
- Vaughan, A., 2022. Slag heaps from steelmaking could absorb CO2 and fight climate change. New Sci. <https://www.newscientist.com/article/2322641-slag-heaps-from-steelmaking-could-absorb-co2-and-fight-climate-change/#ixzz7VcvZfGQC>.
- Venturelli, G., Capedri, S., Di Battistini, G., Crawford, A., Kogarko, L.N., Celestini, S., 1984. The ultrapotassic rocks from southeastern Spain. Lithos 17, 37–54. [https://doi.org/10.1016/0024-4937\(84\)90005-7](https://doi.org/10.1016/0024-4937(84)90005-7).
- Vicca, S., Goll, D.S., Hagens, M., Hartmann, J., Janssens, I.A., Neubeck, A., Peñuelas, J., Poblador, S., Rijnders, J., Sardans, J., Struyf, E., Swoboda, P., van Groenigen, J.W., Vienne, A., Verbruggen, E., 2022. Is the climate change mitigation effect of enhanced silicate weathering governed by biological processes? Glob. Chang. Biol. 28, 711–726. <https://doi.org/10.1111/gcb.15993>.
- Villaseca, C., Ancochea, E., Orejana, D., Jeffries, T.E., 2010. Composition and evolution of the lithospheric mantle in central Spain: inferences from peridotite xenoliths from the Cenozoic Calatrava volcanic field. Geol. Soc. Spec. Publ. 337 (1), 125–151. <https://doi.org/10.1144/SP337.7>.
- Vogeli, J., Reid, D.L., Becker, M., Broadhurst, J., Franzidis, J.P., 2011. Investigation of the potential for mineral carbonation of PGM tailings in South Africa. Miner. Eng. 24, 1348–1356. <https://doi.org/10.1016/j.mineng.2011.07.005>.
- White, S.K., Spang, F.A., Schaefer, H.T., Miller, Q.R.S., White, M.D., Horner, J.A., McGrail, B.P., 2020. Quantification of CO2 mineralization at the Wallula basalt pilot project. Environ. Sci. Technol. 54, 14609–14616. <https://doi.org/10.1021/acs.est.0c05142>.
- Wilkin, R.T., Digiulio, D.C., 2010. Geochemical impacts to groundwater from geologic carbon sequestration: controls on pH and inorganic carbon concentrations from reaction path and kinetic modelling. Environ. Sci. Technol. 44, 4821–4827. <https://doi.org/10.1021/es100559j>.
- Wilson, S.A., Dipple, G.M., Power, I.M., Thom, J.M., Anderson, R.G., Raudsepp, M., Gabites, J.E., Southam, G., 2009. Carbon dioxide fixation within mine wastes of ultramafic-hosted ore deposits: examples from the Clinton Creek and Cassiar chrysotile deposits, Canada. Econ. Geol. 104 (1), 95–112. <https://doi.org/10.2113/gsecongeo.104.1.95>.
- Wilson, S.A., Harrison, A.L., Dipple, G.M., Power, I.M., Barker, S.L.L., Ulrich Mayer, K., Fallon, S.J., Raudsepp, M., Southam, G., 2014. Offsetting of CO2 emissions by air capture in mine tailings at the Mount Keith Nickel Mine, Western Australia: rates, controls and prospects for carbon neutral mining. Int. J. Greenh. Gas Control 25, 121–140. <https://doi.org/10.1016/j.ijggc.2014.04.002>.
- WorldData.info, .. Spain <https://www.worlddata.info/europe/spain/index.php#>.
- Xing, L., Pullin, H., Bullock, L., Renforth, P., Darton, R.C., Yang, A., 2022. Potential of enhanced weathering of calcite in packed bubble columns with seawater for carbon dioxide removal. Chem. Eng. J. 431, 134096. <https://doi.org/10.1016/j.cej.2021.134096>.
- Zalduegui, J.S., Schärer, U., Ibarra, J.G., Girardeau, J., 1996. Origin and evolution of the Paleozoic Cabo Ortegal ultramafic-mafic complex (NW Spain): U–Pb, Rb–Sr and Pb–Pb isotope data. Chem. Geol. 129 (3–4), 281–304. [https://doi.org/10.1016/0009-2541\(95\)00144-1](https://doi.org/10.1016/0009-2541(95)00144-1).
- Zarandi, A.E., Larachi, F., Beaudoin, G., Plante, B., Sciortino, M., 2016. Multivariate study of the dynamics of CO2 reaction with brucite-rich ultramafic mine tailings. Int. J. Greenh. Gas Control 52, 110–119.
- Zarza, L.F., Novo, C., .. Spanish desalination know-how, a worldwide benchmark <https://smartwatermagazine.com/news/smart-water-magazine/spanish-desalination-know-how-a-worldwide-benchmark>.
- Zeyen, N., Wang, B., Wilson, S.A.S., Paulo, C., Stubbs, A.R., Power, I.M., Steele-MacInnis, M., Lanzirrotti, A., Newville, M., Paterson, D.J., Hamilton, J.L., 2022. Cation exchange in smectites as a new approach to mineral carbonation. Front. Clim. 98. <https://doi.org/10.3389/fclim.2022.913632>.
- Zhou, Y., Ning, X., Liao, X., Lin, M., Liu, J., Wang, J., 2013. Characterization and environmental risk assessment of heavy metals found in fly ashes from waste filter bags obtained from a Chinese steel plant. Ecotoxicol. Environ. Saf. 95, 130–136. <https://doi.org/10.1016/j.ecoenv.2013.05.026>.